

HIGH PERFORMANCE EXACT LINEAR ALGEBRA

by

Bryan Youse

A dissertation submitted to the Faculty of the University of Delaware in partial fulfillment of the requirements for the degree of Doctor of Philosophy in Computer & Information Sciences

Spring 2015

© 2015 Bryan Youse
All Rights Reserved

HIGH PERFORMANCE EXACT LINEAR ALGEBRA

by

Bryan Youse

Approved: _____
Errol Lloyd, Ph.D.
Chair of the Department of Computer & Information Sciences

Approved: _____
Babatunde A. Ogunnaike, Ph.D.
Dean of the College of Engineering

Approved: _____
James G. Richards, Ph.D.
Vice Provost for Graduate and Professional Education

I certify that I have read this dissertation and that in my opinion it meets the academic and professional standard required by the University as a dissertation for the degree of Doctor of Philosophy.

Signed: _____

B. David Saunders, Ph.D.
Professor in charge of dissertation

I certify that I have read this dissertation and that in my opinion it meets the academic and professional standard required by the University as a dissertation for the degree of Doctor of Philosophy.

Signed: _____

Jeremy Johnson, Ph.D.
Member of dissertation committee

I certify that I have read this dissertation and that in my opinion it meets the academic and professional standard required by the University as a dissertation for the degree of Doctor of Philosophy.

Signed: _____

Michela Taufer, Ph.D.
Member of dissertation committee

I certify that I have read this dissertation and that in my opinion it meets the academic and professional standard required by the University as a dissertation for the degree of Doctor of Philosophy.

Signed: _____

John Cavazos, Ph.D.
Member of dissertation committee

I certify that I have read this dissertation and that in my opinion it meets the academic and professional standard required by the University as a dissertation for the degree of Doctor of Philosophy.

Signed: _____

David Wood, Ph.D.

Member of dissertation committee

ACKNOWLEDGEMENTS

I would like to deeply thank all of those friends and family who believed in me from the beginning. I simply could not have proceeded without your support. Special thanks are owed to:

- My parents, for the various opportunities for growth they provided me throughout my life, by virtue of their own hard work.
- My grandfather, who had been calling me “doctor” long before it was clear that I would complete this work.
- My advisor, Dave, who devoted countless hours in aiding my journey. His enthusiasm for the subject matter was contagious. I will forever fondly recall the late evenings of pair-programming in the various labs that our somewhat nomadic group occupied at one time or another. I view this time spent as collaboration of not mere colleagues, but friends.
- Finally my wife, Leah, earns my deepest gratitude. She unflinchingly encouraged, reassured, and cared for me at all times, but most especially when I needed it.

I love you.

TABLE OF CONTENTS

LIST OF TABLES	ix
LIST OF FIGURES	x
LIST OF ALGORITHMS	xi
LIST OF SYMBOLS	xii
ABSTRACT	xiii
 Chapter	
1 INTRODUCTION	1
2 FINITE FIELD DATA COMPRESSION	4
2.1 Introduction	4
2.1.1 Prior work	5
2.2 Bit-packing	5
2.2.1 Faster bit-packing	12
2.2.2 Extending to other prime fields	14
2.3 Bit-slicing	19
2.3.1 Specialized arithmetic	22
2.4 Summary	25

3	STRONGLY REGULAR GRAPH 3-RANKS	27
3.1	Introduction	27
3.1.1	Prior work	28
3.2	Obtaining rank($D(3, 7)$)	29
3.2.1	Space and time efficient p -Rank	30
3.2.2	Certified 3-Rank	40
3.3	Obtaining rank($D(3, 8)$)	44
3.3.1	Motivation	44
3.3.2	Size & scope	45
3.3.3	Producer/consumer: A first try	46
3.3.3.1	Broad implementation	48
3.3.3.2	The building blocks	58
3.3.3.3	A failure	62
3.3.4	Producer/consumer: cut out the middle-man	64
3.3.4.1	Revised big-picture layout	65
3.3.4.2	Revised building blocks	68
3.3.4.3	Shared-memory parallelism	70
3.3.5	Obtaining rank(M)	72
3.3.6	A final barrier	74
3.3.6.1	The panacea	75
3.3.7	Further applications	77
3.4	Summary	78

4	EXACT RATIONAL LINEAR SYSTEM SOLVER	80
4.1	Introduction	80
4.1.1	Relation to prior work	80
4.2	Background	83
4.3	Confirmed continuation and output sensitivity	86
4.3.1	An adaptive approach	86
4.3.2	Overflowing doubles	88
4.3.3	Early termination	89
4.4	Dyadic rational to rational reconstruction	90
4.5	Experiments	95
4.6	Summary	102
5	SUMMARY	103
5.1	Future Work	105
	BIBLIOGRAPHY	106
	Appendix	
A	REMOTE OBJECTS WITH PYRO	111
B	\mathbb{F}_3 BIT-SLICING “STEPPER”	113
B.1	File-stepper	115

LIST OF TABLES

2.1	Best bit-packing for small prime fields of interest.	10
2.2	<i>Semi-normalized</i> bit-packing performance improvements.	18
2.3	Speed of vector operations over \mathbb{F}_3	26
3.1	Running time for computing the ranks of Dickson adjacency matrices, with summation and certificate.	44
3.2	Running time for computing the ranks of Dickson adjacency matrices: fully parallelized implementation.	75
3.3	Known ranks for adjacency matrices of certain strongly regular graph families.	79
4.1	Examples of numeric failure to converge.	96
4.2	Dixon, Wan, and Overlap algorithm performance comparison.	101

LIST OF FIGURES

2.1	A closeup of a machine word utilizing bit-packing, and a view of the savings bit-packing affords.	7
2.2	Performance and space gains using vanilla bit-packing for small prime fields.	11
2.3	Flowchart depicting the four bit-operations needed for <i>semi-normalization</i> for bit-packed \mathbb{F}_3	13
2.4	A repetition of Figure 2.2(c) including <i>semi-normalization</i> data	17
2.5	The flow of a series of <i>SN3</i> operations.	19
2.6	A closeup of two machine words utilizing bit-slicing to store \mathbb{F}_3 values, and a view of savings bit-slicing affords.	20
2.7	Figure 2.2(a) updated with data points for <i>semi-normalized</i> bit-packing and bit-slicing.	24
3.1	Butterfly construction for $b = 8$	32
3.2	Decomposition and compression of the matrix A	50
3.3	Filesystem activity during parallel build of $D(3, 8)$	63
3.4	A contrast of Figure 3.3 with the real time file-system activity of the revised parallel decomposition.	68
3.5	Multithreaded parallel scalability for the routine of building a column block.	73
4.1	Dense and sparse system performance comparison between the Overlap method and Dixon's method.	100

LIST OF ALGORITHMS

1	Marshalling finite field element data to enable bit-packing.	6
2	Extracting finite field element data from a bit-packed representation.	8
3	Converting <i>semi-normalized</i> values to \mathbb{F}_3 representation.	14
4	General <i>semi-normalization</i> for bitpacking Mersenne-prime fields. .	16
5	Bit-slice a finite field element.	21
6	Extracting finite field element data from a bit-sliced representation.	22
7	\mathbb{F}_3 addition with bit-slicing.	23
8	\mathbb{F}_3 negation/multiplication by two.	23
9	Confirmed continuation iterative refinement to solve $Ax = b$	87
10	Confirmed continuation iterative refinement with Early Termination to solve $Ax = b$	89
11	Vector conversion from dyadic to rational.	94

LIST OF SYMBOLS

	Bitwise-OR.
&	Bitwise-AND.
\oplus	Bitwise-XOR.
\sim	Bitwise-NOT.
\ll	Bitshift left.
\gg	Bitshift right.
++	Increment operator.
%	Modulus operator.
[]	Integer floor.
[]	Integer ceiling.
$\ A\ $	Matrix norm.
$\ A\ _\infty$	Infinity norm.

ABSTRACT

This is a study in exact computational linear algebra consisting of two parts. First the problem of computing the p -rank of an integer matrix with particular emphasis on the case when the matrix is large and dense, the rank is relatively small, and the prime is tiny (such as $p = 3$). Second is a numeric-symbolic rational linear system solver using an iterative refinement approach.

The rank problem arises from the study of difference sets of finite groups and their corresponding strongly regular graphs. The ranks of the adjacency matrices representing these graphs are sought. These matrices, defined in sequences, grow too large for previously known rank algorithms. Prior solutions either require too much memory or are too computationally costly for the scenario of a large matrix with much lower rank. The expected low rank invites us to find a space- and time-efficient algorithm for this special case. The heuristic methods detailed here form a Monte Carlo algorithm which is essentially optimal when the rank is sufficiently small. Several tools are used in concert with the new algorithm which are vital in computing the rank of some of the larger matrices of the sequences, which contain on the order of peta-entries. A suite of finite-field data compression tools is discussed. Additionally, a framework for distributed- and shared-memory parallelism is detailed.

The rational linear system solver produces, for each entry of the solution vector, a rational approximation with denominator a power of two. From this representation, the correct rational entry can be reconstructed. Our method is a numeric-symbolic hybrid in that it uses an approximate numeric solver at each iteration together with a symbolic (exact arithmetic) residual computation and symbolic rational reconstruction. It is able to be output sensitive (i.e. terminate early) with provably correct result. Alternatively, the algorithm may be used without the rational reconstruction to obtain

an extended precision floating point approximation of *any* specified precision. The chief contributions of the method and implementation are confirmed continuation, highly tuned rational reconstruction, and fast, robust performance.

All work contained herein contributes to the LINBOX library for exact linear algebra.

Chapter 1

INTRODUCTION

The purpose of this study is to explore and synthesize methods to increase the efficiency of selected exact linear algebra problems. Traditional numerical approximation methods, prevalent in scientific and engineering computing today, provide solutions at best accurate to the level of the precision of the machines on which they run. This approach is nevertheless popular due to generally fast computations and the approximate nature of some input data. Symbolic techniques, those used to solve linear algebra problems exactly, offer the significant feature of providing answers completely free of error. This benefit often comes at the cost of additional computational resources than analogous numerical methods would employ. Still, there exists healthy demand for exact results; many applications stand to benefit from exact computation even if the nature of the input data is approximate. Thanks to advances in computing hardware, namely cheaper, vaster memory and faster, more numerous processors, exact computations are in the realm of practical possibility for many problems. This growing complexity in the computing landscape offers many avenues for improving algorithmic performance. Tailoring algorithms to diverse architectures, cache sizes, hardware arithmetic methods, and parallel computation models is necessary to achieve peak performance. The work in this thesis takes advantage of these strategies to improve efficiency of algorithms found in the software library LINBOX [1].

LINBOX is a high performance, exact linear algebra C++ template library that provides solutions for problems over arbitrary precision integers, rational numbers, and

finite fields. Particular problems include matrix rank, determinant, minimal polynomial, characteristic polynomial, linear system solving, and Smith normal form. Solutions exist for general dense matrices as well as sparse matrices, those matrices populated primarily with zeroes. Many specializations are offered for both dense and sparse matrix variants that are specifically structured so that certain characteristics can be algorithmically exploited.

An important area to the realm of exact computation is that of finite field arithmetic. In Chapter 2 we will discuss various ways to improve arithmetic over small prime finite fields. Special forms of compression have been developed to the end of lowering both algorithm running time and memory footprint. Here we describe two known compression schemes that greatly benefit computing with small prime fields, here called bit-packing and bit-slicing. We provide an implementation of the compression methods in LINBOX, and detail our key innovations to the schemes. We demonstrate the value of our specializations with experimental data.

The specific innovations will be illustrated by their inclusion in a solution to the exact rank computation investigated in Chapter 3. In this chapter, the ranks we are searching for are conjectured to be considerably smaller than the size of the matrices on which we compute. We provide a novel, Monte Carlo algorithm tailor-made for such a scenario, one wherein previously existing algorithms for computing rank prove either too time-consuming, too memory-hungry, or both. In fact we compute with matrices so large that shared and distributed parallelism is a necessity. We develop and outline a multi-tiered parallel solution to computing the ranks of matrices peta-scale in storage requirement. We explore and learn from some of the failures encountered along the way. This completed work shows large performance gains over the previous state of the art, and has achieved results that encourage pushing the algorithm to ever-larger problems.

Chapter 4 discusses an entirely new topic under the wide umbrella of exact computational algebra, that of rational linear system solving. In this chapter we employ

the aforementioned approximate numeric arithmetic within the confines of an exact-answer algorithm in a hybrid solution known as a numeric-symbolic method. The idea behind the marriage of numeric and symbolic computing is to exploit the gigaFLOPS of power found in current floating-point units while still producing exact results. This can prove advantageous over either using software extensions for representing large integers, or resorting to finite field methods, two common symbolic techniques. We offer a novel method of detecting overlap between successive numeric computations, which we call the confirmed-continuation method. This key improvement helps a pre-existing algorithm achieve improved performance and increased stability for solving rational linear systems, a key solution offered by LINBOX.

Chapter 2

FINITE FIELD DATA COMPRESSION

2.1 Introduction

Let \mathbb{F}_p denote the finite field of size p . The field elements are $0 \dots p - 1$ with arithmetic modulo the prime p . Small finite field elements can be represented by many fewer bits than are in a typical machine word. In this chapter let r be the number of bits required to represent each element in a field. \mathbb{F}_p elements require $r = \lceil \log_2 p \rceil$ bits to fully represent. For instance \mathbb{F}_5 requires $r = 3$, e.g. $0 = 000_2, 1 = 001_2, 2 = 010_2, 3 = 011_2, 4 = 100_2$.

“Machine word” refers to the fixed-size number of bits that a given computer architecture uses as its computational unit. In this chapter let l be the bit-length of a machine word. Modern general purpose computers commonly have $l = 32$ or 64 bits. Thus special compression for in-memory storage of small finite-field elements can be used, appreciably decreasing both data-storage space requirements and common kernel running times. The space-efficiency is of course an inherent property of our data compression, while the running time efficiency follows from being able to perform arithmetic operations on multiple elements simultaneously. This scheme is a form of Single Instruction, Multiple Data (SIMD) Parallelism as defined in Flynn’s taxonomy of parallel architectures [2]. Typically, the SIMD designation would refer to an architecture specifically designed for performing instructions on multiple words simultaneously. While of course our methodology does not preclude the use of such SIMD-capable hardware, it achieves the end of the SIMD-parallelism model from within basic machine words. In other words, though specialized hardware would certainly still prove beneficial, the benefits of our improved data representation can be seen on general-purpose hardware

as well. Specifically, we employ variations on two compression schemes, bit-packing and bit-slicing, each with different strengths and weaknesses.

Before these schemes can be illustrated in depth, first we must establish a language for discussing finite-field compression. First let f_x represent the *space-efficiency factor* of a compression scheme, x , over the naive storage method of word-per-element. The values of x used will be b for “basic bit-packing”, p for “bit-packing” and s for “bit-slicing”. That is, f_x describes the number of field elements representable with a single machine word, since the elements-per-word in the naive scheme is always 1.

2.1.1 Prior work

Modern high-level languages and machinery replete with memory have both served to limit the need to resort to bit-fiddling. But the concept of storing separate but related values within singular inherent types has been well-explored. An early instance of packing single bits into larger inherent types is the implementation of “bit-fields” in the C Programming Language [3]. Later the C++ Standard Template Library [4] would extend this concept to store arbitrary-length bit vectors with its “bitset” object. Although these examples are primarily aimed at saving storage space, programmers have exploited the SIMD nature of computing with word-compressed data. Boothby and Bradshaw [5] detail some history with classical bit-packing methods, and introduce the concept and key features of bit-slicing for small prime fields. Albrecht, Bard, and Hart [6] have implemented bit-packing/bit-slicing for \mathbb{F}_2 in the M4RI software [7]. The combination of their thorough exposition and optimized implementation has been highly influential on our development of the \mathbb{F}_3 compression technologies detailed here.

2.2 Bit-packing

Bit-packing involves marshalling field elements to fit alongside one another within a single machine word. Using the defined values l and r from Section 2.1, we can immediately calculate the *basic* bit-packing factor, $f_b = \lfloor \frac{l}{r} \rfloor$. If data storage

were the only concern, this would be sufficient, but almost always we desire to perform arithmetic operations on the compressed data. We must account for potential bit-overflow during, say, addition or multiplication. Therefore we allocate a bit buffer to catch this bit-overflow and let b refer to its bit-length. For general bit-packing, b is adjustable and negotiable to best serve a given application's needs. Thus, $r + b$ denotes the number of bits available to store each packed field element. Then the *bit-packing factor* is $f_p = \lfloor \frac{l}{r+b} \rfloor$. For instance, consider packing \mathbb{F}_3 values into sixty-four bit words and allocating a single bit for carries, i.e. $b = 1$. Using the formula above, $r = 2$ for \mathbb{F}_3 . So the compression factor $f_p = \lfloor \frac{64}{2+1} \rfloor = 21$. The preceding can be visualized with the aid of Figure 2.1, including the role of values l , r , and b .

Insertion of values into packed form is accomplished with two bit-operations per element to be stored: a bitwise OR to incorporate the value and a bit-shift to adjust each value to its correct slot within the larger word. Of course, employing bit-packing means that accessing individual elements is costly, but such action is typically unnecessary. We value performing operations in bulk on many elements over accessing elements directly. The marshalling of data to achieve bit-packing is seen in Algorithm 1.

Algorithm 1 Marshalling finite field element data to enable bit-packing. Input bit-packed data *packedvector* gets filled with input array [*Field Elements*].

```

i ← 0 // counter
packedword ← packedvector[0] // pointer into storage

for e in [Field Elements] do
    *packedword ← *packedword | e // bitwise-OR in the element

    *packedword ≪ (r + b) // left-shift the element, making room for the next
    if i++ =  $f_p$  then
        i ← 0 // reset counter
        packedword++ // next storage
    end if
end for

```

Clearly the smaller b is, the more space-efficient the packing scheme is, i.e. f_p increases. The luxury of this space-efficiency of course comes at a cost. When

bit-packed value (1) bit-packed value (2) bit-packed value (0) $b = 1$ $r = 2$

0|010|001|000|010|010|001|000|010|001|000|001|000|000|001|000|010|001

$l = 64$

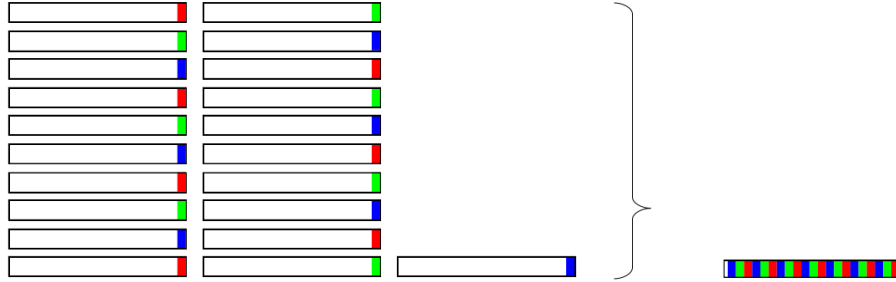


Figure 2.1: A closeup of a machine word utilizing bit-packing illustrating l , r , and b . This is followed by a broad view of the savings bit-packing affords. The rectangular outlines represent machine words while the shaded portions represent finite field data. The different colors representing individual field values are marshalled next to one another in the compressed form. One word is used to store what would take twenty-one without the compression.

the arithmetic-overflow buffers are full, performing further arithmetic could overflow them. This scenario is tantamount to the very problem the buffers are employed to ameliorate: data corruption. Once again, overflow destroys bit-packed data and individually packed values bleed together, rendering them meaningless. So, the trade-off of decreasing the buffer size b means having to normalize the data more frequently to avoid this overflow. Normalization is the act of clearing the overflow buffer while maintaining data integrity. A naive approach to normalization would be to unpack the values, perform a modular reduction on each value to rid the overflow, and re-pack the data into compressed form. Standard, one-value-per-word integer implementations using, say **int** or **long** data types, need not normalize until values would overflow the words. Since these primitive integer types on modern processors leave ample room for overflow, normalization is merely an afterthought.

However with bit-packing, proper normalization is no insignificant step. Repacking the data involves a bitwise-OR and a bit-shift left. Unpacking bit-packed

data is a matter of performing Algorithm 2, containing inverse operations to those in Algorithm 1. Each finite-field element is extracted from the packed vector via a bitwise-AND with an all-ones bit-mask, $2^{r+b} - 1$. Then the packed vector is bit-shifted to the right by $r + b$ in order to align the next field element for unpacking. Thus, rote normalization requires four bit operations per field element, in addition to some counters and loop bookkeeping in the typical case of having more than one packed-word full of data. Between all this, each value must be normalized to clear the overflow buffer. In the case of prime finite fields, which is the primary focus of our work, normalization is accomplished via modular reduction, which is generally slow (as described in [8]). In summary, the process of fully normalizing values in this manner is computationally costly and steps should be taken to limit its need.

Algorithm 2 Extracting finite field element data from a bit-packed representation. *values* gets filled with the data stored in input *packedvector*.

```

values ← [ ]           // array to hold field elements
mask ← 2r+b - 1      // bit-mask to extract packed values

for packedword in [packedvector] do
  for i in [fp..0] do
    // extraction/insertion into vector
    e ← packedword ≫ ((r + b) × i) & mask
    values.append(e % F)
  end for
end for

```

How can we choose the most advantageous value for b ? Let \mathcal{B} be the set of legal values for b . Here, legal means a buffer size sufficiently large enough to hold the information from a single application of any possible field arithmetic without overflowing. For the field \mathbb{F}_p , $\mathbf{min}(\mathcal{B}) = \mathbf{bitlength}((p-1)^2) - r$. That is the number of bits needed to represent the square of the largest field element unnormalized less the number of bits needed to represent that element normalized. Obviously setting $b = \mathbf{min}(\mathcal{B})$ results in the most space-efficient packing scheme. But it turns out that the most runtime-efficient value for b varies based on the field. A balance must be found between small

values for b which require more frequent normalization and the loose, SIMD-inefficient packing for large b values. This can be accomplished with a simple experiment on a given computational platform. Run a series of repeatably random vector multiplication/additions (or mul-adds, or *axpy* in LINBOX parlance) for each buffer size and find the fastest runtime. The curves in Figure 2.2 illustrate this approach, with the maxima of the charted lines indicating best packing width. Table 2.1 summarizes the data for some small-prime fields. All experimental data reported in this chapter was collected using a single-thread of execution on an AMD Opteron 6164 HE Processor clocked to 1700 MHz. Codes were compiled by the GNU Compiler Collection’s (GCC) `g++`, using the `-O3` optimization level. One interesting note is that GCC was not able to automatically vectorize the codes to make use of wide registers and SIMD instruction sets on modern processors. Analysis of compiler debugging output suggests the relevant arithmetic loops are too deeply nested and consist of too many control-flow structures to intelligently auto-vectorize. The deep level of specialization inherent in our small-prime finite field arithmetic helps explain this complication. With few field values that can serve as input, branching is worthwhile as it can save having to multiply an entire structure by, say, zero or one. Still, manual vectorization is possible, and would indeed be quite worthwhile. Such a step would extend by a small factor the benefits we already enjoy by compressing data into a single machine word.

It is worth noticing from Table 2.1 that the b column firmly correlates with the p_f column, given change in the r column. Both four-bit primes do best with eight bits of overflow, providing five values per word. Out of the five bit primes, all but the smallest devote eleven bits to the overflow, totalling sixteen bits for the packing and a neat four values per word. In this case, there are no unused bits being wasted, as $16|64$. The smallest five-bit prime field, \mathbb{F}_{17} , can do with only seven bits devoted to an overflow buffer, as working with the smaller values means normalization is less frequent at this packing factor. Note also the correlation between p_f and performance. Quite evidently, the general trend is that performance dips as we pack less tightly. But even between prime fields with the same best- p_f , performance slightly dips as the fields

Table 2.1: Best bit-packing for small prime fields of interest. Optimal choice for b is displayed along with the speedup of the vector mul-add (axy) operation. The p_f column assumes sixty-four bit words. Measured and reported is relative performance, or how many times faster bit-packing is than the same operations using an unpacked representation.

Field	r	b	p_f	axy Speedup
\mathbb{F}_3	2	6	8	40.4
\mathbb{F}_5	3	6	7	26.71
\mathbb{F}_7	3	7	6	21.16
\mathbb{F}_{11}	4	8	5	17.23
\mathbb{F}_{13}	4	8	5	16.74
\mathbb{F}_{17}	5	7	5	15.11
\mathbb{F}_{19}	5	11	4	14.19
\mathbb{F}_{23}	5	11	4	14.1
\mathbb{F}_{29}	5	11	4	13.97
\mathbb{F}_{31}	5	11	4	13.88
\mathbb{F}_{127}	7	14	3	10.56

get larger; more frequent normalization is required of the larger values resultant from arithmetic. For example, note the small performance degradation between bit-packing for \mathbb{F}_{19} and \mathbb{F}_{31} , despite both being packed four-per-word.

Figure 2.2 demonstrates the dual benefits of bit-packing. Each chart is organized left-to-right from tighter to looser packings. Memory footprint is diminished considerably with the tighter packings, as evidenced by the smaller bars toward the left of the x-axes. Performance of vector operations, as depicted by the lines, is improved by at least an order of magnitude. Each component is normalized against LINBOX’s **plain-domain**, the data-agnostic, and currently best, implementation for finite-field matrix operations in LINBOX. The reduction of storage space is a constant. The relative performance is a ratio of the running-times for 10^9 compressed to uncompressed, but otherwise identical, finite-field operations. The computation is highly regular; over hundreds of repetitions of the experiment, the variance between the ratios is less than 10^{-5} .

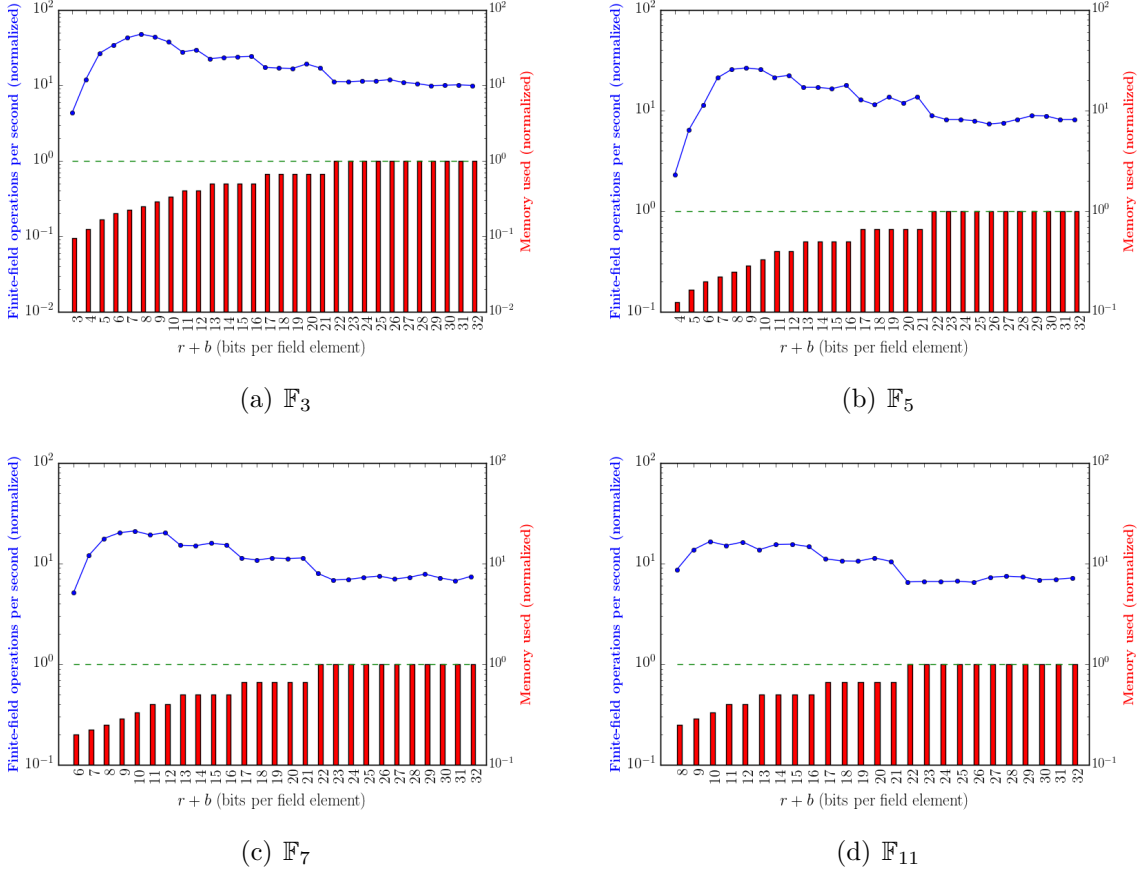


Figure 2.2: Performance and space gains using vanilla bit-packing for the vector *axpy* operation (multiply/add) over small prime fields. The x-axis charts the number of bits ($r + b$) used to store each element in the packed representation. Normalized running time performance is denoted by the line, measuring finite field operations per second (thus higher is faster/better). Normalized memory usage is denoted by the bar (thus lower is smaller/better). In both cases, the line $y = 10^0$ (1) is the measuring stick, representing the {performance, size} of the standard uncompressed representation.

2.2.1 Faster bit-packing

For \mathbb{F}_3 , $b = 1$ would be ideal from the SIMD point of view; fewer bits allotted for overflow means more bits per word devoted to data we care about, and thus a higher degree of inherent SIMD parallelism. However using a one-bit overflow buffer, normalization would have to be performed after each element-wise addition or multiplication, as each of these arithmetic operations has potential for bit-overflow. Therefore performing two consecutive operations would potentially overflow the buffer. Such a runtime-costly burden, that of normalization, works against or even fully negates the benefits of compressing finite-field data in the first place.

To overcome the obstacle of frequent normalization while using small arithmetic buffers is the innovation of *semi-normalization* [9]. Over \mathbb{F}_3 with $b = 1$, this technique clears out the highest-order, buffer bit of each bit-packed finite field value whilst maintaining data integrity, all without performing the tedious unpack-mod-pack routine outlined above. With the “buffer bit” off, values can be doubled or added together safely. Thus, arithmetic performed during a linear algebra routine can continue unfettered by the aforementioned costly naive normalization. *Semi-normalization* requires exactly four bit operations— not per element, but per machine word (or f_p elements). Essentially, the overflow bit is isolated with a bit-mask, right-shifted, and added back into the lower-order two bits (which were isolated with a bit-mask themselves). These operations on the seven possible *semi-normalized* values in \mathbb{F}_3 are illustrated by the flowchart in Figure 2.3.

Note that the bit-sequence $111_2 = 7$ is omitted from the flowchart. This sequence is in fact impossible to obtain under this scheme, because the largest *semi-normalized* value is $(011_2 = 3)$. We restrict multiplication to seminormalized \times normalized values only. Through arithmetic operations, the *semi-normalized* value can only ever be doubled, either by way of addition with itself or multiplication by two, the largest \mathbb{F}_3 element. *Semi-normalization* being performed after each operation means $110_2 = 6$ is the largest bit triplet obtainable. This is a relief, as attempting the *semi-normal* algorithm on $111_2 = 7$ would result in the bit-sequence $100_2 = 4$. A second

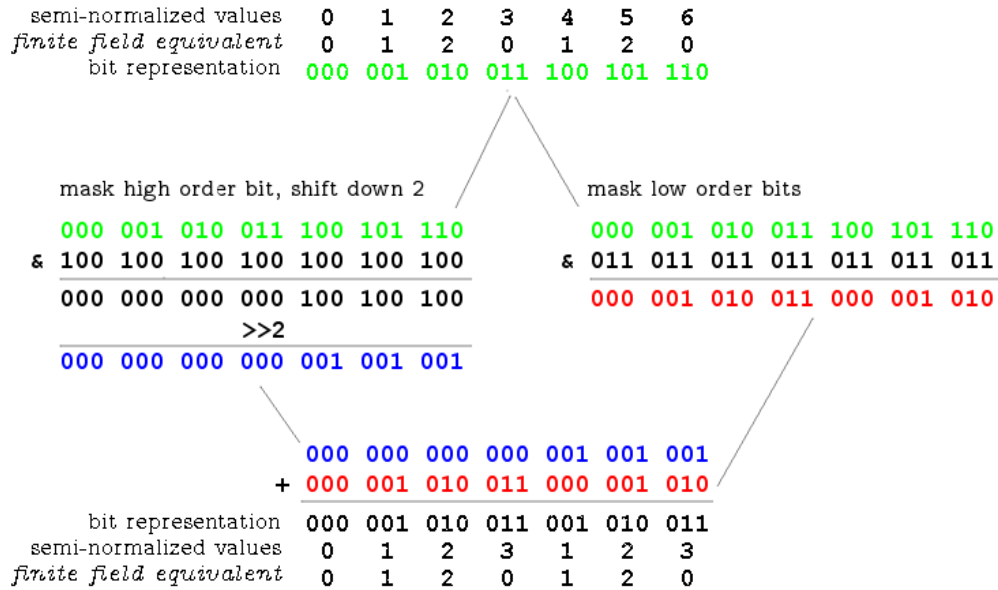


Figure 2.3: Flowchart depicting the four bit operations needed for *semi-normalization* for bit-packed \mathbb{F}_3 . The seven possible 3-bit sequences that exist whilst using *semi-normalization* ($000_2 \dots 110_2$) are detailed. Note that the \mathbb{F}_3 value of each triplet of bits maintains its integrity over this field by the end of the routine. At finish, the highest order bit in each set is shown to be off, which is the central concept that allows for further arithmetic on the packed values.

semi-normalization would be required to switch off the high-order bit in this case. This second step would otherwise be required after every arithmetic operation, so not having to perform it is a performance boon.

When true field values are called for, *semi-normalized* \mathbb{F}_3 values can be fully normalized by converting all of the threes, the highest possible semi-normalized value, to zeros. This operation can be done using nine bit operations per 64-bit word, in similar fashion to the core *semi-normalization* routine. This is demonstrated in Algorithm 3. Though retrieving fully-normalized, pure field elements is generally infrequently necessary (for instance, only upon an algorithm’s completion), nine bit-operations is significantly computationally faster than the naive unpack-and-mod approach given in Algorithms 1 and 2. This tandem of specialized normalization techniques ensures the run-time savings is commensurate with the memory-space savings that bitpacking offers over uncompressed finite field storage.

Algorithm 3 Converting *semi-normalized* values to \mathbb{F}_3 representation. Input bit-packed word w gets fully normalized.

```

word ones, twos, both           // helper words
ones ← w & 111...18           // mask for lowest-order bit in each triplet
twos ← w & 222...28           // mask for middle bit in each triplet

// check for both bits on
both ← (twos & ones ≪ 1) | (ones & twos ≫ 1)

w ← w & ~both                   // zero out both bits if they are on

```

2.2.2 Extending to other prime fields

Recall the terms from Section 2.2: r , the number of bits needed to store a value, l , the length of a machine word, and b , the number of bits needed for arithmetic carries. The key to *semi-normalization* in the case of \mathbb{F}_3 values being packed into two-bits each is the arithmetic carry $((r + 1)^{th} = 3^{rd})$ bit being equivalent to the “unit” bit mod 3. In short, the third bit represents $2^2 = 4 \equiv 1 \pmod{3}$. Similarly, the ability to quickly *semi-normalize* can be easily generalized over fields \mathbb{F}_p where p is an r -bit Mersenne

prime (i.e. $p = 2^r - 1$). For these \mathbb{F}_p , every r^{th} bit is a “unit” bit mod p . Therefore if your values are packed into r bits and then you perform arithmetic on the packed values, the overflow itself acts as an additive component of the new value.

How many bits-per-value must we earmark for overflow? As shown, *semi-normalized* \mathbb{F}_3 can get away with just a single bit for arithmetic carry. In general we may wish to multiply our *semi-normalized* representations, which use r bits. Thus, a further r bits are necessary to store the product (i.e. set $b = r$). All told, $2r$ bits are required to store each packed value. Therefore to utilize SIMD bit-packing at all, it is necessary that $r \leq \frac{l}{4}$.

This means we can specialize standard bit-packing using 64-bit words for the following list of Mersenne prime fields: $\mathbb{F}_3, \mathbb{F}_7, \mathbb{F}_{31}, \mathbb{F}_{127}, \mathbb{F}_{8191}$. The *semi-normalization* process in the general case is similar to what is done over \mathbb{F}_3 , only r high-order bits are isolated and accumulated into the r low-order “value” bits, instead of just the single carry bit. Unlike as demonstrated for \mathbb{F}_3 in Figure 2.3, a single iteration of the *semi-normal* subroutine may not be enough to clear the high-order “carry” bits to be all zeroes. Performing this process once is sufficient following any addition operation, but following a multiplication it is possible that this action would again overflow the “value” bits. However we are in luck, the *semi-normalization* operation is idempotent, and can simply be applied once more, to assuredly clear the b high-order “carry” bits. All of this sums to eight bit-operations per machine-word of packed values, as each iteration of *semi-normalization* still requires four bit-operations.

The isolation of the high- and low- order bits is accomplished with yet another bit-mask. By way of example, in the case of \mathbb{F}_7 we can mask the three high-order “carry” bits out of the six-bits-per-element with a mask of 70_8 . We start with these six bits and repeat them—going right-to-left—to arrive at a 64-length bit-mask of 7070707070707070_8 . For completeness, the low order bits are masked with an inverse mask 0707070707070707_8 . The general *semi-normalization* algorithm is outlined in Algorithm 4. These masks will be referred to in the pseudocode as `MASK_HI` and `MASK_LO`, respectively.

Algorithm 4 General *semi-normalization* for bitpacking Mersenne-prime fields. Input bit-packed word w containing r -bit prime field elements gets *semi-normalized*.

```

word highs                                // helper word

// do this twice
for i in 1..2 do
    highs ← w & MASK_HI                    // overflow bit-mask
    w ← w & MASK_LO                        // zero out overflow bits
    w ← w + (highs ≫ r)                   // add in overflow to data
end for

```

This is all well and good, but we can actually go one step further. It turns out that Mersenne prime fields do not have a strict monopoly on the ability to *semi-normalize* effectively. The sufficient condition is that the prime p for a field \mathbb{F}_p divides a number one less than a power of two. This fact enables an especially efficient bit-packing representation for \mathbb{F}_5 , as 5|15. Setting r and b to four for this field means again that the overflow bits can be added back into the base bits to maintain the field values. This works because the fifth bit represents $2^5 = 16 \equiv 1 \pmod{5}$. Note that this is a less efficient packing than is used for the larger field \mathbb{F}_7 , eight bits to six, but such is the price we pay for 5 not being a Mersenne prime. Table 2.2 demonstrates the performance gains earned by the use of *semi-normalization* in certain prime fields over “dumb” bit-packing. Note that the Mersenne prime fields (e.g. \mathbb{F}_7 , \mathbb{F}_{31} , \mathbb{F}_{127}) enjoy more of a performance boost than their counterparts (e.g. \mathbb{F}_5 and \mathbb{F}_{17}). These other fields nevertheless consistently display performance improvement when eschewing “slow” normalization for the more streamlined *semi-normalization*. Additional small prime fields which qualify for *semi-normalization* include $\mathbb{F}_{73}(73|511)$, $\mathbb{F}_{89}(89|1023)$, $\mathbb{F}_{151}(151|32767)$, and $\mathbb{F}_{257}(257|65535)$.

While extending r in order to manufacture *semi-normalization* for some prime fields showed performance benefits, it is worth mentioning another technique that did not prove beneficial. The thought was to devote (the minimum) three bits to represent \mathbb{F}_5 values with three additional bits for overflow. The overflow then begins with the

Normalized performance and memory of compressed forms

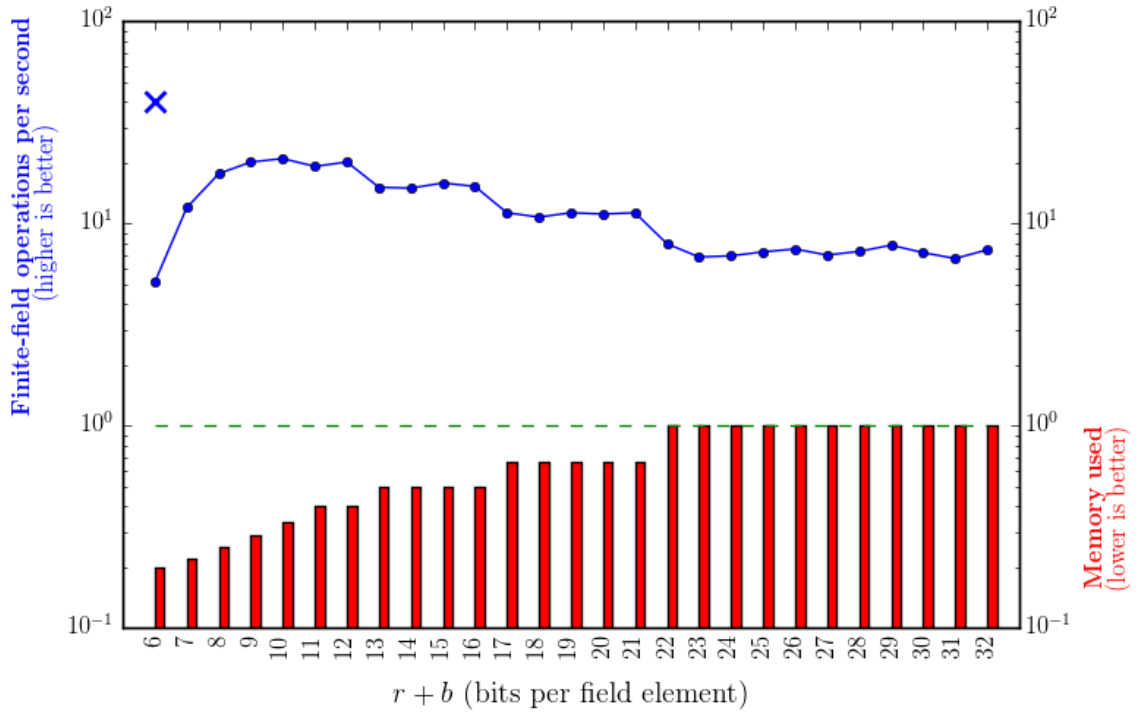


Figure 2.4: Figure 2.2(c), detailing bit-packing for \mathbb{F}_7 , updated with a data point (denoted by \times) where *semi-normalization* is employed. The best of all worlds is achieved: faster than the fastest bit-packed time (line) paired with the smallest possible memory usage (bars).

Table 2.2: *Semi-normalized* bit-packing performance improvements, measured against the fastest-running vanilla bit-packing. The p_f column assumes sixty-four bit words. Measured and reported is relative performance, or how many times faster *semi-normalized* packing is than the same operations using the *most efficient* choice for b with basic bit-packing.

Field	r	b	p_f	<i>axpy</i> Speedup
\mathbb{F}_3	2	1	21	2.21
\mathbb{F}_5	4	4	8	1.05
\mathbb{F}_7	3	3	10	1.58
\mathbb{F}_{17}	8	8	4	1.04
\mathbb{F}_{31}	5	5	6	1.7
\mathbb{F}_{127}	8	8	4	1.51

fourth bit. Bit indices are zero-based, so the fourth bit is equivalent to $2^3 = 8 \equiv 3 \pmod{5}$. Thus, to get *semi-normalization* out of this structure, one would have to mask, shift, then add *three times* the overflow component into the original component. Call this routine *SN3*. *SN3* can be achieved through bit operations alone by first adding in the overflow shifted to the right by three bits (standard *semi-normalization*, this is adding in *one times* the overflow), then adding in the overflow shifted two bits to the right (this is adding in an additional *two times* the overflow). This uses six bit-operations: the four from basic *semi-normalization* combined with a second shift/addition pair. This kernel indeed maintains data integrity over \mathbb{F}_5 , but it does not rid the overflow bits quickly enough. Figure 2.5 contains a disjoint tree with the root nodes representing clean *semi-normalized* values, i.e. those with empty overflow bits. All non-root nodes are possible arithmetic outcomes of \mathbb{F}_5 data in this representation. The parent/child relationships, or edges, indicate output/input of the *SN3* routine, respectively.

Neither 0, 1, nor 2 are present as root nodes in the tree because they actually have no children. It is easy to understand why: *SN3*'s minimum output is 3. The important takeaway from the tree is the maximum depth being three. This depth is equivalent to the worst-case number of applications of the idempotent *SN3* routine

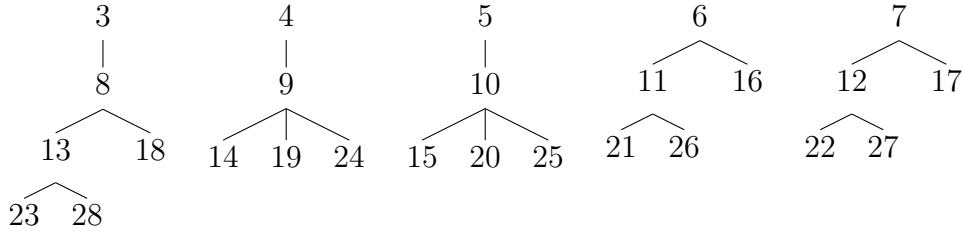


Figure 2.5: The flow of a series of *SN3* operations.

needed to clear the overflow bits after any arithmetic operation. That amounts to eighteen bit-operations, a far cry from the mere four that makes vanilla *semi-normalization* such an estimable performer. In fact, basic experiments show that employing *SN3* runs 2.1 times slower than the best (nine bits-per-value) vanilla bit-packing scheme per Table 2.1 and 2.25 times slower than the specialized eight bits-per-value *semi-normalized* scheme from Table 2.2. The slowdown is despite operating at an optimal six bits-per-value. The conclusion here is that excessive bit operations of *SN3* definitively override the benefits of the tighter packing it affords.

2.3 Bit-slicing

A better scheme for very small finite fields is known as bit-slicing. Here, the few bits used to represent field elements are striped across parallel machine words, as shown in Figure 2.6. The set of separate but logically connected words that holds bit-sliced finite field data is called a *sliced unit*. These stripings can then be marshaled next to one another in machine words, achieving compression in the same manner as bit-packing. A key improvement here is the elimination of any arithmetic buffer ($b = 0$). Each and every bit used in bit-slicing is devoted to data storage. This fact makes the slicing compression factor very clean, $f_s = \frac{l}{r}$. Also notice that the floor function is not needed in calculating the compression factor. With bit-slicing there will never be unused high-order bits because single bits are “packed” together into machine words. Taking the view from a single word (one half of a *sliced unit*), bit-slicing is essentially bit-packing with $r = 1$, which will quite evenly divide any word size. Thus, machine

$$r = 2 \left\{ \begin{array}{ccc} \text{bit-sliced value (0)} & \text{bit-sliced value (1)} & \text{bit-sliced value (2)} \\ 01101010000110110100100010101010101010100000101011111010111 & & \\ 010010100010011000010000000010001010101000000101010101011000 & & \end{array} \right.$$

$l = 64$

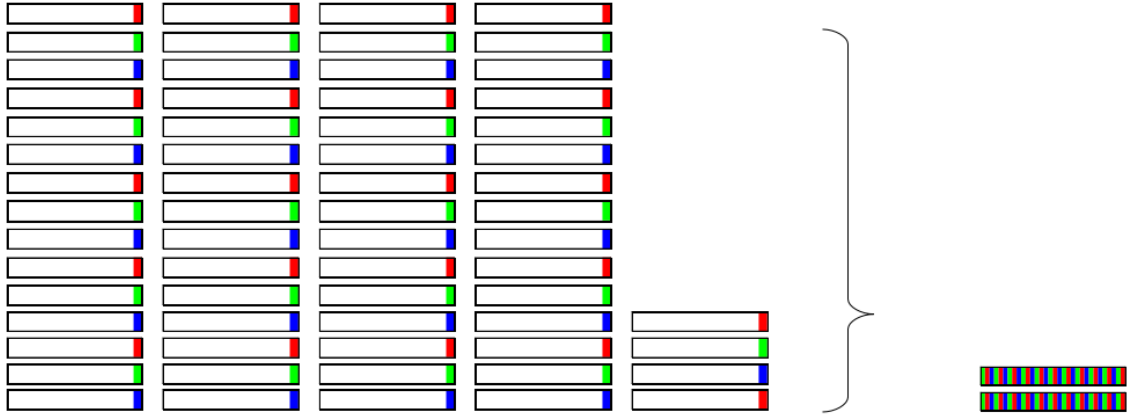


Figure 2.6: A closeup of two machine words utilizing bit-slicing to store \mathbb{F}_3 values. We call this pair of words a *sliced unit*. This is followed by a broad view of the savings bit-slicing affords. The rectangular outlines represent machine words while the shaded portions represent finite field data. Notice that the colors, representing individual finite field values, are striped in parallel fashion between the two bit-sliced words. Two words are used to store what would take sixty-four without the compression.

words comprising vectors of bit-sliced data can always be filled out completely. This is in contrast to bit-packing, where high-order bits remain unused when $(r + b) \nmid l$.

Algorithm 5 demonstrates the insertion of a finite field value into a bit-sliced vector. Once again we notice that converting uncompressed data to our specialized representation is computationally costly. And once again we assert that there is plenty of value in the scheme despite this stipulation. The benefits of performing arithmetic in bulk with the compressed representation vastly outweigh the costs in arriving at the compression. Insertion of a value into sliced form is accomplished by pinpointing

Algorithm 5 Bit-slice a finite field element. Input \mathbb{F}_3 element e gets inserted into the i^{th} position of bit-sliced vector V (i.e., an array of *sliced units*). To be consistent, l is the length in bits of a machine word.

```

// first slice the bits of input
unit  $\leftarrow \lfloor i/l \rfloor$  // sliced unit's index within  $V$ 
index  $\leftarrow i \% l$  // element's index within unit
word b0, b1 // helper machine words
b1  $\leftarrow (e \& 2) \gg 1$  // isolate  $2^1$  bit
b0  $\leftarrow (e \& 1)$  // isolate  $2^0$  bit
// now incorporate value into vector
V[unit].b0  $\leftarrow V[\text{unit}].b0 \& \sim(1 \ll \text{index})$  // zero out place for value in first word

V[unit].b1  $\leftarrow V[\text{unit}].b1 \& \sim(1 \ll \text{index})$  // zero out place for value in second word

V[unit].b0  $\leftarrow V[\text{unit}].b0 | (b0 \ll \text{index})$  // bitwise-OR in the data

V[unit].b1  $\leftarrow V[\text{unit}].b1 | (b1 \ll \text{index})$ 

```

exactly where in the sliced vector the value belongs. This slot is zeroed out via bitwise-AND with a negative bit-mask to both words in the *sliced unit* (here called $b0$ and $b1$). The entire routine would for instance be found within a function called `setEntry()`, which is a canonical method in LINBOX to initialize a data structure.

Extracting bit-sliced data, should that be desired, involves the application of Algorithm 6. This is essentially the inverse of Algorithm 5. It is a simpler routine in that the formation of a bit-mask specific to the value in question is not needed. We simply shift the words comprising the appropriate *sliced unit* such that the bits we care about are lowest-order. Then, our bit-mask is reliable old 1. The two lower order bits can be added together because of the special two's complement representation. ($2 \equiv -1$ is represented by the bit-sequence 11 instead of 10). If both bits (in $b0$ and $b1$) are on, the value is 2. Otherwise, the value is dependent on the bit in $b0$. This routine would fit into LINBOX's common interface function `getEntry()`, which retrieves a scalar from a data structure for linear algebra.

Algorithm 6 Extracting finite field element data from a bit-sliced representation. Output \mathbb{F}_3 element e gets the i^{th} value in bit-sliced vector V .

```

unit ←  $\lfloor i/l \rfloor$  // sliced unit's index within  $V$ 
index ←  $i \% l$  // element's index within unit
// perform extraction from both words in the proper unit
 $e \leftarrow (V[\text{word}].b1 \gg \text{index}) \& 1 + (V[\text{word}].b0 \gg \text{index}) \& 1$ 

```

2.3.1 Specialized arithmetic

Devoting no storage space for arithmetic overflow is quite convenient. Of course this makes storage more efficient, as every bit is devoted to the data itself. On top of that the burdensome normalization required by bit-packing is rendered entirely unnecessary. It seems too good to be true; just how is this accomplished? Well, the large caveat here is that specialized arithmetic is required on a per-field basis— an arithmetic engineered from the ground up to avoid carries. This problem is equivalent to circuit minimization across a truth table of an r -variate Boolean function describing the mapping from binary inputs and outputs across an arithmetic operation. The size of the circuit is the number of bit-operations needed to perform the arithmetic. This problem is computationally NP-Indeterminate, and in practice quite difficult. Hence this scheme is only practical for very small prime fields where custom arithmetic can be worked out.

For instance, also given by [5], in \mathbb{F}_3 regular addition (Algorithm 7) requires only six bitwise operations per pair of words. This can be done using the following representation for \mathbb{F}_3 values: $0 = 00_2, 1 = 10_2, -1 = 11_2$. Negation (Algorithm 8), which is in this field is equivalent to multiplication by $2 \equiv -1$, requires only one bitwise operation. Trivially applying addition and negation, subtraction can be accomplished in seven bit operations. However, a different formula exists for subtraction in just six. Multiplication by $2 \equiv -1$ is the only non trivial multiplicand for this field; multiplication by zero simply empties the sliced words, and multiplication by one is a no-op. In Algorithms 7 and 8, the accessors “bit0” and “bit1” respectively refer to the words of the *sliced units* that hold the lower order bits (those switching 2^0 in the field element)

and the high order bits (those switching 2^1). Similarly clever games can be played with certain subsets of arithmetic in \mathbb{F}_5 , \mathbb{F}_7 , and some extension fields of small prime fields. Please see [5] for further discussion of bit-slicing for those fields, as they are not a focus of this thesis. The application contained in Chapter 3 concerns \mathbb{F}_3 bit-slicing, so this is the only field for which we implemented bit-slicing in LINBOX thus far.

Algorithm 7 \mathbb{F}_3 addition with bit-slicing. *sliced unit* $x \leftarrow left + right$. The example given demonstrates each of the nine possible pairwise additions in \mathbb{F}_3 .

```

a ← left.bit0 ⊕ right.bit1
b ← left.bit1 ⊕ right.bit0
s ← a ⊕ left.bit1
t ← b ⊕ right.bit1
x.bit0 ← s | t
x.bit1 ← a & b

```

A minimal example: ($left = 000\ 111\ 222_3$) + ($right = 012\ 012\ 012_3$).

```

left.bit0 = 000 111 111
left.bit1 = 000 000 111
right.bit0 = 011 011 011
right.bit1 = 001 001 001
a ← 001 110 110
b ← 011 011 100
s ← 001 110 001
t ← 010 010 101
x.bit0 ← 011 110 101
x.bit1 ← 001 010 100

```

Thus $x \leftarrow 012\ 120\ 201_3$.

Algorithm 8 \mathbb{F}_3 negation/multiplication by two. *sliced unit* $x \leftarrow x \times 2$

```

x.bit1 ← x.bit1 ⊕ x.bit0

```

An interesting case regarding finite field compression is that of \mathbb{F}_2 . The cardinality of this field is two, which by definition can be represented with a single bit. Clearly, as we have done for the general case, we can push multiple \mathbb{F}_2 bits together into

Normalized performance and memory of compressed forms

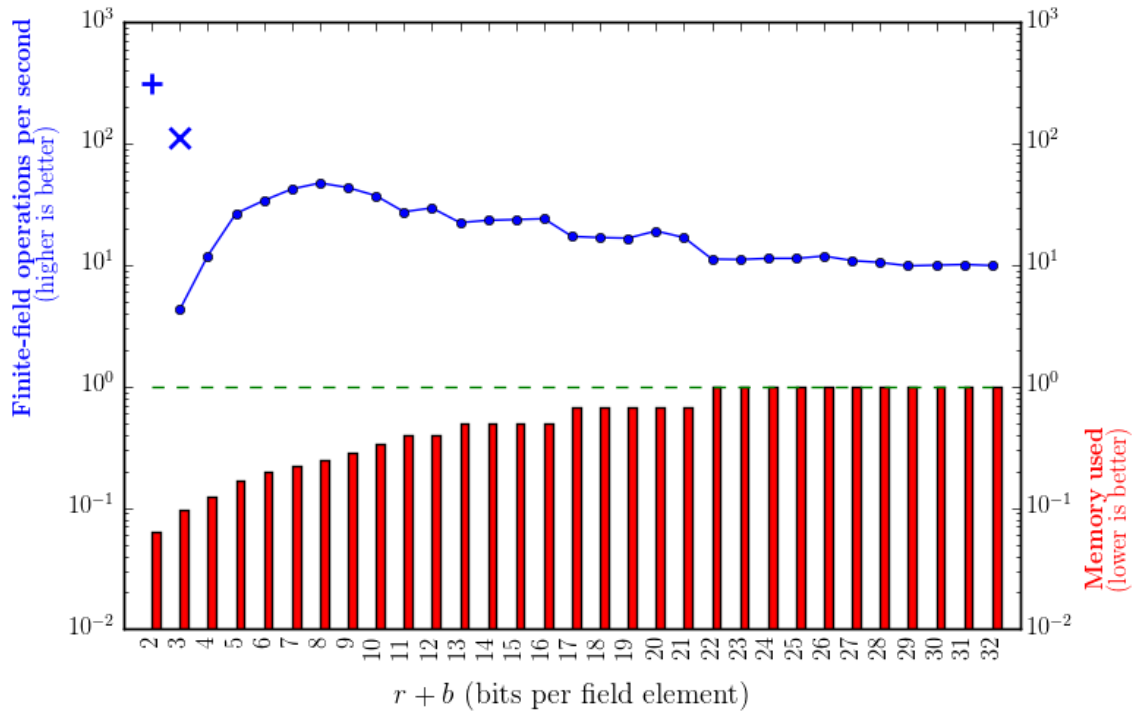


Figure 2.7: Figure 2.2(a), detailing \mathbb{F}_3 compression, updated with two data points: *semi-normalized* bit-packing denoted by \times and bit-slicing denoted by $+$. Bit-slicing being the optimal compression scheme for \mathbb{F}_3 is quite evident, as it more than doubles the performance of the best (*semi-normalized*) bit-packing. On top of this, it uses the optimal two bits per finite field element, so it is also the most efficient compression scheme from a memory/storage standpoint, using 6.25% of the memory of the naive approach.

single machine words. When we do this, we are in fact simultaneously achieving both bit-packing *and* bit-slicing! Adding two \mathbb{F}_2 *sliced units* is simple: bitwise-XOR them. Multiplying two \mathbb{F}_2 *sliced units* is equally simple: bitwise-AND them. Component-wise *sliced unit* multiplication is not something currently provided by \mathbb{F}_3 bit-slicing in LINBOX. \mathbb{F}_2 matrix-vector product is accomplished by word-wise bitwise-AND between matrix rows and vector, then an accumulation of these words with bitwise-XOR. The parity of the word resulting from this accumulation is the matrix-vector product for the given row. Sub-cubic matrix-matrix multiplication is possible as an extension of this method. Also detailed by Albrecht, et al. [6] are other very fast matrix-matrix multiplication routines over \mathbb{F}_2 , Strassen-Winograd and the Method of Four Russians.

2.4 Summary

The most attractive attribute of bit-packing is its flexibility. Any field with the property $r \leq \frac{l}{4}$ for a given machine can utilize bit-packing. Bit-packing has memory savings and arithmetic efficiency built in; when you use it, your program runs faster and smaller. Additionally, some small prime fields can take advantage of the specialized *semi-normalized* variant to squeeze out even more runtime savings.

Bit-slicing however, is the clear-cut best compression scheme when compact, custom no-carry bit arithmetic can be worked out for the desired finite field. Therein lies the rub, but such is certainly the case for compressing \mathbb{F}_3 . \mathbb{F}_3 bit-slicing far outperforms even the formidable *semi-normalized* edition of \mathbb{F}_3 bit-packing. It also uses $\frac{2}{3}$ the data storage that even the tightest bit-packing needs. When computing with matrices or vectors containing entries over \mathbb{F}_3 , **always** use bit-slicing.

Figure 2.3 shows the relative merits of bit-packing and bit-slicing using a special metric, called MegaFFops. This is shorthand for “millions of finite field operations per second”. Performance is provided for the three major arithmetic kernels: vector addition, vector scalar multiply, and their combination (vector *axpy*).

We might initially expect operations using packing or slicing to run 21 or 32 times faster than their non-compressed counterparts, respectively. However, we notice

Table 2.3: Speed of vector operations over \mathbb{F}_3 , using elements that are a) stored as floats and using BLAS, b) stored as ints, c) packed, and d) sliced. Timings of arithmetic were done on random vectors of length 10^7 .

\mathbb{F}_3 Arithmetic Comparison (MegaFFops)				
Operation	float	int	packed	sliced
add $x + y$	120.65	165.9	4492	6100
scalar mul αx	81.15	136.5	21008	65112
axpy $\alpha x + y$	77.96	98.46	6165	8806

improvement much better than that in the experiment of adding two vectors. Multiplying a vector by a random scalar from the field is an even more impressive win for the bit-packed and bit-sliced representations. Here we may be seeing memory hierarchy benefits from compressing to a smaller memory footprint. Also helping is the high level of specialization our compression schemes provide that the other implementations lack. With bit-packing we use only a single bit shift to accomplish multiplication by two, followed by semi-normalization. With bit-slicing we again employ a single bit-operation with no need for normalization. Axy runs slightly faster than addition. This is an encouraging sign, considering addition is part of axpy. The ground gained on addition is explained by the third of the time where the random multiplication scalar is zero and no addition is necessary.

In conclusion, the suite of bit-packing and bit-slicing greatly improves efficiency of arithmetic in small prime finite fields. Having faster arithmetic in these fields benefits many of the kernels in LINBOX. For example Dumas and Villard highlight many applications for exact computation using small finite fields in [10]. The applications listed there, including factoring large integers, computing Smith form, and homology all stand to improve with the new compressions. In Chapter 3 we will discuss a specific problem that has certainly benefited, if not outright relied upon, bit-slicing for \mathbb{F}_3 .

Chapter 3

STRONGLY REGULAR GRAPH 3-RANKS

3.1 Introduction

Matrix rank has been perhaps the most widely used exact linear algebra computation to date. It has often been the goal of computations requested by users of the LINBOX software library for exact linear algebra computations over the integers and over finite fields. Besides being of interest itself in numerous applications, rank plays an important role in solving singular systems and computing invariants. For example the rank is used in solving large sparse linear systems [11] computing homology groups [12], and in computation of Gröbner bases [13].

The goal for this chapter is to compute the ranks in a sequence of adjacency matrices of strongly regular graphs as defined by Dickson and detailed by Xiang et al. in [14]. We will refer to the matrices in the Dickson graph sequence as $D(p, e) : e \in \mathbb{N}$, where p is a prime number. Of specific interest to us is $p = 3$, where the matrices consist of entries over \mathbb{F}_3 . The 3-rank is sought, meaning all arithmetic is also done over \mathbb{F}_3 . The rank of $D(3, e)$ has been previously computed for $e \in 1 \dots 6$, e.g. in [15, 16, 14]. More recently we obtained the rank of $D(3, 7)$ [9], which evinced a conjecture that the rank of $D(3, 8)$ could help confirm. The difficulty in computing the 3-ranks for $D(3, 7)$ and $D(3, 8)$ stems from the sheer volume of data these matrices contain. Each Dickson adjacency matrix is $p^{2e} \times p^{2e}$, however the ranks are considerably smaller, on the order of 2^{2e+1} . Thus, $D(3, 7)$ contains $(3^{14})^2 \approx 22.9$ tera-entries, but only a rank near $2^{15} \approx 32000$ is expected. Similarly $D(3, 8)$ contains $(3^{16})^2 \approx 1.85$ peta-entries, with expected rank near $2^{17} \approx 131000$. The small rank estimate nudges this problem into being practically solvable by current computing resources. The basic idea is to

losslessly compress the larger matrix into a roughly rank-sized block, on which to do final, classical rank computations. “Small” rank notwithstanding, this is enough data to present considerable challenges not just in computing the rank, but also in merely generating, representing, and storing the Dickson matrix itself.

This chapter will highlight these challenges, after beginning with the methodology of solving for the rank of $D(3, 7)$. Specialized bit-packing was used by the original computation [9], but bit-slicing has been the compression of choice for more recent duplicate computations. Construction for the Dickson family of matrices will be detailed. Following will be an exploration of techniques used in solving for the rank of $D(3, 8)$. A matrix decomposition strategy is required due to the volume of data stored in the matrix. Different data-decomposition strategies were attempted with varying degrees of success. Before detailing what ultimately worked, a failed attempt at solving the problem is outlined; often failures can be just as illuminating and worthy of discussion as successes.

Naturally given the decomposed nature of the matrix data, some well-known distributed and shared-memory parallel computing mechanisms were deployed to generate a compressed form of the matrix. Shared-memory parallelism was also used in the rank algorithm on this compressed form. Bit-slicing was employed throughout the computation, vastly improving arithmetic efficiency over \mathbb{F}_3 . Recall the infrastructure of bit-slicing instantly provides chip-level data parallelism. Finally, there is still room to expand; the methods presented here are both applicable to, and foundational for computing a suite of related problems. In this light, a discussion of potential directions for this strong base of work to grow is included.

In this chapter log is base 2.

3.1.1 Prior work

There are various well-studied approaches for computing the rank of a matrix. Singular value decomposition is a common approach on matrices containing real or complex numbers that is not applicable here due to the finite-field arithmetic needed.

Two common approaches are found in exact linear algebra: classical Gaussian elimination or LU -decomposition [17], and probabilistic blackbox methods, for example the Wiedemann approach [18, 19]. From a complexity point of view, for an $n \times n$ dense matrix of rank r , the rank may be computed in $O(rn^2)$ field operations and storage of n^2 field elements, using Gaussian elimination. Blackbox methods can be run in time $\mathcal{O}^\sim(rn^2)$, using $\mathcal{O}^\sim(n)$ storage. Here we use $\mathcal{O}^\sim()$ to mean we ignore log factors. In particular, for rank over a small field, this notation hides the necessity to work over an extension field of degree $O(\log(n) \log(1/\epsilon))$, where ϵ denotes the desired upper bound on the probability of failure of the Monte Carlo algorithm. This is in order to have sufficiently many elements for the random choices. Also the blackbox approach requires accessing each entry of the matrix $O(2r)$ times, which is costly for the too-large-to-store but entry-on-demand-by-formula matrices of our intended application. In the paper of May, Saunders, and Wan on this topic [15] several Monte Carlo algorithms that run in time $\mathcal{O}^\sim(rn^2)$ and require varying amounts of memory were reported and used on the Dickson matrices. The algorithm discussed in Section 3.2.1 improves the time complexity to $\mathcal{O}^\sim(n^2)$ and storage to $O(r^2)$ (beyond the requirement to access each matrix entry exactly once). Also given is a Monte Carlo certification algorithm that is useful for verifying rank after use of heuristics. It is simpler and of lower space and time costs than the certificates of prior work [15]. While the prior work done on this topic provided the basic structure for computing the ranks of the large Dickson matrices, the improvements that follow in this chapter have made the computation itself readily possible.

3.2 Obtaining rank($D(3, 7)$)

$D(3, 7)$ is understandably a challenge computationally in view of the fact that its storage would require over 22 terabytes at one byte per entry. Each entry of $D(3, 7)$ is determined by a straightforward but somewhat expensive formula involving arithmetic in \mathbb{F}_{37} . Fortunately, it is not necessary to work with the completely constructed matrix at one time. We have found it effective to work at any one time with about one billion

entries, roughly one part in 20,000 of the matrix. We gain efficiency of both space and time by employing either specialized \mathbb{F}_3 bit-packing or bit-slicing.

3.2.1 Space and time efficient p -Rank

For this section let A be an $n \times n$ matrix of rank r over a finite field K . If A is large and dense and yet the rank is small, how may we compute $\text{rank}(A)$ efficiently?

We present a method that is a Monte Carlo algorithm for large enough fields and runs in $\mathcal{O}(n^2 + r^3)$ time and using $O(r^2)$ space. This is essentially optimal when $r \in O(n^{2/3})$. Here “ $\mathcal{O}(\cdot)$ ” and “essentially” mean that we ignore log factors. Independently, a very similar observation concerning optimality of matrix operations in a low rank setting has been made by Kaltofen [20], who showed optimality of an algorithm for system solving for sufficiently over- or under-determined systems. We also give a Monte Carlo certificate that works for all fields, and is important to the 3-rank computation discussed in the following section. This uses random linear combinations of rows and columns, a projection technique that was also used for handling low rank matrices by Cooperman and Havas [21].

The main idea of our rank algorithm is to use butterfly preconditioners. We know that if B and C are butterfly matrices, then the matrix BAC has generic rank profile with high probability [22, 23]. *Generic rank profile* means the leading principal minors are nonzero up to the rank. A leading principal minor, order k , of a matrix order n is the leading $k \times k$ block, obtained by deleting the last $(n - k)$ rows and columns from the matrix. One could imagine trying to compute larger and larger leading principal minors until a zero minor is encountered. This is precisely one of the earlier methods [24, 22], but it requires too much time and space for our current problems. Let us set out to achieve a helpful leading submatrix with nonsingular leading principal minors by another means. We propose a sum of blocks, with each block preconditioned. Let b be the block size, a number to be discussed further. For now keep in mind that the

goal will be that b is slightly larger than the rank of the matrix. Consider

$$M = \sum_{i \in 0.. \frac{n}{b}} \sum_{j \in 0.. \frac{n}{b}} B_i A_{i,j} C_j,$$

where all terms are $b \times b$ matrices, $A_{i,j}$ being the block in the i -th row of blocks and j -th column of blocks in a partitioning of A into $b \times b$ blocks. This will create an advantage of small space and time requirement. Only one block of A is needed in memory at a time so the algorithm requires a block of A , a block for the partial sum, and whatever storage is required for the preconditioning blocks, the B_i and C_j . The runtime is evidently $O((\frac{n}{b})^2(b^2 + T(b)))$ field operations, where $(\frac{n}{b})^2$ counts the number of summands, the b^2 represents the cost of adding one block, and $T(b)$ is the cost of preconditioning (the operations to produce a product $B_i A_{i,j} C_j$). The memory cost is for storage of M (as a partial sum during the algorithm), and one block of A at any one time, so $O(b^2)$ for these entries. The storage cost is then $O(b^2 + (\frac{n}{b})S(b))$, where b^2 accounts for storing one block of A and (a partial sum of) M at any one time, with $2\frac{n}{b}$ preconditioning blocks (B_i and C_j) at space $S(b)$ each. It will turn out that $T(b)$ is $O(b^2 \log(b))$ and $S(b)$ is $O(b \log(b))$, because the preconditioners are butterfly matrices (discussed next). Then we have overall costs of $O(n^2 \log(b))$ time and $O(n \log(b))$ space for the construction of M . We can then efficiently compute the rank of $M \ll A$.

When b is a power of 2, a $b \times b$ *butterfly* matrix is a product of $\log(b)$ *stage* matrices each of which is a direct sum of $\frac{b}{2}$ two-by-two *switches*. The direct sums are organized so that in the i -th stage there is a switch for each pair of rows and columns whose indices, expressed in binary notation, differ only at the i^{th} bit.

Let us illustrate the butterfly matrix construction with the case $b = 8$. For example when $i = 2$, rows $5 = 101_2$ and $7 = 111_2$ are engaged by one switch at stage 2. Figure 3.1 demonstrates.

Each switch is determined by 4 components, $\alpha, \beta, \gamma, \delta$. These components represent a decision to transpose or not transpose two rows or columns (via the values $\alpha, \beta, \gamma, \delta = 0, 1, 1, 0$ or $1, 0, 0, 1$) when the stage multiplies a matrix from the left or

Figure 3.1: Butterfly construction for $b = 8$. There are $\log(8) = 3$ stage factors, each comprised of $\frac{8}{2} = 4$ two-by-two switches, denoted by $*$.

$$B = \begin{pmatrix} * & * & . & . & . & . & . & . \\ * & * & . & . & . & . & . & . \\ . & . & * & * & . & . & . & . \\ . & . & * & * & . & . & . & . \\ . & . & . & . & * & * & . & . \\ . & . & . & . & * & * & . & . \\ . & . & . & . & . & . & * & * \\ . & . & . & . & . & . & * & * \end{pmatrix} \times \begin{pmatrix} * & . & * & . & . & . & . & . \\ . & * & . & * & . & . & . & . \\ * & . & * & . & . & . & . & . \\ . & * & . & * & . & . & . & . \\ . & . & . & . & \alpha & . & \beta & . \\ . & . & . & . & . & . & * & * \\ . & . & . & . & \gamma & . & \delta & . \\ . & . & . & . & . & * & . & * \end{pmatrix} \times \begin{pmatrix} * & . & . & . & * & . & . & . \\ . & * & . & . & . & * & . & . \\ . & . & * & . & . & . & * & . \\ * & . & . & . & * & . & . & . \\ . & * & . & . & . & * & . & . \\ . & . & * & . & . & . & * & . \\ . & . & . & * & . & . & . & * \\ . & . & . & * & . & . & . & * \end{pmatrix}$$

right, respectively. We may expand the concept to allow any 4 values for $\alpha, \beta, \gamma, \delta$ (subject to nonzero determinant, $0 \neq \alpha\delta - \beta\gamma$), and the action is then a “scrambling” of rows or columns via linear combinations. The cost of application of a switch is

$$\begin{pmatrix} \alpha & \beta \\ \gamma & \delta \end{pmatrix} \times \begin{pmatrix} \text{col}_i \\ \text{col}_j \end{pmatrix} = \begin{pmatrix} \alpha \text{col}_i + \beta \text{col}_j \\ \gamma \text{col}_i + \delta \text{col}_j \end{pmatrix}.$$

is $O(b)$ field ops, hence a stage costs $O(b^2)$, and a full butterfly uses time $T(b) = O(b^2 \log(b))$ and space $S(b) = O(b \log(b))$.

With that thumbnail sketch of butterfly matrices, we move on now to their use in our preconditioners. Noting that

$$M = \sum_{i \in 0.. \frac{n}{b}} B_i M_i,$$

where

$$M_i = \sum_{j \in 0.. \frac{n}{b}} A_{i,j} C_j,$$

consider the construction of the right preconditioners in building M_i .

Our column preconditioning is to be applied to each block row A_i of A . The

argument applies to column operations performed on any matrix, so we simplify notation by referring to A rather than A_i . We have A partitioned into blocks of columns. The block size b should be no less than the rank. Later we will address how to find such a block size. Assume $b|n$ so that there are $\frac{n}{b}$ blocks of size b with $r < b$. If n is not a multiple of b , pad A with zero columns until this property is true.

We operate to achieve a matrix of the same rank whose leading r columns are independent. The argument style is the familiar one of considering the random preconditioners as random evaluations of correspondingly structured polynomial matrix preconditioners in which the random values have become independent variables. The first step of the argument is to show there exists an evaluation of the polynomial matrices with desired properties. The second step (via Zippel-Schwartz [25, 26]) is to show the desired property is to be expected when random values replace the variables.

The structure of our construction is *select-permute-sum*. Each preconditioning block is of the form $C_i = D_i U_i$, where D_i is diagonal and U_i is a butterfly, for $i \in 1..\frac{n}{b}$. The n diagonal entries and $(\frac{n}{b})(b \log(b))$ butterfly nonzero entries are distinct independent variables over K . In the existence-proving step of the argument we assign either 0 or 1 to each variable.

First, let us suppose we have identified r columns which are independent. This is possible and our columns will form a basis for the column space, since $r = \text{rank}(A)$. We multiply from the right by a diagonal matrix D which has 1's in in the diagonal positions corresponding to the desired columns and zeroes everywhere else. Then AD has the designated r columns the same as A 's and all other columns zero. View D as partitioned into diagonal blocks D_i which select those of the designated i columns lying in the i -th column block of A .

To illustrate, we may have selected thus (vertical bars used to separate blocks):

$$\left(\begin{array}{cccccc|cccccc|cccccc} 0 & * & 0 & 0 & 0 & 0 & * & * & 0 & 0 & 0 & * & 0 & * & 0 & 0 & 0 & 0 \\ 0 & * & 0 & 0 & 0 & 0 & * & * & 0 & 0 & 0 & * & 0 & * & 0 & 0 & 0 & 0 \\ \vdots & \vdots & \vdots & \vdots & \vdots & \vdots & \vdots & \vdots & \vdots & \vdots & \vdots & \vdots & \vdots & \vdots & \vdots & \vdots & \vdots & \vdots \\ 0 & * & 0 & 0 & 0 & 0 & * & * & 0 & 0 & 0 & * & 0 & * & 0 & 0 & 0 & 0 \end{array} \right).$$

Let b_j denote the number of designated columns in block j , and let c_j denote the prefix sum, $c_j = \sum_{i \in 1..j} b_i$. We permute the columns so that the designated columns in block j are moved to the contiguous area in positions $(c_{j-1} + 1)..c_j$ (with $c_0 = 0$). Call such a permutation a *scramble* (so named because we will soon move from a specified permutation to a randomized linear combination process). We have scrambled:

$$\left(\begin{array}{cccccc|cccccc|cccccc} * & 0 & 0 & 0 & 0 & 0 & 0 & * & * & * & 0 & 0 & 0 & 0 & 0 & * & 0 \\ * & 0 & 0 & 0 & 0 & 0 & 0 & * & * & * & 0 & 0 & 0 & 0 & 0 & * & 0 \\ \vdots & \vdots & \vdots & \vdots & \vdots & \vdots & \vdots & \vdots & \vdots & \vdots & \vdots & \vdots & \vdots & \vdots & \vdots & \vdots & \vdots \\ * & 0 & 0 & 0 & 0 & 0 & 0 & * & * & * & 0 & 0 & 0 & 0 & 0 & * & 0 \end{array} \right)$$

Finally, we sum the blocks obtaining a $n \times b$ matrix of the same rank as A :

$$\left(\begin{array}{cccccc} * & * & * & * & * & 0 \\ * & * & * & * & * & 0 \\ \vdots & \vdots & \vdots & \vdots & \vdots & \vdots \\ * & * & * & * & * & 0 \end{array} \right)$$

Analogously, if we applied the same select-scramble-sum process on the left (acting on the rows of this $n \times b$ matrix, we would achieve a $b \times b$ matrix with leading $r \times r$ minor nonsingular. The left and right preconditioning multipliers are products of 0,1 matrices (a diagonal, a permutation, and a stack of $b \times b$ identity matrices for the summing).

The desired permutations, moving a designated set of objects to a specified

contiguous block, can be achieved by butterfly permutation matrices. See Lemma 5.1 in [22].

Intuitively the benefit of butterfly preconditioners with random values in the switches is that they quite thoroughly scramble things up (getting one to an approximation of the generic case where nonsingularity of the leading $r \times r$ minor is to be expected) while being economical to use (costing $O(b^2 \log(b))$ field ops to multiply with a dense block). This cost results from the application of $\log(b)$ stages, each calling for b row or column operations. When the set of values from which the switch entries are chosen at random is large enough, the probability that the preconditioned matrix has generic rank profile (leading principal minors nonzero up to the rank) is high [22]. Thus for these preconditioners, $T(b)$ is $O(b^2 \log(b))$ and $S(b)$ is $O(b \log(b))$, as stated for these complexities earlier. Note that the diagonal block factor is absorbed in this complexity, being of lower cost, $O(b^2)$ time and $O(b)$ space.

To prepare for the use of randomness we turn to consider what we have if we populate the diagonal selectors and butterfly switches with independent variables.

Theorem 1. *Let K be a field and let A be an $n \times n$ matrix of rank r , where n is a power of 2. Let b be a power of 2, with $b \leq n$. Let B_i and C_i , for $i \in 1.. \frac{n}{b}$ be $b \times b$ butterflies whose defining entries are distinct variables over K . Let D_i and E_i , for $i \in 1.. \frac{n}{b}$ be $b \times b$ diagonal matrices each of whose b diagonal entries are further distinct variables. Let A be partitioned into $b \times b$ blocks $A_{i,j}$ and let $M = \sum_{i \in 0.. \frac{n}{b}} B_i D_i \sum_{j \in 0.. \frac{n}{b}} A_{i,j} E_j C_j$. Finally Let X denote the set of $2n(\log(b) + 1)$ variables involved ($2n \log(b)$ from the butterflies and $2n$ from the diagonals). Then any $k \times k$ minor of M is a homogeneous polynomial of degree $2kb(\log(b) + 1)$ in $K[X]$, if $k \leq r$, and is zero otherwise.*

Proof. In a $b \times b$ butterfly B_i , the entries of each stage are single variables (in the switches) or zero (outside the switches). Thus the entries of B_i , the product of $\log(b)$ stages, are homogeneous polynomials of degree $\log(b)$ in the variables. Multiplication by a diagonal increases the degrees of all terms by 1, so the entries of $B_i D_i$ are homogeneous polynomials of degree $\log(b) + 1$. Then each term $B_i D_i A_{i,j} E_j C_j$, in the sum

constituting M , has entries which are homogeneous polynomials of degree $2b(\log(b)+1)$. Hence the same can be said of the sum M . Finally, the k -th leading principal minor is a determinant whose terms are products of k entries, hence of degree $2kb(\log(b) + 1)$. That is so, unless through cancellation of the coefficients of every monomial, it is actually the zero polynomial. But our previous select-scramble-sum construction showed that if $k \leq r$ we can arrange to put k independent columns in the leading column positions and then do the same for rows, by suitable choice of $\{0, 1\}$ values for the variables, thus proving this minor is non zero. M has rank no more $\text{rank}(A)$ because it is a product of matrices including A ,

$$M = \begin{pmatrix} B_1 & B_2 & \dots \end{pmatrix} A \begin{pmatrix} C_1 \\ C_2 \\ \vdots \end{pmatrix}$$

Hence all minors of order greater than r are zero. Thus this determinant polynomial is a non-zero homogeneous polynomial of the stated degree if and only if $k \leq r$. \square

The power of 2 restriction is not necessary, but simplifies the explanation. It is an easy matter to extend to non power of 2 values for n and b .

Let us make the defining entries of our select-scramble-sum process neither restricted to 0,1 nor distinct variables. Instead let us choose them at random from a set S . By a standard application of the Zippel-Schwartz lemma, the probability that the leading $k \times k$ minor of M is zero is bounded above by $\frac{2kb(\log(b) + 1)}{|S|}$. We are ready to prove

Theorem 2. *Let M be the $b \times b$ matrix computed from A , a matrix of rank $r < b$, by the select-scramble-sum procedure with preconditioner entries chosen at random in a set of size s . Then $\text{rank}(M) \leq \text{rank}(A)$, and the probability that $\text{rank}(M) < \text{rank}(A)$ is bounded by $\frac{4b^2(\log(b) + 1)}{s}$. Thus for large enough s , $\text{rank}(M) = \text{rank}(A)$ with high probability.*

Furthermore, M may be computed using $O(n^2 \log(b))$ field operations and uses space for $O(b^2 + 2n \log(b))$ field elements, assuming a A can be produced from an external source one $b \times b$ block at a time.

Proof. Let $r = \text{rank}(A)$ and $r' = \text{rank}(M)$. $4b^2(\log(b) + 1) = 2d$, where d is the degree of $\det(M)$ as a polynomial in the preconditioner entries. If $r' < b$ then $\det(M)$ is zero, which implies $r < b$ with probability of failure less than $\frac{d}{s}$. Noting that $r' \geq r$ is impossible (the rank of a matrix product is bounded by the rank of its factors), we have $r' \leq r < b$. But $r' < r$ can only happen if every $r \times r$ minor of M is zero, an event again bounded by $\frac{d}{s}$ (which bounds the probability that any one of them be zero). Then the overall probability of the algorithm failing is less than the failure of the $b \times b$ plus the failure of an $r \times r$ conditional on the success of the $b \times b$, in other words, $\frac{d}{s} + (1 - \frac{d}{s})\frac{d}{s} < 2\frac{d}{s}$.

□

The probability estimate in theorem 2 is not sharp. In particular, the probability that the rank is erroneous conditional on $b > r$ is clearly lower in general, since the randomization has to evaluate as root of not one but all of the $r \times r$ minors. For a similar reason, if $r' \ll b$ it would seem that we have stronger evidence than our proof suggests that $r < b$. We conjecture that this could provide a good Monte Carlo algorithm for small primes (perhaps with different preconditioner), but we have not proven anything to this end. Instead, we turn to a certifying tool for small primes.

Theorem 3. *Let prime power q be given and $K = \mathbb{F}_q$. Let A be a given matrix in $K^{m \times n}$. Let l and k be an arbitrary positive integers, U and V be in $K^{n \times l}$ and $K^{n \times k}$, respectively with U an arbitrary matrix and V having random entries chosen uniformly from K .*

If $\text{rank}(AU) = \text{rank}((AU|AV))$, then $\text{rank}(AU) = \text{rank}(A)$, with probability of error bounded by $\frac{1}{q^k}$.

Proof. The columns of AU are linear combinations of the columns of A . As such combinations, they lie in the column space, $C(A)$, of A and span a subspace, $C(AU)$,

of it. This subspace is possibly the full column space of A , in which case A and AU have the same rank. So consider the case that $C(AU)$ is a proper subspace of $C(A)$. A basis of $C(AU)$ can be extended to a basis of $C(A)$ which includes at least one additional vector, call it w . A uniform random vector v of $C(A)$ has uniformly random coefficients in any basis (invertible change of basis preserves uniformity). Therefore the coefficient of w has probability $1/q$ of being zero. When it is not zero, v is not in $C(AU)$ and $\text{rank}((AU|v))$ is greater than $\text{rank}(AU)$. This applies independently to each of the k columns of V , hence we have the stated probability of error bound $\frac{1}{q^k}$. \square

Theorem 3 and its proof evidently transpose to the case of U and V applied from the left and acting on the row space of A . From this we get the 2 sided version,

Corollary 1. *Let K, A, U, V be as in Theorem 3 (likewise q, m, n, l, k) and let U' and V' be in $K^{l \times n}$ and $K^{k \times n}$, respectively with U' an arbitrary matrix and V' having random entries chosen uniformly from K .*

If $\text{rank}(U'AU) = \text{rank}\left(\begin{pmatrix} U'AU & U'AV \\ V'AU & V'AV \end{pmatrix}\right)$, then $\text{rank}(U'AU) = \text{rank}(A)$, with probability of error bounded by $\frac{2}{q^k}$.

Proof. Let

$$B = \begin{pmatrix} U'AU & U'AV \\ V'AU & V'AV \end{pmatrix}.$$

Augmenting a matrix with rows or columns cannot decrease rank so we have $\text{rank}(U'AU) \leq \text{rank}\left(\begin{pmatrix} U'AU & U'AV \\ V'AU & V'AV \end{pmatrix}\right) \leq \text{rank}(B)$. By hypothesis the first and last of these have the same rank, hence the middle matrix also has this rank. Applying theorem 3, to the first and middle matrices, we see $U'A$ has this same rank, with probability at least $1 - \frac{1}{q^k}$.

Again augmenting a matrix with rows or columns cannot decrease rank so we have

$$\text{rank}(U'AU) \leq \text{rank}\left(\begin{pmatrix} U'AU \\ V'AU \end{pmatrix}\right) \leq \text{rank}(B).$$

By hypothesis the first and last of these have the same rank, hence the middle matrix also has this rank. Applying theorem 3, to the middle and last matrices, we see

$$C = \begin{pmatrix} U'A \\ V'A \end{pmatrix}$$

also has this rank. Applying theorem 3 in transpose to $U'A$ and C , which have the same rank with probability at least $1 - \frac{1}{q^k}$, we conclude A has this rank with probability at least $(1 - \frac{1}{q^k})(1 - \frac{1}{q^k})$ making the probability of error less than $\frac{2}{q^k}$. \square

In summary, our Monte Carlo rank algorithm, suitable for a low rank $n \times n$ matrix A over \mathbb{F}_q , has the following four steps.

1. First choose a suitable value of b (an *a priori* estimate of the rank if you have it, otherwise a small value: $b = 1$ will do).
2. compute

$$M' = \begin{pmatrix} B \\ U \end{pmatrix} DAE (C \ V),$$

where B is $b \times n$, consisting of $b \times b$ random butterfly blocks and C is similarly $n \times b$ vertical stack of random butterfly blocks, D and E are $n \times n$ random diagonal, and U and V are respectively $k \times n$ and $n \times k$ random matrices.

3. Let M be the initial $b \times b$ block of M' . Compute $r' = \text{rank}(M')$ and $r = \text{rank}(M)$.
4. If $r' = r$, then return it as $\text{rank}(A)$. Otherwise repeat from step 2 with b doubled.

For simplicity we ignore the certificate parameter k in the $\mathcal{O}^\sim()$ complexity analysis because it will be small, logarithmic in n say, for any imaginable error probability demand. For instance, $k = 20$ assures error less than one time in a million for all values of n, r, q .

It is also true that the diagonal matrices D, E are not necessary for Theorem 1 to apply.

$$\begin{pmatrix} B \\ U \end{pmatrix} A (C \ V) \iff \begin{pmatrix} B \\ U \end{pmatrix} DAE (C \ V),$$

provided that D, E are uniformly random in \mathbb{F}_3 . Since the B, C, U, V are already uniformly random, multiplication by uniformly random diagonals D and E does not, by definition, add any more randomness to the product.

By theorem 3, the probability of error (returning an incorrect rank) is bounded by $\frac{1}{q^k}$. The number of repetitions to obtain $b > \text{rank}(A)$ is at most $\log(r)$, and by theorem 2, the probability of excessive repetitions, i.e. $r' < r$ when $b > \text{rank}(A)$, is bounded by $\frac{4b^2 \log(b)+1}{q}$. So for large enough q (an extension field may be used),

Theorem 4. *the algorithm runs in $\mathcal{O}^\sim(n^2 + r^\omega)$,*

where the $\mathcal{O}^\sim(n^2)$ is for construction of the projected matrix M' and the $\mathcal{O}^\sim(r^\omega)$ is for computing the ranks in M' .

Here $\omega < 3$ denotes the complexity of matrix multiplication.

3.2.2 Certified 3-Rank

Our focus in this section is on the pragmatics of the computation of the 3-rank of the order 3^{14} matrix $D = D(3, 7)$. We begin by describing the adjacency matrix construction of $D(p, e)$, then discuss the implementation strategies that make computation of the 3-rank of our 22 tera-entry matrix feasible.

The study of difference sets and of strongly regular graphs are closely intertwined. There is about a page of discussion on this topic in [15]. That paper described the computation of the 3-ranks of $D(3, e)$ for $e \leq 6$, but those methods run into excessive time and space demand when working with $D(3, 7)$. For a good entry point into the mathematical literature on difference sets and partial difference sets, we refer to [27, 16]. Here we just describe the construction of Dickson's family of strongly regular graphs which are part of the computational task of computing the p -rank of their adjacency matrices $D(p, e)$.

The Dickson matrix, $D(p, e)$, is of order 3^{2e} , and is defined in terms of a semifield $K \times K$, where $K = \mathbb{F}_{p^e}$. This $K \times K$ is endowed with componentwise addition/subtraction and multiplication

$$(a, b) * (c, d) = (ac + jb^\sigma d^\sigma, ad + bc).$$

Here j is a generator of the multiplicative group of K and σ is a non-trivial automorphism of K . This semifield multiplication is plainly commutative, and distributive over addition, but is not associative. For our computations we used the generator chosen by the software package Givaro's implementation of \mathbb{F}_q and as σ the Frobenius automorphism $x \rightarrow x^p$ [28].

For our purposes, the important semifield operations are squaring and subtraction. This is because the rows and columns of $D = D(p, e)$ are indexed by the semifield elements, and the entries are determined by whether or not the difference of these semifield elements is a square in $K \times K$.

$$D_{i,j} = \begin{cases} -1(\text{mod } p), & \text{if } i = j, \\ 1, & \text{if } i \neq j \text{ and } i - j(\text{semifield subtraction}) \text{ is a square,} \\ 0, & \text{otherwise.} \end{cases}$$

The p -rank of $D(p, e)$ is independent of the generator or automorphism chosen for the definition of multiplication in the semifield. It is also independent of the order in which row and column indices are associated with semifield elements (a matter just of row/column permutations).

In our computations, we use the GivaroGFq implementation of \mathbb{F}_{3^e} . GivaroGFq is the LINBOX [1] wrapper of the Zech's logarithm table approach implemented in Givaro[28].

Our matrix construction works by first computing a table of squares of the semifield. This is a length 3^{2e} array of $\{0, 1\}$ values, 1's denoting squares of the semifield. For fixed e , the cost of this construction is linear in the array size. Then the (i, j) entry

of D is determined by casting i and j into the semifield, performing a subtraction, and casting the result back to an index. Finally, the squares table for that index determines if the entry is 1 or 0. This is sufficiently expensive that it is a significant advantage of our algorithm that we only construct the (i, j) entry once, even though we cannot afford to remember (store) too many of these entries at one time.

If we combine the preconditioning of the select-scramble-sum method with the certificate of corollary 1, we have the block sum

$$M = \sum_{i \in 0..\frac{n}{b}} (B_i D_i | U_i) \sum_{j \in 0..\frac{n}{b}} A_{i,j} \begin{pmatrix} E_j C_j \\ V_j \end{pmatrix}.$$

The select-scramble (diagonal and butterfly preconditioners) may not be necessary, and in any case, have no guarantee of working over the small prime field $\text{GF}(3)$. Therefore we have replaced these preconditioners with order b identity matrices. We have the random certifying samplers of the row and column space, U_i and V_j . Here then is our computation illustrated when $\frac{n}{b} = 3$:

$$M = \begin{pmatrix} I_b & I_b & I_b \\ U_1 & U_2 & U_3 \end{pmatrix} \left[\begin{pmatrix} A_{1,1} & A_{1,2} & A_{1,3} \\ A_{2,1} & A_{2,2} & A_{2,3} \\ A_{3,1} & A_{3,2} & A_{3,3} \end{pmatrix} \begin{pmatrix} I_b & V_1 \\ I_b & V_2 \\ I_b & V_3 \end{pmatrix} \right]$$

The association shown is there to point out that we can sum the blocks on one row and at the same time multiply these blocks by the column certifiers V_j , obtaining

$$M_i = \left(\sum_j A_{i,j} \mid \sum_j A_{i,j} V_j \right). \quad (3.1)$$

$$M = \begin{pmatrix} \sum_i M_i \\ \sum_i U_i M_i \end{pmatrix} = \begin{pmatrix} \sum_{i,j} A_{i,j} & \sum_{i,j} A_{i,j} V_j \\ \sum_{i,j} U_i A_{i,j} & \sum_{i,j} U_i A_{i,j} V_j \end{pmatrix}. \quad (3.2)$$

This requires one block of A , our $A_{i,j}$, along with one block of (partial) row sum, M_i , and one block of (partial) final sum M at any one moment in the computation, thus storage

of $3b^2$ block entries. In addition we have the storage of the random preconditioners U and V . Notice that the V_j are needed as each row of blocks are summed, but the U_i are used only once (or vice versa). Thus half of the preconditioners can be generated at random, used once and immediately discarded, whereas the other side must be stored for $\frac{n}{b}$ uses. With a pseudo-random generator, as a further time-space tradeoff, one can even just store a seed and regenerate the pseudo-random entries for each use.

The computations in this section were written using the LINBOX library with a new packed dense matrix type for matrices over the integers modulo a small prime. They were run on a Sun Fire X4600 M2 having two quad core Opteron processors running Solaris (SunOS 5.11) and with 32 GB of shared RAM. The 2007 runs reported again in Table 3.1 were on a Xeon with 6GB RAM at clock rate 3.2GHz.

The experiments reported here are with sequential programs using one processor. In Table 3.1 we repeat the results reported in [15] (this is the column 2007t) followed by the times using the algorithm described in this section (columns 2009r and 2009t). The ‘t’ stands for total time and the ‘r’ stands for rank time. We broke out the rank times in the 2009 columns to illustrate their relative modesty. The $O(n^2)$ build times completely overshadow the $O(r^3)$ rank elimination times for this problem. Further, since r seems to be growing like 4^e while n grows like 9^e , the relative importance of the rank computation is decreasing as problem size increases.

The dramatic effects of an asymptotically faster algorithm together with high performance implementation details is evident in the contrast with the 2007 experiments.

The expected ratio of successive entries in the last column is 81. The ratios are not quite that large, which we guess to be attributable to relatively large coefficients on the near-dominant but non-dominant monomials in the actual cost formula for the program (in the matrix order and rank parameters). Also, perhaps we are seeing some memory hierarchy effects.

Table 3.1: Running time for computing the ranks of Dickson adjacency matrices, with summation and certificate. The time units are 's' for seconds, and 'h' for hours.

Dickson SRG					
e	dimension	Rank	2007t	2009r	2009t
2	81	20	0.021s	0.0003	0.0012s
3	729	85	0.35s	0.003s	0.022s
4	6,561	376	33.3s	0.046s	0.95s
5	59,049	1654	0.5h	1.4s	0.017h
6	531,441	7283	46.7h	80s	1.2h
7	4,782,969	32064	-	1.2h	96.4h

3.3 Obtaining rank($D(3, 8)$)

3.3.1 Motivation

The sequence of ranks in Table 3.1 indicate a three-term linear recurrence. Six terms from the sequence are needed to define this three-term recurrence relation. This is demonstrated by using said terms as an argument to the following command in the Maple software [?].

```
> with(genfunc):
> rgf_findrecur(3, [4, 20, 85, 376, 1654, 7283], t, n);
      t(n) = 4 t(n - 1) + 2 t(n - 2) - t(n - 3)
```

Here, Maple shows us that each term is dependent on the previous three terms. After obtaining the seventh rank in sequence $\text{rank}(D(3, 7)) = 32064$, we can test the predictive validity of the equation. To do this, we plug the ranks of $D(3, 4..6)$ into the equation for comparison.

```
> 4 * 7283 + 2 * 1654 - 376;
      32064
```

The result is the same. Thus the seventh result serves only to confirm the initial conjectured recurrence. However we had no *a priori* reason to suspect such a low-order

relation. For this reason, the rank of $D(3, 8)$ is sought to strengthen the conjectured relation. If the rank we compute matches the conjectured rank, the recurrence will be more strongly verified.

3.3.2 Size & scope

The number of entries in $D(3, 8)$, hereafter called A , is $(3^{16})^2 \approx 1.85 \times 10^{15}$. Fortunately, as was also true with $D(3, 7)$, the matrix need not be persistently or even simultaneously stored. It can again be generated on demand by formula in what we will call just-in-time (JIT) fashion. Using the smallest inherent machine type, a byte each per the 1.85 peta-elements, A would occupy about 1.65 pebibytes ($\approx 1.65 \times 1024^5$ bytes). In short, a blocking scheme is required not only for division of labor but also for distribution of matrix storage. Additionally bit-slicing is the clear choice of data representation for this job, due to both the space and runtime savings it affords.

The ranks of $D(3, e)$, $e \in 1..7$ are generally slightly smaller than 2^{2e+1} , which had been the choice for the block size b . As mentioned, our $e = 7$ run was comprised of blocks containing a billion entries each ($(b = 2^{15})^2$). However in the case of $e = 8$, the conjectured recurrence hints at a rank slightly above 2^{17} . The author can now with some levity recount, as time heals all wounds, that this detail was left unnoticed for a few frantic months of fruitless work. A prerequisite for the algorithm's success is that $b < \text{rank}(A)$. Ultimately, the day was saved after setting $b = 2^{17} + 2^{14}$, which is sufficiently large to capture the conjectured rank of A . This means each block contains roughly twenty-one billion entries each ($(2^{17} + 2^{14})^2$). Each block, at four entries-per-byte, occupies circa 5 gigabytes of memory. Working with units of this size is quite agreeable on modern computer systems.

The considerable computational problem arises, however, when considering the number of blocks needed. Imagine a grid formed by logically laying these $b \times b$ blocks out on a plane. Such a grid must of course, provide full coverage over A . Therefore the number of blocks in each dimension of this grid is $\lceil \frac{3^{16}}{2^{17} + 2^{14}} \rceil = 292$. Thus A is composed of around eighty-five thousand (292^2) such blocks. Continuing to speak approximately,

even with bit-slicing we are still occupying 425 terabytes. This amount of data is obviously impractical to work with concurrently, as was done for the smaller matrices in the sequence. At current time, it is too much data for even an out-of-core storage system to keep for any system short of a large data-center.

If we cannot use, or even store, A simultaneously, it is clear that the solution is to work individually with $b \times b$ blocks of A . The vital step, from a storage perspective, is in discarding the blocks after accepting their contribution to M . Seeing that A is defined by a formula, the A_{ij} blocks of A can be both created and used by independent processes. Ideally these processes can be run concurrently. This course-grained, “outer” parallelism would be characterized by Dijkstra as “loosely connected processes” [29]. That is to say processes that, while related to one another, can each operate entirely autonomously with no restrictions on the relative speed of any process. This flow of work lends itself to a producer/consumer relationship between groups of processes. These processes can, and in this case do, individually employ a second tier of parallelism: a fine-grained multithreading to get the most out of ubiquitous multicore architectures.

3.3.3 Producer/consumer: A first try

The first attempt at decomposing this problem for parallel computation was ultimately unsuccessful. However it is worth describing for two reasons. First, similar concepts will be employed by the ultimately successful parallel decomposition to be discussed later. This section therefore serves as an introduction of the general structures used. Second, it will be instructive to see what did not work about the failed configuration, and how it was modified to create the working model.

In this iteration, there were actually three classes of processes, as the consumer class is split into two parts. The classes are as follows:

Producers

The producer processes are tasked with simply generating the blocks of A , called

A_{ij} and employed by Equations 3.1 and 3.2. These raw blocks are generated in JIT fashion and subsequently written to files for consumption later. JIT generation is a computationally significant step, as intensive semi-field arithmetic is performed to generate each of the collective 1.85 peta-entries of A . The upside to JIT generation is the lack of any significant memory demand on these processes. For smaller e , we would create the A_{ij} blocks in memory and work with them directly. Because the producers merely generate entries without being asked to do further arithmetic on them, the step of creating blocks in memory is needless. In fact it is counterproductive, since the goal is to parallelize the production step and each block requires some gigabytes to store, even bit-sliced. We can instead write raw bit-sliced data directly to open files. This work flow serves to both keep system memory uncluttered and push the data needed by the consumer processes to disk faster by cutting out the memory middle-man. Every time eight values from the parent matrix are computed, two bytes of bit-sliced data can be written to file without intermediary storage. See Appendix B for a detailing of this mechanism, which we call a “file-stepper”. With scant memory demands, the idea is to run JIT generation code at a one-per-core level on our producer machines, likely ensuring saturation of the network with our block data.

Column-block creators

These processes work with the raw blocks generated by the producers, essentially performing the summation and multiplication seen in Equation 3.1. “Essentially” is used because in order to optimize for bit-slicing, in practice we do the transpose operation. Instead of creating the M_i row-wise, we create them column-wise. Thus, as is more natural, we can refer to the column-blocks as M_j rather than M_i . Once a raw block file is consumed by these processes its data can be discarded. These deletions ameliorate the problem of running out of storage space

for A , provided the ratio of consumed to produced raw blocks is sufficiently high. Consumer processes, unlike producer processes, are performing arithmetic on the blocks. Despite that fact, the production step is more expensive computationally, as the producers are working in the semi-field \mathbb{F}_{3^e} while consumers take advantage of very fast bit-slicing over \mathbb{F}_3 . Thus the aforementioned ratio is in practice high enough so that data can be incrementally deleted fast enough to avoid overloading storage capacities.

Final-block creators

The second stage of consumption deals with the output from the first class of consumers. These processes perform the summation and multiplication of Equation 3.2 (technically, the equivalent transpose operation). This amounts to combining the column blocks, M_j , into our final block M . Just as the first class of consumers could delete the A_{ij} after consumption, so too can this class of consumers delete the M_j after they have been incorporated into M . This is not quite as large an issue as j is bounded by $\frac{n}{b}$ whereas there are $(\frac{n}{b})^2$ raw blocks to generate. Still, using the 5 gigabytes-per-block number from Section 3.3.2, the M_j if combined would occupy over 1.4 TB. While we could account for this particular amount of data, the code is robust enough to handle deleting the M_j . This would be useful in computing, say, $D(3, 9)$. When this stage is complete, we can then compute $\text{rank}(M)$. If this rank is certified by our heuristic given in Section 3.2.2, with high probability $\text{rank}(M) = \text{rank}(A)$.

3.3.3.1 Broad implementation

With the extra tier of consumers, this distributed layout is slightly more complex than a canonical producer/consumer model. Even so, this division of labor fits well within the master/slave parallel programming paradigm, an example of which is given by Gropp et al. in [30]. Under this paradigm a central master process oversees, divides,

and delegates the necessary work to (typically many) distributed slave processes. Of the diverse set of parallel programming approaches, two main archetypes come to mind for accomplishing master/slave parallelism: remote procedure calls (RPC) and message passing. For a variety of reasons, we chose to employ RPC for inter-process communication, specifically via the Python Remote Objects (PyRO) module. RPC solutions typically operate at a higher level of abstraction than message passing does (in fact, RPC may employ message passing). Therefore, RPC-based programs are often less complicated to write and administer. This fact — combined with the choice of an interpreted, cross-platform language such as Python — enabled rapid prototyping and deployment of our management system.

The diverse set of target machines and heterogeneity of our groups of processes both also played a role in this decision. PyRO allows workers to communicate with a central host by essentially making a TCP connection to it. Message passing on the other hand, would involve a non-trivial amount of additional set-up costs. Such costs would include administering a compatible message passing standard (such as MPI, for example) between the wide array of candidate worker machines. Certainly, not electing for message passing foregoes a certain degree of flexibility and generally advanced features. However we have to consider our use-case. We require no more than maintaining shared work queues; this is one of the simplest possible methods of task delegation.

RPC, plainly speaking, allows hosts across a shared network to access remote procedures, or program functions, and call them as if they were local. PyRO extends this concept to an object-oriented programming model by allowing for, as the acronym suggests, remote objects. For the reader uninitiated with the Python programming language, everything (class, method, function, even each basic type) is an object. An object in classical parlance means something that encapsulates data via attributes and act on that data via methods. In Python, as in many languages, an object can always be assigned to a variable and passed as an argument to a function. A class is the standard programming concept used to define an object. The basic strategy is to

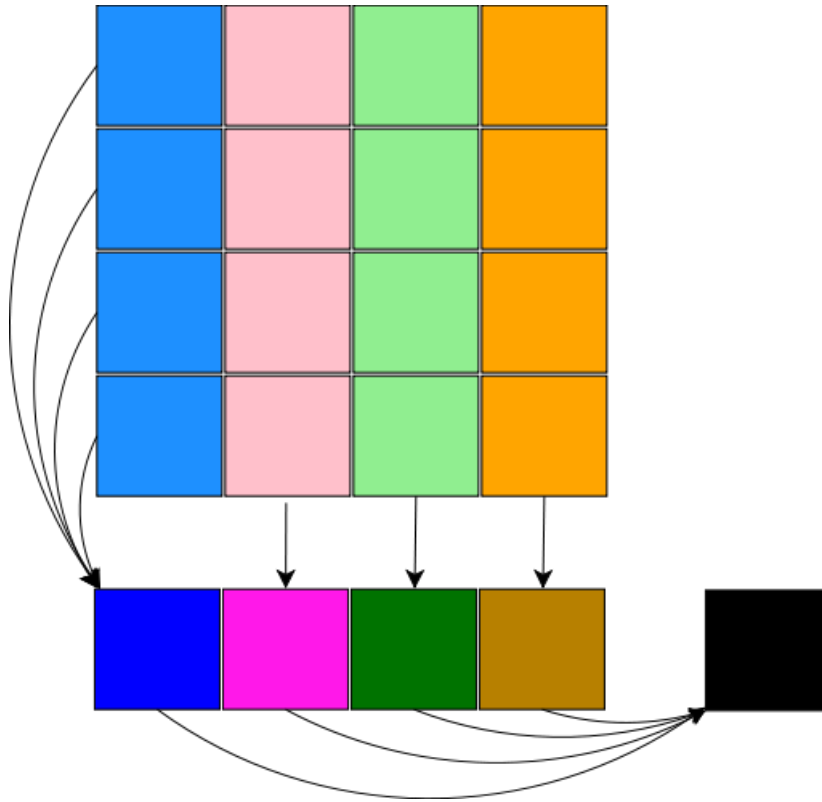


Figure 3.2: Decomposition and compression of the matrix A . Represented vertically is the result of performing Equation 3.1 to create the M_j column-blocks (represented as a darker version of their lighter-colored A_{ij} components). These are combined into the final block, represented by the horizontal flow of data at bottom. This represents the action of Equation 3.2.

create a class to carefully manage work queues, then instantiate an object from this class to share between the slaves.

Following are some loose method sketches, presented directly in Python code (or comments) rather than in pseudo-code. Python, which uses indentation rather than character delimiters to logically group code, reads enough like pseudo-code that further abstraction is unnecessary. That said, a brief illumination of some Python details is in order:

- the **import** keyword is used to make use of external Python modules (loadable code). In the following fragments, we will import some modules from Python's standard library (code distributed with Python itself) as well as some custom modules.

- keywords **class** and **def** are used to define classes and functions or methods, respectively.
- an object is always passed as the first argument to its methods. **self** is merely the conventional name given to this argument.
- square braces `[]` denote lists (with array-like semantics). Lists can be both generated and initialized with data in a single expression. These expressions are known as *list comprehensions*, which will be employed here.
- curly braces `{}` denote dictionaries. A Python dictionary acts like an associative array, or key-value store. Dictionary values can be accessed or mutated by using the key within square braces on the dictionary, e.g. `my_dict['three'] = 3`.
- the **subprocess** module from the Python standard library will be used. Specifically, `subprocess.call()` is used in order to run an external command. The distributed framework is written in Python, but the nuts and bolts linear algebra is done by LINBOX and in C++.

Presented are simplistic code outlines, just enough to demonstrate basic interoperability between components. Mundane programming details regarding things such as error handling, stopping conditions, thread-safe locking, etc. have been omitted in the name of simplicity and clarity. All complete code employed by this project can be accessed via [31] for review and/or experiment replication, in conjunction with LINBOX.

First shown is a local module which aids in data persistence and communication between processes. Python's **pickle** module is used, which quickly serializes binary representations of python objects to-and-fro disk for fast data storage and/or sharing between processes.

```
# persist.py: helps store/retrieve algorithm state
import pickle

# returns object that was pickled to file_name
def load_obj(file_name):
    with open(file_name, 'r+b') as f:
        return pickle.load(f)

# pickle object to file
def dump_obj(obj, file_name):
    with open(file_name, 'w+b') as f:
        pickle.dump(obj, f)
```

These functions are modularized to reduce code repetition and more easily share them between the following scripts, many of which will require this functionality. Without further ado, the bare-bones sketch of the single shared object that controls the flow of the algorithm:

```
from Queue import Queue
from persist import load_obj, dump_obj

class BlockManager():
    def __init__(self):
        self.work_out = Queue()
        self.work_in = Queue()

        # queue each block for production
        for i in range(0, n, b):
            for j in range(0, n, b):
                block = (i, j)
                self.work_out.put(block)

    # methods for remote invocation:
    def get_work(self):
        return self.work_out.get()

    def work_done(self, block):
        self.work_in.put(block)

    def get_produced_block(self):
        return self.work_in.get()

    def consumed_block(self, block):
        #if all blocks in a column have been created:
        j = block[1]
        created = load_obj("created.dict")
        created[j] = True
        dump_obj(created, "created.dict")
```

PyRO allows us to distribute this master object to any machine that can aid in computation, to process work acquired from the queues. See Appendix A for more details on how this object is made available for RPC. This object will be referenced as the variable `manager` in the remotely-run worker scripts.

Essentially two queues are kept. One each for block creation (as performed by the producers) and block processing (handled by column-block creators). What is placed in the queues is a **tuple** containing i and j . This pair describes which A_{ij} block to build. The producer slaves must interact with the master object and are roughly coded thusly:

```
import Queue
from subprocess import call
from threading import Thread, BoundedSemaphore

semaphore = BoundedSemaphore(num_workers)

# target function for new threads
def do_work(block):
    call("buildBlock %d %d" % block)
    manager.work_done(block)
    semaphore.release() # up semaphore

while True:
    try:
        block = manager.get_work()
    except Queue.Empty:
        break

    semaphore.acquire() # down semaphore
    Thread(target=do_work, args=(block,)).start()
```

This script simply loops while the master's **work_out** queue contains blocks to build. It gets a block from this queue via the **get_work()** interface, and spawns a new thread to create it. This thread outsources the computation to a pre-compiled C++ application, here called **build-block**. This sub-routine relies on LINBOX matrix structures and also makes use of our bit-slicing library to store the data. An important note is that this process will write the block it generates out to a file, named appropriately (e.g. of the form "block_ i - j "). Upon creation, the producer adds back to the master's **work_in** queue via the **work_done()** interface. A semaphore is used to limit the number of workers per invocation of this script. Python's **BoundedSemaphore** provides a thread-safe interface to decrementing the semaphore (with **acquire()**) or incrementing

it (with `release()`). When the semaphore's value is zero, no new threads can be spawned. This initial value of the semaphore is denoted by the `num.workers` variable, which is not shown to be set here. In practice, we typically set this via command-line argument to this script, to be flexible toward the resources available on the machine(s) hosting these producers. A good value to use is the number of CPUs available.

Column-block creators are a bit more complicated:

```
import Queue
from subprocess import call
from threading import Thread

# maintain a queue of work for each consumer
qs = [Queue.Queue() for i in range(num_consumers)]

# target function for new threads
def consume(tid):
    while True:
        block = qs[tid].get()
        call('addBlock %d %d' % block)
        manager.consumed_block(block)
        call('removeBlock %d %d' % block)

# create a list of consumer threads
ts = [Thread(target=consume, args=(i,))]

for thread in ts:
    thread.start()

# get work and assign it to a consumer
while True:
    try:
        i, j = manager.get_produced_block()
        consumer_index = (j/b)%consumers
        qs[consumer_index].put((i, j))
    except Queue.Empty:
        break

for thread in ts:
    thread.join()
```

The gist is that as blocks are produced, they are subsequently placed in a queue

such that `get_produced_block()` will return them. This indicates to the consumers that a new block exists and is ready to be incorporated into a column-block. This step is again delegated to a pre-compiled C++/LINBOX program, here called `addBlock`. `addBlock`, in short, reads in a column-block from file (representing M_j and initialized to the zero-matrix) then reads in the new block, also from file. It adds the two blocks together, as well as left-multiplies the new block by the appropriate U_i to obtain its random linear contribution to the strip of rank-certifying rows along the bottom of the column-block. After doing this, the column-block is written back to its file. This means we do not want more than one consumer contributing to the same column block at any one time. If there were multiple column-block creators attempting to work in the same column, they could end up overwriting the work of one another. Therefore, a locking mechanism would need to be designed. Code spending time waiting for a lock on a file to open is precious concurrency wasted. In order to keep processors saturated with work, the simplest solution is to restrict individual threads to work on their own column-blocks. In the code, this is accomplished by creating a child-queue per each intermediate consumer. When a signal is received of a freshly-written raw block, the code does a division (with remainder) to determine which thread “owns” the column-block to which the raw block belongs. Each thread checks its own child-queue, performs any work, and informs the master process that the block has been consumed. Most importantly, after a successful block consumption, the block is deleted to free up disk space (by routine `removeBlock`). To reiterate, this step is necessary as we lack the physical resources to store every block simultaneously. As with the producers, a special variable is used (`num_consumers`) to determine how many jobs will run in parallel.

So, the column-blocks (M_j) are created. The final step is to combine these to form the final matrix M . In this first iteration of design, there is only one final-block creator. The completion of a column-block is infrequent enough such that combinations of the blocks can be done sequentially without much opportunity for overlapping work (i.e. potential parallelism). Thus, there is no third queue informing the final-block creator when column blocks are ready. Instead, it can afford to loop indefinitely,

checking for the existence of new column-blocks on the fly. The final structure ends up looking like this:

```
from subprocess import call
from persist import load_obj, dump_obj

consumed = load_obj("consumed.dict")

while True:
    created = load_obj("created.dict")

    # loop over every possible column-of-blocks
    for j in range(0, n, b):
        if created[j]:
            if not consumed[j]:
                call("addColBlock %d" % j)
                consumed[j] = True
                call("removeColBlock %d" % j)
                dump_obj(consumed, "consumed.dict")
```

Here, we use our persistence module to use and maintain two Python dictionaries. Both dictionaries detail the state of column-blocks: one to keep track of those that have been created, and another to keep track of those consumed. The keys are the column numbers, and the values are simple booleans. The dictionary of created column-blocks is maintained by the `consumed_block()` method of our central `BlockManager` object. Under this design, this final consumer can simply loop over each column index. If a column-block is encountered that has been created but not yet consumed, then the consumer incorporates it into the final block with `addColBlock`, thus consuming it. Then, the consumer marks the column off in the “consumed” dictionary, checkpointing the results to disk. Again, as with the first tier of consumer, we delete the data which we have just read and processed to free up room for further blocks to be created.

These four simple scripts unify the three stages of work by a central manager. Any machine where we can compile the basic C++ components, `buildBlock`, `addBlock`, and `addColBlock`, we can use in the framework of the algorithm (provided also that they also have access to the networked file system where we store the blocks (A_{ij}) , column-blocks (M_j) , and master-block (M)). In addition to ease-of-deployment,

we created some additional design goals. Communication both asynchronous and modular is desirable — we want to be able to pause our computation and add or remove contributing slave processes as shared resource availability fluctuates. Asynchronous communication also makes fault tolerance an easier proposition. Given how large and long-running this task is, a design goal is to be able to checkpoint algorithm progress so that recovery from error is feasible, be it a single failed job or a more widespread ill (such as a system failure or power outage). This is doubly true when considering how much data is necessarily generated and discarded for this job. In addition to CPU time, disk and network bandwidth are shared, finite resources. Designing a framework to minimize duplication of effort is crucial.

Already briefly discussed was a dictionary-pickling mechanic, which kept track of which column-blocks had been produced, and also finally incorporated into the master-block. In addition to providing enough communication to the final-block creator process, this also serves as a fingerprint of the current algorithm’s progress. If a column block has been marked as produced, the basic blocks from which it is composed would not need to be computed were some condition encountered that required restarting computation. This feature has been extended to keeping track of which A_{ij} have been combined into the column-blocks themselves, to eliminate the need for their potential regeneration. Another concern is a potential loss of power during a file-write operation. Remember, we are dealing with writing blocks stored in files that exceed 5 gigabytes, even when writing raw bit-sliced data. It does not matter what modifications are made to the code, disks have a physical write-speed limit. These files will take plenty of time to read and write. For this reason, any time a file being is written which will be read again as input later, it will be written to a temporary file. In this algorithm, column-block files and the master-block file qualify for this treatment. Upon completion of the write-to-temporary, the temporary file can be safely used as the up-to-date file for future reads, and the appropriate dictionary-checkpoint can be registered.

3.3.3.2 The building blocks

Up to now we have laid out a high-level framework to accomplish the creation of $D(3, 8)$, but have only made passing mention to the exact linear algebra kernels that perform the meat of the algorithm. Of course we are referring to the compiled C++ programs using LINBOX. These will now be illustrated in similar fashion to the previous section. Briefly, some important LINBOX convention to note:

- Function arguments are always pass-by-reference. In practice, this helps limit the amount of data movement needed during an algorithm.
- The first argument provided to a function that performs arithmetic with, or otherwise initializes linear algebra data structures, acts as the return value of that function. In other words, the first argument doubles as a function's output; any subsequent arguments serve as input.
- LINBOX is a template library, meaning algorithms are typically written once, in a generic style that accepts different underlying storage containers and configurations of data. The complexity of the template system will be omitted in the provided code in this written work in favor of simplicity and clarity.

In the author's opinion, C++ is a fair bit more obscure to read than Python, so a more surgical approach to code demonstration will be used. We will be highlighting the critical sections of the code rather than sketching entire files. The full source code is available in [31]. Let us begin with `buildBlock`, the kernel that takes as input block indices i and j , and generates A_{ij} :

```
void buildBlock(size_t e, size_t b, size_t i, size_t j){  
    // a just-in-time (JIT) matrix representing all of A  
    JIT A(e);  
  
    // builds a single block of A  
    SlicedDomain::Matrix A_ij;  
    A_ij.init(b, b);  
    A.getSubmatrix(A_ij, i, j);  
    A_ij.writeBinaryFile(i, j);  
}
```

Here, arguments \mathbf{e} (exponent, determines size of the problem), \mathbf{b} (order of the block to generate), and \mathbf{i} & \mathbf{j} (indices of the block to generate) are known ahead

of time. As mentioned, the entries comprising the parent matrix A are determined by formula in a semifield $K \times K$ where K is \mathbb{F}_{3^e} . Recall the formula as provided in Section 3.2.2.

$$D_{i,j} = \begin{cases} -1(\bmod p), & \text{if } i = j, \\ 1, & \text{if } i \neq j \text{ and } i - j \text{ is a square,} \\ 0, & \text{otherwise.} \end{cases}$$

Our **JIT** object performs this arithmetic and can provide arbitrary windows into this matrix. Obtaining submatrices, here called blocks, in this fashion is a common routine for this and other codes used in this computation. Here, we create a compressed matrix (our **SlicedDomain** class encapsulates working with matrices that are bit-sliced) and initialize it to its proper size with **init()**. Then we simply fill our matrix with the data and write it to disk. A helper function **writeBinaryFile()** is used to write out the data to the file name that a consuming process expects. In practice, we opt to write to disk directly within the call to **getSubmatrix()** through a mechanism that can write bit-sliced data just as soon as a *sliced unit* has been filled. See Appendix B for a brief outline of said mechanism, which we call a “file-stepper”.

It is the **addBlock** routine that uses these raw block files:

```
void addBlock(size_t b, size_t c, size_t i, size_t j){
    typedef SlicedDomain::Matrix Matrix;
    SlicedDomain MD; // provides GF(3) matrix arithmetic

    // M_j is the column-block under construction.
    Matrix M_j;
    M_j.init(b + c, b);

    // Read in current state
    M_j.readBinaryFile(j);

    // A_ij is the raw-block to process
    Matrix A_ij;
    A_ij.init(b, b);
    A_ij.readBinaryFile(i, j);
```

```

// U_i is our random strip matrix
Matrix U_i;
U_i.init(c, b);
MD.random(U_i);

// Divide B_j into its two parts
Matrix M_j_Sum, M_j_Cert;
M_j_Sum.submatrix(M_j, 0, 0, b, b);
M_j_Cert.submatrix(M_j, b, 0, c, b);
// incorporate A_ij
MD.addin(M_j_Sum, A_ij);
MD.axpyin(M_j_Cert, U_i, A_ij);

// Write new state back
M_j.writeBinaryFile(j);
}

```

We have some familiar arguments in this snippet joined by a new one, **c**, which represents the number of certification rows we wish to use. This ends up serving as the row height of our random U_i matrices and consequently the product of our certification rows, $U_i A_{ij}$, which pad the bottom of the M_j block we are building. The calls to `readBinaryFile()` will read the appropriate block into program memory from file, given a consistent underlying file-naming scheme. Notice the signature for our extensively used `Matrix.submatrix()` function. The first argument is the matrix that the calling object wishes to refer to (i.e. the parent matrix). The next two arguments are the indices within the parent matrix containing the top-leftmost element of the submatrix. In other words, these integers represent the starting corner of the submatrix in the parent. The final pair of integer arguments represent the height and width of the submatrix, respectively.

The matrix arithmetic is all performed via the calls to `addin()` and `axpyin()`. The `axpyin()` call made within this phase is fast. This mul-add operation needs to uncompress the left matrix (i.e. extract singleton elements from a bit-sliced compressed block). We discussed in Chapter 2 that while bit-sliced arithmetic is fast, retrieving raw elements from bit-sliced data is computationally costly. Here, the U_i on the left are

comparatively small matrices, therefore so is the penalty for extracting the bit-sliced elements.

The core, compiled application at the heart of the final-block consumer reads very similarly:

```
void addColBlock(size_t b, size_t c, size_t j){
    size_t m = b + c;

    // M is the final_block we are building
    Matrix M;
    M.init(m,m);

    // Read in current state
    M.readBinaryFile();

    // M_j is the j-th column block
    Matrix M_j;
    M_j.init(m,b);
    M_j.readBinaryFile(j);

    // V_j is the random wide vector strip
    Matrix V_j;
    V_j.init(b,c);
    MD.random(V_j);

    // Divide M into its two parts, then incorporate M_j
    Matrix M_Sum_k, M_CertCols;
    M_Sum_k.submatrix(M, 0, 0, m, b);
    M_CertCols.submatrix(M, 0, b, m, c);
    MD.addin(M_Sum_k, M_j);
    MD.axpyin(M_CertCols, M_j, V_j);

    // Write new state back
    M.writeBinaryFile();
}
```

Here we introduce a variable, **m**, which is simply **b + c**. This shorthand makes it easy to reference the final block size, which is **m × m**. A key difference is that our call to **axpyin()** in this stage takes much longer than the previous phase. As before, both multiplicands are compressed with bit-slicing. However in this case the

left multiplicand– that which is to be extracted entry-by-entry– is $\mathbf{m} \times \mathbf{b}$. Fortunately, this kernel need only be performed once per column block ($\frac{n}{b}$ times in total).

3.3.3.3 A failure

The framework outlined above was tested and found to work for generating compressed blocks which maintained original rank for $D(3, e), e < 8$. In theory it could also be used to eventually generate $D(3, 8)$. In practice, it was not successful given our usage of the framework. To analyze why, let's begin by loosely crunching some numbers. Our test machine is the Chimera supercomputer at the University of Delaware. This energy-efficient machine contains compute nodes containing 4 AMD Opteron 6164HE 12-core 1.7GHz CPUs, for a total of 48 cores-per-node total. On this machine, a single A_{ij} block could be generated in about two minutes and added into its M_j column-block in about five minutes. Remember, these tasks are being performed independently and thus can be performed simultaneously. Therefore the total time we can expect the algorithm to take is roughly the number of blocks multiplied by five minutes, divided by the number of mid-level consumer processes we devote to the run. The number of blocks is known, it is $(\frac{n}{b})^2$. Sequentially (number of block creators = 1), this would take nearly 300 days. Fortunately, or so it would seem, parallelism would work in our favor: devote enough processes to this task and, so long as you can keep the work queue occupied, have your block built after a couple of weeks.

Therein lied the faulty assumption. Recall from the code outlines in the previous section the calls to `readBinaryFile()` and `writeBinaryFile()`. Communication between the groups of processes is entirely file-based. A central file-server is used to share files to processes running on separate hardware. As it turned out, the amount of parallelism desired out of the mid-level column-block producers was too large a burden on the combination of network and disk. Preventing the supply of A_{ij} blocks from running out meant producing at least one such block *per consumer* every five minutes. This is not even accounting for the top-tier of consumers, which of course use the file space as well to read and write their own data, albeit less frequently. Having

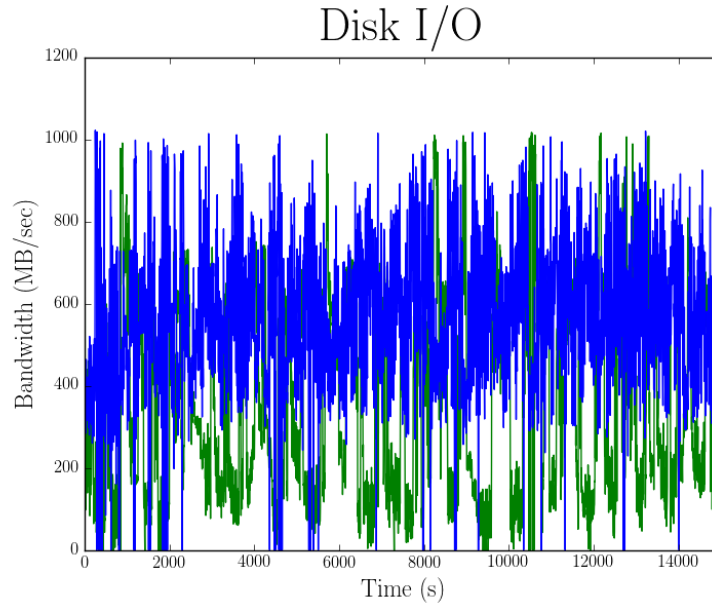


Figure 3.3: Filesystem activity during parallel build of $D(3,8)$. Green line is read bandwidth and blue line is write bandwidth. Bandwidth is measured in MB/sec and plotted every 5 seconds.

multiple processes constantly reading and writing files on the order of gigabytes to the same networked file-system was simply not scalable. Such over-activity would prove too much for our file server, which would on occasion even drop network link in the middle of our operations, rendering our code unable to continue at all. Scaling back the amount of parallelism was an option that would eventually lead to success, but with only a few processes working, we would still be waiting months on end to simply build our compressed block M , to say nothing of computing its rank.

Figure 3.3 demonstrates the utter chaos endured by the networked file system during our attempted runs. Witness the disk frantically trying to keep up with the sheer volume of simultaneous write requests. Under these conditions, column-block creator processes would take tens of minutes, even over an hour, to complete their task which under ideal conditions would only take five minutes. Blocks were being built in memory quickly but written to disk slowly.

Practical failings aside, another limitation of the first decomposition of labor

is that there can only exist a single group of each type of process (producer and consumers). Without intensive micromanagement (which would break a previously stated design goal) multiple groups of column-block creators could trample each other's work. It is clear that a different approach is necessary, one that learns from the failures of our first attempt.

3.3.4 Producer/consumer: cut out the middle-man

Writing each A_{ij} block to a file to be consumed by another process turned out to be a needless endeavor. One of the side goals in initially deciding on that model had to do with testing the installation of a new 10-Gigabit Ethernet backbone at the University of Delaware. Our ability to quickly generate useful, non-synthetic data was only limited by the amount of processing power we had available. Therefore our algorithm, as originally written, was an excellent candidate to test the operation of the new link between buildings on campus, in cooperation with Central IT services. The idea was to employ machines from various buildings each generating A_{ij} blocks and write them to files accessed remotely over the new link. The network handled the data with aplomb, but the single point of failure was the workhorse file-server that simply could not keep up with such load. Network properly tested, but algorithmic goals unmet, the following simplified decomposition was devised.

Producers (column-block creators)

The bottom two tiers of parallelism from the failed labor-decomposition have been merged together. Producer processes are now tasked with generating column-blocks of A , called M_j . The JIT procedure for generating raw A_{ij} blocks is the same as before. Instead of being the end goal, the JIT procedure is used as a kernel of this new process, which no longer bothers to write intermediate blocks to memory. This means producers will now be (significantly) longer running, but keeping the A_{ij} in memory as opposed to writing them to disk, is much less burdensome on the hardware. Unlike before, these producers will now have some

memory demand, approximately 10 GB worth: 5 for the raw-block being calculated at any given time, and another 5 for the column block ultimately being produced. Such demand is not unreasonable on modern hardware. These producers will avoid saturating the disk controller with writes while the consumers are reading data.

Final-block creators

This class of processes is identical to the highest-tier of parallelism from the previous iteration (see p. 48). Briefly, again, these processes perform the summation and multiplication of Equation 3.2.

3.3.4.1 Revised big-picture layout

As before, a central communication hub is used to coordinate efforts of the slave processes. The low level details (PyRO RPC model) are all the same, but the high-level operations have changed slightly. Of course, only dealing with two categories of slaves makes things simpler:

```
from Queue import Queue
from persist import load_obj, dump_obj

class ColBlockManager():
    def __init__(self):
        self.created = load_obj("created.dict")
        self.work_out = Queue()
        # queue each column-bloc for production
        for j in range(0, n, b):
            self.work_out.put(j)

    # methods for remote invocation:
    def get_work(self):
        return self.work_out.get()

    def work_done(self, col):
        self.created[j] = True
        dump_obj(self.created, "created.dict")
```

Only one queue is now kept. This time, it is for column-block creation (as performed by the producers). Instead of an (i, j) tuple, integers are passed via the queue denoting which column was produced/consumed.

The producers have changed, but not much:

```
import Queue
from subprocess import call
from threading import Thread, BoundedSemaphore

semaphore = BoundedSemaphore(num_workers)

# target function for new threads
def do_work(col):
    call("buildCol %d" % col)
    manager.work_done(col)
    semaphore.release() # up semaphore

while True:
    try:
        col = manager.get_work()
    except Queue.Empty:
        break

    semaphore.acquire() # down semaphore
    Thread(target=do_work, args=(col,)).start()
```

Rather than accepting which block to build, it accepts the aforementioned integer as signal for which M_j column-block to generate. Queue input/output works exactly as described before. This time, our thread's pre-compiled C++ heavy-lifter is called `buildCol`. Once again, this application relies on bit-slicing and LINBOX. We will again write column-block output to a conventionally-named file (containing the column number), but less frequently. There are now exactly $\frac{n}{b}$ producers required to fully build our block M , whereas the prior method called for $(\frac{n}{b})^2$ writes.

With no intermediary consumer, this leaves discussion of the column-block consumers (which are the final-block producers). Their purpose mirrors the final-block creator (2^{nd} consumption stage) of the prior parallel layout. Rather than a single process, however, these consumers are implemented with more parallelism in mind. In this

second iteration of design, there can be multiple consumers or final-block creators, each writing output to their own matrix. At algorithm's end, these independent matrices can be added together to form the final block M . More on this point shortly. Once again, the consumption phase can afford to loop indefinitely, checking for the existence of new column-blocks. When a new column-block has been generated, it is queued for consumption by one of the worker threads. Here is the full listing:

```
from subprocess import call
from Queue import Queue
from threading import Thread
from persist import load_obj, dump_obj

ready_queue = Queue()
consumed = load_dict("consumed.dict")

# target function for new threads
def consume(tid):
    # continuously check for new column blocks to combine
    while True:
        j = ready_queue.get()
        if j is None:
            break
        call("addColBlock %d %d" % (j, tid))
        consumed[j] = True
        call("rmColBlock %d" % j)
        dump_obj(consumed, "consumed.dict")

while True:
    created = load_dict("created.dict")
    queued = consumed.copy()

    # create the parallel workers
    threads = [Thread(target=consume, args=(i,))
               for i in range(num_workers)]
    # spawn them
    for t in threads:
        t.start()

    # loop over every possible column-of-blocks
    for j in range(0, n, b):
        if created[j]:
            if not queued[j]:
```

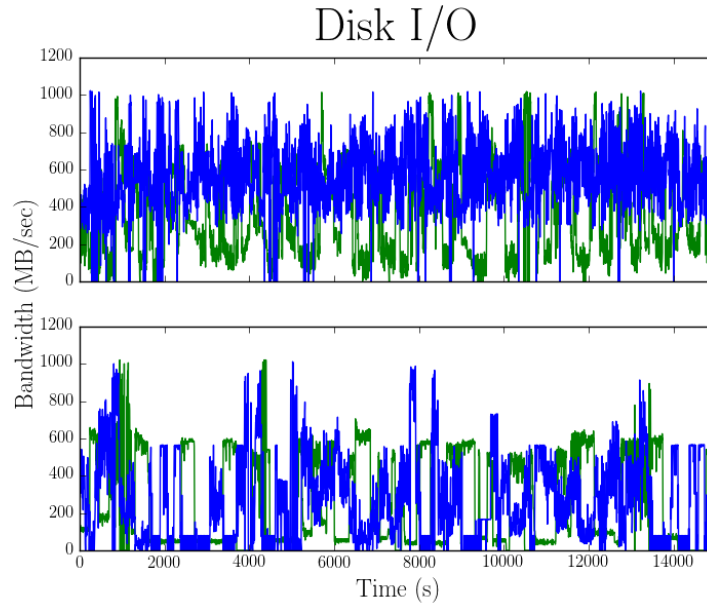


Figure 3.4: A contrast of Figure 3.3 (top chart) with the real time file-system activity of the revised parallel decomposition (bottom chart). Green line is read bandwidth and blue line is write bandwidth. Bandwidth is measured in MB/sec and plotted every 5 seconds. Notice that although reads are performed at a similar rate, the demand for writes is kept much lower in the bottom chart.

```
ready_queue.put(j)
queued[j] = True
```

3.3.4.2 Revised building blocks

We now detail the changes to the underlying compiled LINBOX programs in accordance with the new parallel layout. Here we begin with `buildCol`, the kernel that takes as input column index j , and generates M_j :

```
void buildCol(size_t e, size_t n, size_t b, size_t c, size_t j){
    SlicedDomain MD(); // provides GF(3) matrix arithmetic
    typedef SlicedDomain::Matrix Matrix;

    // a just-in-time (JIT) matrix representing all of A
    JIT A(e);
    // A_ij will be used to represent a block of A
    Matrix A_ij;
```

```

A_ij.init(b, b);

// M_j is the column-block under construction.
Matrix M_j;
M_j.init(b + c, b);
// Divide it into two parts
Matrix M_j_Sum, M_j_Cert;
M_j_Sum.submatrix(M_j, 0, 0, b, b);
M_j_Cert.submatrix(M_j, b, 0, c, b);

// U_i is our random strip matrix
Matrix U_i;
U_i.init(c, b);

// For each block in this column, row-wise
for(size_t i = 0; i < n: i += b){
    // Retrieve the block
    A.getSubmatrix(A_ij, i, j);

    // incorporate block
    MD.addin(M_j_Sum, A_ij);k
    MD.random(U_i);
    MD.axpyin(M_j_Cert, U_i, A_ij);
}

// Write block to file
M_j.writeBinaryFile(j);
}

```

Naturally this is just an amalgamation of the producer and the first consumer from before. Once again, the important point is that there are no intermediate file writes.

The `addColBlock` routine is unchanged from the listing given in [3.3.3.2](#), save one detail. In this computational layout the consumer is written to take advantage of multiple worker threads, each of which could be consuming a column block simultaneously. Of course, this means the threads would be adding to a master block simultaneously. Such a mechanism is thread-unsafe. Workers could overwrite each other's partial work, leaving the master block in an unknown (but almost certainly meaningless) state. So

in practice, each thread has its own master block to write to, and this is subtly distinguished by having the call to `addColBlock` take as input the thread identification number. As long as each thread used in this stage of the parallelism has a unique identification number, no thread-collisions can occur at the file level.

Thus we are left with the following construction. If there are w workers devoted to column-block consumption, there will be w *sums* of column-blocks, call them the M_w . Let the set \mathcal{J} be the set of all columns-of-blocks needed by the algorithm, denoted by that column's leftmost column index of A . Let the set \mathcal{J}_w be the set of all columns incorporated into M_w by a worker w , denoted the same way. The \mathcal{J}_w are mutually disjoint partitions of the set \mathcal{J} . For any pair \mathcal{J}_x and \mathcal{J}_y , $\mathcal{J}_x \cap \mathcal{J}_y = \{\}$. In other words, no two workers will combine the same column-block into their private sum-block M_w . Then,

$$\mathcal{J} = \{ib : 0 \leq i < \frac{n}{b}\}$$

$$\mathcal{J} = \bigcup \mathcal{J}_w$$

Therefore,

$$M_w = \sum_{\mathcal{J}_w} M_{\mathcal{J}_w} | M_{\mathcal{J}_w} V_{\mathcal{J}_w}$$

$$M = \sum M_w$$

So, our final block M can be created by a basic summing of the intermediary column-block sums produced by each worker. This is a quite fast operation with bit-sliced matrices, and has negligible effect on overall running time.

3.3.4.3 Shared-memory parallelism

As mentioned, our main compute nodes had four 12-core CPUs, so taking advantage of the available shared-memory parallelism is paramount. For this feature we turned to the ready-made OpenMP [32] framework. OpenMP is a portable, flexible

API for using shared memory parallelism from within C++ (among other languages) via simple directives. For example, a revamped `buildCol` routine to take advantage of OpenMP parallelism:

```
#include <omp.h>

void buildCol(size_t e, size_t n, size_t b, size_t c, size_t j){
    ... // set up matrices as before

    // Submatrices employed per-thread
    Domain::Matrix sub, msub;

    // For each block in this column, row-wise
    for(size_t i = 0; i < n: i += b){

#pragma omp parallel private(tid, rpt, sub, msub) shared(nthreads)
    {
        tid = omp_get_thread_num();
        nthreads = omp_get_num_threads();

        rpt = b / nthreads; // rpt = Rows Per Thread

        // Retrieve the sub-block for this thread
        sub.submatrix(A_ij, rpt*tid, 0, rpt, b);
        A.getSubmatrix(sub, i+rpt*tid, j);

        // add in sub-block to correct slab of M_j
        msub.submatrix(M_j_Sum, rpt*tid, 0, rpt, b);
        MD.addin(msub, sub);
    }

    MD.random(U_i);
    MD.axpyin(M_j_Cert, U_i, A_ij);
}

    ... // write file as before
}
```

Set-up and tear-down have been omitted as they are unchanged from the listing on page 68. The internal loop has been re-written to take advantage of multi-core

processing. The `#pragma omp parallel` directive will automatically separate its containing “for” loop into equal chunks for separate threads to tackle. The `private()` and `shared()` clauses indicate which variables are to be shared among all threads, and which variables should be copied to thread-local memory for individual usage. Once again our oft-used `submatrix` archetype is used. In this modification it is doubly useful: a sub-matrix called `sub` is created by each thread which can be used to generate entries from A_{ij} , and another submatrix called `msub` is used to reference the appropriate slice of the column-block, M_j to which the thread can simply add `sub`. The A_{ij} generation can be done entirely independently, meaning each thread can proceed as if it were its own process, entirely ignorant of the work of the other threads. Of course, the step that cannot be parallelized so simply is the call to `axpyin()`, which is left outside of the OpenMP code block.

3.3.5 Obtaining $\text{rank}(M)$

Computing the rank of the compressed adjacency matrix of the strongly-regular graph that we have built is the final step in our rank algorithm. Last, but not least: calculating rank even on this vastly compressed form can still take on the order of days with current computing resources. The algorithm we use is essentially canonical Gaussian Elimination [17], one of the same methods that was not viable to use on the uncompressed adjacency matrix. However, a few key improvements make this computation faster. We perform a special bit-sliced and multithreaded implementation of Gaussian elimination. Performing Gaussian elimination means converting the matrix to row-echelon form. In this form, the nonzero rows precede the zero rows and the number of nonzero rows is the rank of the matrix. The leading entries in the nonzero rows are called the pivots; the columns of the pivots are in increasing order. The exact details are not so important, but the algorithm relies on two subroutines: swapping rows and vector-*axpy*. Swapping memory is easy enough, but bit-slicing makes it significantly faster as every word-swap exchanges many values instead of just one. Vector-*axpy* is of course also improved by virtue of the data being bit-sliced, but even

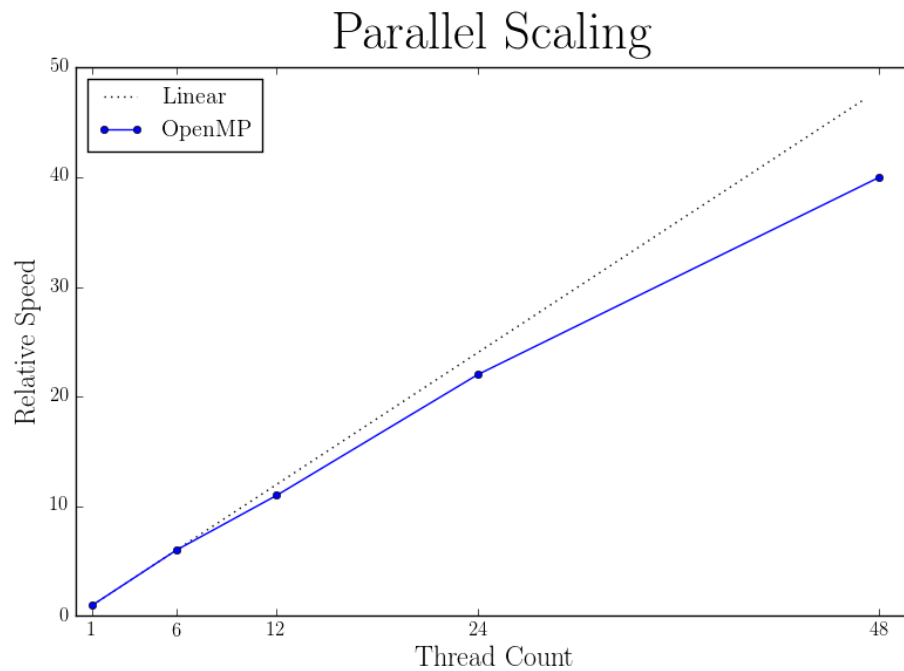


Figure 3.5: Multithreaded parallel scalability for the routine of building a column block, `buildColBlock`. Relative performance is charted versus the single-threaded application, with linear speedup displayed on the graph as a reminder of the best-case scenario. The multicore scalability of this algorithm is quite favorable, further illustrating the embarrassingly parallel, CPU-bound nature of generating matrix entries.

more time is saved by again resorting to shared-memory parallelism. Each time a pivot is found, elimination (by way of axpy) must be performed on all subsequent rows. This step can be performed entirely independently on each row, yet another embarrassingly parallel routine. Therefore these rows can be evenly pooled into t groups, where t is the number of OpenMP threads available. Each thread then eliminates the rows for which it is responsible. Table 3.2 repeats Table 3.1 with new data showing the marked improvement bit-slicing and OpenMP have made on our simple Gaussian elimination kernel, in the “2014r” column. Specifically, contrasting this with the “2009r” column shows an order of magnitude difference in computing the rank of the compressed $D(3, 7)$.

Full disclosure: the comparison over the years is not apples to apples. The times reported in the 2014 columns were run on the Chimera supercomputer. The considerable improvement seen in Table 3.2 between the “2009t” and “2014t” column in computing $\text{rank}(D(3, 7))$, and indeed the very ability to compute $\text{rank}(D(3, 8))$ owes largely to taking advantage of the parallelism afforded by the new machinery. The “2014t” column, which describes time taken for the matrix compression, employed eighteen Chimera compute nodes, whereas the rank calculation (“2014r” column) enjoyed the contribution of 48 cores of a single node. Despite not being a fair comparison, the new data still serves as a remarkable high level view on just how much runtime savings bit-slicing and massive parallelism have earned us. With a time complexity cubic and the matrix quadrupling in size with each successive entry, we expect an 81-times increase in running time between levels on the table. The fact we have actually *cut* running time between levels by a factor of three (96.4 hours in 2009 to 27.9 hours in 2014) is a great success, and promising for the future of this line of computation.

3.3.6 A final barrier

With the new decomposition of work, we were able to compute final blocks M that should have captured the rank of $D(3, 8)$. However, our rank code performing Gaussian elimination was “dipping” into the certification rows and columns we built

Table 3.2: Repetition of Table 3.1 with data added from the parallel implementation— Running time for computing the ranks of Dickson adjacency matrices. The time units are 's' for seconds, and 'h' for hours.

Dickson SRG							
e	dimension	Rank	2007t	2009r	2009t	2014r	2014t
2	81	20	0.021s	0.0003	0.0012s	-	-
3	729	85	0.35s	0.003s	0.022s	-	-
4	6,561	376	33.3s	0.046s	0.95s	-	-
5	59,049	1654	0.5h	1.4s	0.017h	-	-
6	531,441	7283	46.7h	80s	1.2h	-	-
7	4,782,969	32064	-	1.2h	96.4h	.13h	1.3h
8	43,046,721	141168	-	-	-	8.71h	27.9h

into our block. In fact, the elimination was using up the entirety of this buffer, indicating M was of full rank or M did not capture $\text{rank}(D(3, 8))$, or both. Something was decidedly going wrong. The algorithm would have to be run, re-run, and thoroughly examined in order to figure out the problem. In this light, the performance of the distributed- and shared-memory parallel implementation proved vital. We could also be thankful for the many-core architectures on which the code ran. The job could be re-tried in days, not months.

3.3.6.1 The panacea

Where we stand here is that we have generated a compressed block that has not captured the desired rank. We generated this block without the benefit of the butterfly preconditioners detailed in Section 3.2.1. Butterfly preconditioners would ensure that the true rank would be contained in the compressed block. However, re-engineering the butterflies back into the code would be time-consuming, to say nothing of the massive increase in algorithmic complexity and computational running time this would cause. Remember, the butterfly matrices serve to “scramble” the matrix data, so much of the effectiveness of the shared-memory parallelism detailed in the previous section would be diminished due to inter-thread data dependence. Another factor to consider is that

the butterfly concept of permuting at the individual column-level is incongruent with bit-slicing, our chosen matrix representation, which of course packs multiple matrix columns together.

Instead the heuristic we rely upon, crudely adding the blocks together, has proven ineffective on this iteration of the problem where it had hitherto succeeded. It is likely in this instance that independent rows and columns of A are cancelling each other out. Thus the preconditioning step, whilst clearly not necessary for the computation of the prior ranks in the sequence, would greatly increase the likelihood of capturing $\text{rank}(D(3, 8))$ within our built-block M . So the question now is how can we approximate the scrambling effect of the butterfly preconditioners without losing many of our current advantages? The answer to coarsely permute column-wise the M_j column-blocks before combining them into M with our consumers. This is a desirable solution as the coarse permutation is performed only $\frac{n}{b}$ times per run. The permutation is coarse because the M_j is not permuted by individual columns. Again, such an action would be quite costly given that M_j is bit-sliced; each element to permute would have to be masked and shifted out of its original *sliced-unit* before being shifted and masked back into its final *sliced-unit*. Rather, the permutation occurs on *sliced-unit* boundaries. If bit-sliced data is packed into 64-bit words, then the permutation is of 64 columns at a time. This is one of the least invasive and intensive ways to radically change the construction of the matrix. Yet it was entirely reasonable to attempt first, because after all we have the certification rows and columns. As long as at least some of those remain intact throughout the rank calculation, we can be reasonably sure that M 's rank is $D(3, 8)$'s rank. So of course the plan was to try the simplest things first to get the rank to certify.

In practice, a random permutation generated by a Knuth shuffle [33] is performed on the level of *sliced-units*. A Knuth shuffle is a method of randomly permuting a sequence, which generates permutations uniformly random across the set of all possible permutations, i.e. every permutation is equally likely. This turned out to provide exactly the shifting around needed to avoid independent column cancellation.

After performing this step, the rank algorithm no longer “dipped” into the row or column certifiers containing random linear combinations of $D(3, 8)$. We could once again probabilistically trust that $\text{rank}(M) = \text{rank}(A)$.

The result: 141168. How does that stack up with what was expected? Once again we check by plugging the ranks of $D(3, 5..7)$ into the conjectured recurrence relation for comparison.

$$\begin{aligned} > 4 * 32064 + 2 * 7283 - 1654; \\ & \qquad \qquad \qquad 141168 \end{aligned}$$

At long last, we have successfully confirmed that the rank of $D(3, 8)$ is equivalent to the rank predicted by our formula!

3.3.7 Further applications

Accomplishing the rank computation of $D(3, 8)$, and thus giving further evidence for a linear recurrence for the ranks, engendered a certain interest in exploring similarly defined adjacency matrices of other families of strongly-regular graphs. Some graph families of interest that were also described by Xiang et al. in [14] include the Paley and the Cohen-Ganley series. A graph sequence of more recent interest is known as the Ding-Yuan sequence [?].

The convenient thing about attempting to calculate the ranks of these sequences is the ability for code re-use from the Dickson sequence. In fact, nearly everything about the framework for computing the Dickson ranks remains the same, from the JIT generation step, to the parallel master-slave hierarchy and components, to the final-block compression. There are two main differences between obtaining ranks of the different families of matrices. Most simply is the fact that differently sized ranks are expected in each case. This fact requires a minor tweak in determining the block size b of the compressed block M . Remember, this block must of course be large enough to entirely encompass the rank of the uncompressed JIT A .

The second difference is in pre-calculating a table of squares in the semifield which defines the particular matrix class (e.g. Dickson, Cohen-Ganley, etc.). Recall

that the entry in the (i, j) position of the matrix is 1 if the difference $i - j$ is a square in this semifield. For efficiency we pre-compute a binary listing of every possible value within the semifield. A one in the place of a semifield element denotes it is a square, and a zero denotes that element is not a square. This way, upon computing $i - j$, all that is necessary is a table-lookup to determine the matrix entry at these indices.

Given our success in pinning down a formula for the Dickson sequence, we have been asked by these mathematicians to explore the unknown ranks on the larger end of the scale for the other sequences. The hope here is that similar formulae can be found, or at least upper bounds on the ranks can be proven. Furthermore, no simple linear recurrence has emerged for the Cohen-Ganley and Ding-Yuan ranks as have been computed thus far. Pushing on to even larger sizes is ultimately desirable— this means computing the rank of matrices far larger than $D(3, 8)$. For instance, $DY(3, 8)$ (DY for Ding-Yuan) is actually a matrix order 3^{17} .

The basic heuristic we rely on has proven unreliable in computing the larger matrices in the Cohen-Ganley and Ding-Yuan families. Additional permutation steps are likely needed to tackle these examples.

3.4 Summary

Chapter 2 detailed technologies that greatly benefited this rank problem, among other small finite field applications. Chapter 3 motivated the rank problem, then attacked it with a new theoretical approach. This approach parallelizes easily, and a new parallel framework has been necessarily developed to compute rank of the larger matrices of interest. The framework has been applied successfully to solve for $\text{rank}(D(3, 8))$ using about nine hundred cores over the course of days. Work is ongoing to adjust the algorithm for the non-Dickson families, meaning ever-larger computations will follow. As the asymptotic complexity indicates cubic growth, we can expect these runs to take on the order of months with the same hardware. The end of this chapter concludes discussion on this problem. Chapter 4 turns to a completely different application falling under the umbrella of exact linear algebra: rational linear system solving.

Table 3.3: Known ranks for adjacency matrices of certain strongly regular graph families. The powers for the Ding-Yuan family are all one less than the power listed, e.g. the Ding-Yuan matrix in 3^2 row is 3×3 , and the matrix in the 3^{16} row is $3^{15} \times 3^{15}$.

<i>Order</i>	Paley	Dickson	Cohen-Ganely	Ding-Yuan
3^2	4	4	4	2
3^4	16	20	20	8
3^6	64	85	94	42
3^8	256	376	448	226
3^{10}	1024	1654	2084	1232
3^{12}	4096	7283	9652	6646
3^{14}	16384	32064	44651	35862
3^{16}	-	141168	-	185868
Known Formula	✓	✓	?	?

Chapter 4

EXACT RATIONAL LINEAR SYSTEM SOLVER

4.1 Introduction

We address the problem of solving $Ax = b$ for a vector $x \in \mathbb{Q}^n$, given $A \in \mathbb{Z}^{m \times n}$ and $b \in \mathbb{Z}^m$. Also, in this chapter we are concerned with dense matrices, which is to say, matrices that do not have so many zero entries that more specialized sparse matrix techniques should be applied. We do anticipate that the refined numeric-symbolic iterative approach presented here will also apply effectively to sparse systems.

4.1.1 Relation to prior work

We present a method which is a refinement of the numeric-symbolic method of Wan [34, 35]. Earlier work of Geddes and Zheng [36] showed the effectiveness of the numeric-symbolic iteration, but used higher precision (thus higher cost) steps in the residue computation. However, Wan’s method has had only sporadic success as deployed in the field in LINBOX. Here we present a new *confirmed continuation method* which is quite robust and effective. In general, numerical iteration methods are intended to extend the number of correct digits in the partial solution x' . The confirmed continuation method verifies that these new digits overlap the previous iteration’s partial solution. The concept of “overlap” here will be explained in detail in Section 4.3. This is our assurance of progress, rather than the less reliable matrix condition number small norm of residual, $|b - Ax'|$, which is used in prior methods [34, 35, 37, 38]. Evidence from data suggests that the new version solves a larger class of problems, is more robust, and provides the fastest solutions for many dense linear systems.

Standard non-iterative methods, such as Gaussian elimination, suffer from extreme expression swell when working in exact integer or rational number arithmetic.

In fact, the solution vector x itself is typically a larger object than the inputs. When elimination is used, typically $O(n^2)$ large intermediate values are typically created, with concomitant large time and memory cost.

In view of such expression swell, it is remarkable that iterative methods provide for solution in $n^{3+o(1)}$ time and $n^{2+o(1)}$ space when input entry lengths are constant. (The factor $n^{o(1)}$ absorbs any factors logarithmic in n .) There are two contending approaches.

A classical approach for finding rational number solutions to linear systems is Dixon’s modular method [39]. This method begins by solving the system modulo a prime, p , and proceeds to a p -adic approximation of the solution by Hensel lifting, and finishes with reconstruction of the rational solution from p -adic approximants of sufficient length. The second approach is a numeric-symbolic combination introduced by Wan in his thesis [34, 35]. Our focus is on extending Wan’s method to to a larger class of problems where the size of residuals is too pessimistic.

The more usual iterative refinement of solutions within working floating point precision has excellent exposition in [40]. Historically, the idea of solving exact linear systems to arbitrarily high accuracy by numerical iterative refinement (earlier referred to as binary-cascade iterative-refinement process, BCIR) is attributed to H. Wozniakowski by Wilkinson [41]. Wozniakowski is also acknowledged in a 1981 paper by Kielbasinski [38]. This 1981 paper emphasized “using the lowest sufficient precision in the computation of residual vectors.” The required precision was allowed to vary at each iterative step. The case when doubling the working precision suffices to compute sufficiently accurate residuals was also treated soon after in [37]. An important limitation of these early papers was the assumption that the condition number of the matrix A is known. In practice, the system’s condition number is rarely known and estimators can fail drastically.

Wan introduced two innovations into iterative refinement. The first innovation is that knowledge of condition numbers is not required. Instead, the accuracy of intermediate approximation vectors is estimated by the computed residuals, $|b - Ax'|$. Wan’s

second innovation was to compute these residuals exactly, rather than in variable precision or double precision as in the two earlier papers. Accurate residuals are essential, of course, for the correctness of subsequent iterative steps. However, residuals, even if exact, do not always correctly assess the accuracy of approximate solutions.

Thus, Wan's approach is basically to iterate with a series of approximate numerical solutions, each contributing a possibly differing number of correct bits, and to do exact computation of the current residual (via truncation and scaling) at each iteration in preparation for the next. The exactly computed residual is used to estimate the number of reliable bits in the current numeric approximation, and to provide the required accuracy of the residual that is to be input into the next iterative step. The final step in Wan's method, just as in Dixon's method, is that rational construction of the exact solution is undertaken only after a sufficiently accurate (dyadic, in this case) rational approximation is obtained.

One may say that, as input to the rational reconstruction, Dixon's method produces terms of a Laurent series in powers of the prime p and numeric-symbolic iteration produces terms of a Laurent series in powers of $1/2$. A bound is computed for the maximum length of the series necessary to assure rational reconstruction. These methods have the same asymptotic complexity.

Reconstruction earlier in the process can be tried and will succeed if the rational numbers in the solution have smaller representations than the *a priori* bound. This is not done in the current implementation of Wan's method. Steffy studies this case in [42]. We offer a variant of rational reconstruction which recognizes potential early termination. But we distinguish these speculative results from the results that are *guaranteed* from known properties of the output and length of the Laurent series. Speculative results should be checked to see if they satisfy the original linear system.

One advantage of numeric-symbolic iteration is that the most significant digits are obtained first. One can stop short of the full rational reconstruction and instead take as output the floating point values at any desired precision. A disadvantage of numeric-symbolic iteration is that it does require the numeric solver to obtain at least

a few bits of accuracy at each iteration to be able to continue. Thus it is subject to failure due to ill-conditioning.

Wan’s method has been implemented in LINBOX [43, 1]. Some uses of linear system solving, for instance in Smith Normal Form computation, proceed by trying Wan’s method and, if it fails, resorting to Dixon’s. Unfortunately, past experience is that the numeric-symbolic iteration fails more often than not in this context. The confirmed continuation algorithm variant reported here significantly increases the success rate.

In section 4.2, we explore Dixon’s and Wan’s iterations in more detail. Then in section 4.3 we describe our confirmed continuation method. In section 4.4 the rational reconstruction phase is discussed in detail. Finally our experiments are reported in section 4.5.

4.2 Background

Here is a unified skeleton of Dixon’s p-adic method and the numeric, dyadic iteration for rational linear system solution. To unify the notation note that a rational number x may be written as a Laurent series: $x = \sum_{i=k}^{\infty} x_i p^i$, where either p is a prime (p -adic expansion) or $p = 1/2$ (dyadic expansion). It will be convenient to think of the dyadic expansion in e bit chunks, in other words, use $p = 2^{-e}$. We specify that each x_i is integer and $0 \leq x_i < p$ in the p-adic case, $0 \leq x_i < 1/p$ in the dyadic case. In either case let $x \bmod p^l$ denote $\sum_{i=k}^{l-1} x_i p^i$. This will allow us to use the same modular language when discussing p-adic or dyadic expansions.

The skeleton of iterative refinement schemes to compute a solution x to $Ax = b$ is then the following.

1. Compute B such that $B = A^{-1} \bmod p$. That is, $A * B = I \bmod p$. The needed functionality of B is that for various vectors r , it can be used to accurately compute $A^{-1}r \bmod p$ in n^2 arithmetic steps. For instance, B could be represented by an LU decomposition of A .
2. By Cramer’s rule the solution vector can be represented by quotients of $n \times n$ minors of (A, b) . Compute a bound H (for instance the Hadamard bound) for

these determinants. Let $k = \lceil \log_q(H) \rceil$, where $q = p$ if doing p -adic expansion and $q = 1/p$ if doing dyadic expansion. $2k$ terms of expansion are needed, in the worst case, to reconstruct the rational numbers in the solution vector.

3. Let $r_0 = b, y_0 = 0$. For i in $0..2k$ do the following:

(a) $y_i = A^{-1}r_i \bmod p$.

(b) $r_{i+1} = (r_i - Ay_i)/p$. Do this computation modulo p^2 at least. Since $r_i - Ay_i = 0 \bmod p$, after the division, r_{i+1} is the correct residual modulo p .

(c) $y = y + y_i p^i$.

Each of these steps corrects for the preceding residual by computing y to one more p -adic digit of accuracy. In other words $y = A^{-1}b \bmod p^{2k}$.

4. Apply rational reconstruction to the pair of (y, p^{2k}) to obtain x , the solution vector of rational numbers.

When p is a prime, this is Dixon's method. When $p = (1/2)^{30}$ this is essentially Wan's numeric-symbolic iterative scheme. Wan's method succeeds so long as step (3a) yields at least some bits of accurate data at each iteration. Thus there is the possibility of failure due to insufficient numeric accuracy in the iteration, a problem not present in Dixon's method. On the other hand, it is possible to exploit whatever amount of accuracy is achieved at each step, which could be more or fewer than 30 bits. In other words, there is no need to use the same power of $1/2$ at each iteration. Wan's iteration (and others) adjust the number of bits used at each iteration to the accuracy of the solver.

The trick to this on-line adjustment is to know the accuracy of the solver. The condition number and/or the norm of the residual have been used as guidance here. The residual norm idea is basically that in step (3b) if $r_{i+1} = r_i - Ay_i$ is smaller by e bits than r_i , then also the first e bits of y_i are likely to be accurate. However, this is not always the case.

The first contribution of our approach is to replace the use of the residual norm with an overlap confirmed continuation principle. Suppose it is believed that e bits of an intermediate numeric solution are accurate. The residual norm based iteration would

define y_i as $w \bmod 2^{-e}$. Thus $w = y_i + 2^{-e}q$, ($q \leq 1$) and q is discarded¹. Instead, we choose the exponent e' of $1/2$ used at each iteration slightly conservatively. Let $e' = e - 1$ and use the decomposition $w = y_i + 2^{-e'}q$. We take a little less in y_i so as to be able to make use of q . Since we believe the numeric solver gave us e bits of accuracy, the first bit in each entry of q is presumably accurate. Thus y_{i+1} should agree with q in the leading bits. When this happens we say we have a *confirmed continuation*. When it fails, we recognize that w was not accurate to e bits, and make an adjustment as described in the next section.

Confirmed continuation is a heuristic, since when it succeeds we do not know with certainty that the solution is accurate. It will succeed very well when the numeric solver is unbiased and the intuition is that it will still do very well when bias is present. Let $A \in \mathbb{Z}^{n \times n}$ and let B be a representation of A^{-1} . Suppose B is unbiased, which means that, for any $b \in \mathbb{Z}^n, s \in \mathbb{Z}$, if $y = Bb \bmod 2^s$ and $y \neq A^{-1}b \bmod s$ then the direction of $B(b - Ay)$ is uniformly random. Observe that if B is unbiased then the probability is $1/2^n$ of a false one bit continuation confirmation. This is just the observation that there are 2^n patterns of n bits. This is a rather weak justification for our confirmed continuation heuristic since solvers are rarely if ever unbiased. However, in practice the heuristic is proving to be effective, allowing continuation in some cases in which the residual norm is discouragingly large.

In the next section our confirmed continuation method is described in more detail including the exploitation of techniques to discover the solution sooner when the actual numerators and denominator are smaller than the *a priori* bounds. This is variously called output sensitivity or early termination [44, 45]. Output sensitivity has been used primarily with Dixon's algorithm. The only study of it we know for numeric-symbolic iteration is [42].

¹ It is a central idea of Wan's approach to do this truncation so that the next residual may be computed *exactly*.

4.3 Confirmed continuation and output sensitivity

Our variant on iterative refinement, sketched in Algorithm 15, uses the same basic structure as previous implementations. That is, the system is solved numerically in a loop, with the solution at each iteration contributing some bits to the dyadic numerators and common denominator. Specifically, we call the solution in a step of the iteration \hat{x} , and divide it into two parts, called \hat{x}_{int} and \hat{x}_{frac} . \hat{x}_{int} contains the higher order bits and is incorporated into the dyadic estimate. \hat{x}_{frac} contains the lower order bits and is unused in Wan’s algorithm. The residual vector obtained by applying A to \hat{x}_{int} provides the right-hand side to solve against for the next iteration. The loop ends when it is determined the dyadic approximants contain enough information to reconstruct the true rational solution. As mentioned in Section 4.1.1, this determination is made by checking against a pre-computed bound on the size of the rationals.

To ensure the accuracy of the numeric solver’s solution at each iteration, we verify that there is overlap between the current iteration’s numeric solution, \hat{x} and the discarded fractional portion of the previous solution \hat{x}_{frac} . The two vectors are subtracted and the maximal absolute value in the difference set is checked against a threshold, $\frac{1}{2^k}$, to ensure k overlapping bits. In practice, we find one bit of overlap (i.e. $k = 1$) suffices to confirm continuation except for very small n .

4.3.1 An adaptive approach

Once this verification step is successful, we are able to explore seeking more bits of accuracy from the numeric solver. We treat the value s as an adjustable bit-shift length. Each numeric solution \hat{x} is multiplied by 2^s in order to split into \hat{x}_{int} and \hat{x}_{frac} . That is, it is bit-shifted left by s . Likewise when we update the dyadic numerators N , we shift them left by s , then add the new information to the now zeroed lower s bits.

The value of s is at our disposal and allows the algorithm to adapt to changing accuracy from the numeric solver. Ideally it will hug the true number of accurate bits in the intermediate results as closely as possible. As long as some bits of accuracy are provided by each numeric solve, the iteration can continue. Within the bounds

Algorithm 9 Overlap: Confirmed continuation iterative refinement to solve $Ax = b$.

Input: $A \in \mathbb{Z}^{n \times n}, b \in \mathbb{Z}^n, k$. Output: $x \in \mathbb{Z}^n, 0 < q \in \mathbb{Z}$ such that $Ax = qb$.
 Compute A^{-1} . // Numeric LU decomposition
 $N_{1..n} \leftarrow 0$. // dyadic numerators
 $D \leftarrow 1$. // common denominator
 $\text{loopbound} \leftarrow 2 \times \prod_{i=1}^n \|A_i\| \times b_{\max}$.
 $r \leftarrow b$. // Residue of intermediate solutions
 $s \leftarrow 52 - \text{bitlength}(n \times \|A\|_{\infty} \times \|b\|_{\infty})$.
 $\text{thresh} \leftarrow \frac{1}{2^k}$. // Threshold for overlap confirmation
 $\hat{x} \leftarrow A^{-1}r$.
while $D < \text{loopbound}$ **do**
 $\hat{x}_{int} \leftarrow \lfloor \hat{x} \times 2^s + 0.5 \rfloor$. // Round \hat{x}_{int} entries to the nearest integer
 $\hat{x}_{frac} \leftarrow \hat{x} - \hat{x}_{int}$.
 $r \leftarrow r \times 2^s - A\hat{x}_{int}$. // Update residual
 $\hat{x} \leftarrow A^{-1}r$.
 if $\|\hat{x} - \hat{x}_{frac}\|_{\infty} > \text{thresh}$ **then**
 Shrink s , repeat iteration.
 else
 $N_{1..n} \leftarrow N_{1..n} \times 2^s + \hat{x}_{int}$. // Update dyadics
 $D \leftarrow D \times 2^s$.
 if $r = 0$ **then**
 Return: N, D as x, d .
 end if
 end if
end while
 Return: $x, d \leftarrow$ Algorithm 11 (N, D).

of a 52-bit mantissa of a double-precision floating point number, we seek to maximize the shift length to minimize the number of iteration steps. Program efficiency is the foremost improvement provided by the confirmed continuation method as compared to the residual-norm based iterative refinement.

Finding a good shift length s is a matter of starting at 1 and iteratively doubling until no overlap is evident or the hard ceiling of 52 (bit-length of mantissa of double) is reached. The absence of overlap is an indication that we obtained s or fewer bits of numeric accuracy, and to back off. Backing off requires a copy of the last successful \hat{x} , and involves the following steps. First repeat the extraction of bits using a smaller s , then recompute residual r , and finally solve against this adjusted right-hand side. We use a binary search to determine the maximum value of s that produces overlap, which sits between the failed shift length and the last successful shift length. Algorithm 15 omits these details from its sketch for the sake of conciseness; here s is instead simply initialized to a sensible starting point.

4.3.2 Overflowing doubles

If the step applying A to \hat{x}_{int} is done in double precision and produces values that cannot fit into the mantissa of a double floating point number, this operation computes an inexact residual. The next iteration would then be solving the wrong problem. This error is detected by neither the norm-based approaches nor the overlap method, since both approaches only guard against numerical inaccuracy of the partial solutions themselves. If the numeric solver itself is accurate, repeated divergence from the problem we intend to solve will be undetected. The algorithm completes after sufficiently many iterations, and reports dyadic estimates that have no hope of being reconstructed into the correct rational solution to the original problem.

To avoid this error, we employ big-integer arithmetic (using the GNU Multiprecision Arithmetic Library, GMP [46]) in the residual update, but only when necessary, specifically when $\|A\|_\infty \times \|\hat{x}_{int}\|_\infty \geq 2^{52}$, which is a conservative condition.

The matrix norm is computed beforehand, so it costs only $O(n)$ work per iteration to compute the vector norm. The flexibility of this approach both prevents the aforementioned divergent behavior and allows for the use of quicker, double precision computation of the exact residual in many cases. Our experience is that for borderline problems that require some bignum residual computation, the need is rare amongst iterations.

4.3.3 Early termination

Sometimes the numerators and denominator of the final rational solution are significantly smaller than the worst case bound computed *a priori*. When this is the case, it is possible to obtain dyadic approximants of sufficient length to reconstruct the solution before the iterative refinement would normally end. Our early termination strategy is designed to improve algorithmic running time in these cases. It is sketched in Algorithm 10.

Algorithm 10 Ov-ET: Confirmed continuation iterative refinement with Early Termination to solve $Ax = b$.

This is Algorithm 15, replacing the while loop (iterative refinement) with:

```

bound  $\leftarrow \prod_{i=1}^n \|A_i\|_2$ . // Hadamard bound
while bound < loopbound do
  while  $D < \text{bound}$  do
    while loop body of Algorithm 15.
  end while
  bound  $\leftarrow \sqrt{\text{bound} \times \text{loopbound}}$ .
   $i \leftarrow \mathbf{random}(1..n)$ . // Select random element
  if Algorithm 11 ( $N_i, D$ ) is success then
    if  $x, d \leftarrow$  Algorithm 11 ( $N, D$ ) is success then
      Return:  $x, d$ .
    end if
  end if
end while
Return:  $x, d \leftarrow$  Algorithm 11 ( $N, D$ ).

```

The core iterative refinement loop is still in place, but every so often it is stopped to attempt a rational reconstruction from the current dyadic approximation. Specifically it is initially stopped at the halfway point to the worst case bound, that is, as soon

as D is larger than the Hadamard bound for the determinant of A , which is the initial value of the name *bound* in Algorithm 10. A single-element rational reconstruction is attempted using a random element from the numerator vector N , here called N_i , and denominator D . Success on the scalar reconstruction encourages attempting a full reconstruction on the entire vector N . See Section 4.4 for details of these reconstructions. Success on the full vector reconstruction provides a speculative or guaranteed solution, depending on the reconstructed denominator and length of the dyadic approximation. Here we verify the solution by checking $Ax = b$. Upon successful verification we may terminate, saving potentially many iterations of refinement.

Upon failure to rationally reconstruct the solution on an early attempt the *bound* is set to the bitwise half-way point between itself and *loopbound*, the point at which iterative refinement would end without early termination. The new value of *bound* serves as the next checkpoint for an early termination attempt. This is a binary search that keeps reporting “go higher” after failed guesses. The strategy ensures the number of attempts is logarithmic in the number of iterations required. Also reconstruction attempts are of increasing density as the full iteration bound is approached, which address the expectation that successful early termination becomes increasingly likely. We remark that van Hoeij and Monagan [47] and Steffy [42] also use a logarithmic number of iterations but with increasing density of trials at the low numbered iterations rather than at the end, as we do. Either approach ensures good asymptotic behaviour. Which is better in practice is an open question. For good performance in practice, One might use a more uniform spacing of reconstruction trials with frequency such that reconstruction cost does not exceed a specified fraction of overall cost.

4.4 Dyadic rational to rational reconstruction

Section 4.2 highlights the similarity between numeric approximation and p-adic approximation. When it comes to the rational reconstruction, both may be expressed in terms of extended Euclidean algorithm remainder sequences. However there is a difference. In rational reconstruction from a residue and modulus, the remainder serves

as numerator and the coefficient of the residue as denominator of the approximated rational. The coefficient of the modulus is ignored. In contrast, for dyadic to rational reconstruction we use the two coefficients for the rational and the remainder serves to measure the error of approximation, as is explained next.

First consider a single entry of the solution vector. The input to the reconstruction problem is a dyadic n/d (with d a power of 2) together with a known bound B for the denominator of the approximated rational a/b . Let us say that a/b is *well approximated* by n/d if $|a/b - n/d| < 1/2d$. By this definition, n/d can never well approximate the midpoint between $(n \pm 1)/d$ and n/d . But this midpoint has larger denominator, and the rational reconstruction process described below never finds a/b when $b > d$ in any case. In the system solving application, the rational reconstruction would fail but the next iteration would compute a/b exactly and terminate with residual 0.

Proposition 1. *If two distinct fractions a/b and p/q are well approximated by n/d then $d < bq$.*

The proposition follows from the fact that $1 \leq |pb - aq|$ (nonzero integer) and the triangle inequality: $1/qb \leq |p/q - a/b| \leq |p/q - n/d| + |n/d - a/b| < 1/2d + 1/2d = 1/d$,

Proposition 2. *If a/b is well approximated by n/d and $d \geq bB$, then no other fraction with denominator bounded by B is well approximated. Also n/d well approximates at most one rational with denominator bound B when $d \geq B^2$.*

Proposition 4 follows from the previous proposition since $bq \leq bB$, when p/q is a second well approximated fraction with denominator bounded by B .

This allows for a *guaranteed* early termination (output sensitive) strategy in the numeric-symbolic iteration. In the Dixon method, early termination is a probabilistic matter (the prime used is chosen at random). It cannot be so in numeric-symbolic iteration, because there is no randomness used.

Reconstruction of the sought fraction a/b is done with the extended Euclidean algorithm remainder sequence of n, d . Define this to be (r_i, q_i, p_i) such that $r_i =$

$q_i n - p_i d$, with $q_0 = p_1 = 1$ and $q_i = p_0 = 0$. We have altered the usual treatment slightly so that p_i and q_i are positive (and strictly increasing) for $i > 1$, while the remainders alternate in sign and decrease in absolute value. Let Q be defined by Euclidean division on the remainders: $|r_{i-1}| = Q|r_i| + r$, with $0 \leq r < |r_i|$. Then the recursion is $r_{i+1} = Qr_i + r_{i-1}$, $p_{i+1} = Qp_i + p_{i-1}$, and $q_{i+1} = Qq_i + q_{i-1}$. Also the determinants $p_i q_{i+1} - p_{i+1} q_i$ are alternately 1 and -1. See e.g. [48] for properties of remainder sequences and continued fractions.

Proposition 3. *The coefficients p, q in a term (r, q, p) of the remainder sequence define a rational p/q well approximated by n/d and denominator bounded by B if and only if $2|r| < q \leq B$.*

This follows from $r = qn - pd$ so that $|r|/qd = |p/q - n/d| < 1/2d$ (and $q \leq B$ by hypothesis).

Proposition 4. *Given n, d, B , let (r, q, p) be the last term such that $q < B$ in the remainder sequence of n, d . This term defines the best approximated B bounded fraction p/q of any term in the remainder sequence.*

When n/d well approximates a rational a/b and $d < bB$ then $a/b = p/q$, i.e. is defined by this term of the remainder sequence.

This follows because $|r|$ is decreasing and q increasing in the remainder sequence. The claim that the rational will be found in the remainder sequence follows from Theorem 4.4 in [35]. Half extended gcd computation computation $((r, q)$ rather than (r, q, p)) lowers the cost, with p computed post hoc only for the term of interest.

When this last term below the bound defines a well approximated rational p/q , i.e. $2|r| < q$, we say we have a “guaranteed” reconstruction. When that is not the case, it is still possible that we have found the correct rational. As mentioned in the previous section, sometimes by good luck this leads to successful solutions even when the iteration has not proceeded far enough to have a guaranteed well approximated answer.

Thus we may offer the last approximant from the remainder sequence with denominator bounded by B . It is speculative if $d > bB$ and guaranteed to be the unique solution otherwise. It is never necessary to go beyond $d = B^2$. As the experiments attest, trial reconstructions during the numeric iteration process, can be effective at achieving early termination. The vector reconstruction described next helps keep the cost of these trials low.

To construct a solution in the form of a vector of numerators $x \in \mathbb{Z}^n$ and common denominator q from a vector of $n \in \mathbb{Z}^n$, and common (power of 2) denominator d , we can often avoid reconstructing each entry separately with a remainder sequence computation. We compute x_i as $x_i = [n_i q / d]$. In other words, x_i is the quotient in the division $n_i q = x_i d + r$, with $-d/2 < r < d/2$. The error of the approximation is then $|x_i/q - n_i/d| = r/qd$. If this error is bounded by $1/2d$, x_i/q is well approximated by n_i/d . Thus we have a well approximated result if and only if $2r < q$. When single division fails to produce a well approximated x_i/q , resort to a full remainder sequence. This leads to the following algorithm.

The first loop discovers new factors of the common denominator as it goes along. In practice one or two full reconstructions are needed and the remainder are done by the single division before the if statement. The backward propagation of new factors is delayed to the second loop, to avoid a quadratic number of multiplications. In the worst case this algorithm amounts to n gcd computations. In the best case it is one gcd and $n - 1$ checked divisions with remainder. Experimentally we have encountered essentially the best case, with a very few full gcd computations.

To our knowledge, prior algorithms do not assume n/d well approximates (to accuracy $1/2d$) and so do not exploit the guarantee of uniqueness as we do, particularly when using the early termination strategy. However, Cabay [49] gave a guarantee of early termination based on a sufficiently long sequence of iterations resulting in the same reconstructed rational. This was in the context of Chinese remaindering, but should apply to numeric-symbolic iteration as well.

Algorithm 11 Vector DyadicToRational

Input: $N \in \mathbb{Z}^n, D \in \mathbb{Z}$. Output: $x \in \mathbb{Z}^n, 0 < d \in \mathbb{Z}$, flag, such that flag is “fail” or N/D well approximates x/d and flag is “speculative” or “guaranteed”.

$d \leftarrow 1$.

for i from 1 to n **do**

$x_i \leftarrow \lfloor N_i q / d \rfloor$.

if x_i fails the well approximation test **then**

$x_i, d_i, \text{flag} = \text{ScalarDyadicToRational}(N_i, D)$.

if flag = “fail”, return “fail”.

 Compute the factorizations $d = a_i g, d_i = b_i g$, where $g = \text{gcd}(d, d_i)$. The new common denominator is $d \leftarrow a_i d_i$, so set $x_i \leftarrow x_i \times a_i$. Prior numerators must be multiplied by b_i . Enqueue b_i for that later.

end if

end for

$B \leftarrow 1$.

for i from n down to 1 **do**

$x_i \leftarrow x_i \times B$;

if $b_i \neq 1$ **then**

$B \leftarrow B \times b_i$.

end if

end for

return x, d, flag . [If any scalar reconstruction was speculative, flag = “speculative”, otherwise flag = “guaranteed”.]

4.5 Experiments

For test matrices, we use the following 8 matrix families $H_n, J_n, Q_n, S_n, m_n, M_n, R_n, Z_n$ described next.

H_n : The inverse of the $n \times n$ Hilbert matrix. This is a famously ill-conditioned matrix. The condition number of H_n

$$\kappa(H_n) = \|H_n\|_2 \|H_n^{-1}\|_2 \approx c 33.97^n / \sqrt{n}$$

where c is a constant, is quoted in [50]. We find that our numeric solvers – both the residual norm based and the overlap confirmed continuation approach – can handle this matrix only up to $n = 11$. On the other hand, Dixon’s p -adic iteration can handle any size, provided p is chosen large enough to insure the nonsingularity of $H_n \pmod p$. For instance, Dixon does the $n = 100$ case in 12 seconds. This class is introduced only to illustrate the potential for numeric solver failure due to ill-condition.

J_n : This matrix is twice the $n \times n$ Jordan block for the eigenvalue $1/2$. We multiply by 2 to get an integer matrix. It is a square matrix with 1’s on the diagonal, and 2’s on the first subdiagonal. Numerical computations for matrices with repeated eigenvalues are notoriously difficult. The inverse matrix contains $(-2)^j$ on the j -th subdiagonal. For $n > 1023$, the matrix J_n^{-1} is not representable in double precision (infinity entries), and for smaller n it poses numerical challenges.

Table 4.1 shows that the numeric-symbolic solvers are faster than the p -adic lifting when they work, but they have difficulties with J_n .

For n larger than 1023, infinities (numbers not representable in double precision) defeat all numeric solving. The bottom left entry of J_n^{-1} is 2^{n-1} which is not representable when $n \geq 1024$. However, the overlap solver fails at $n = 1023$. Although the inverse matrix itself is just barely representable, some numbers which occur in the matrix-vector products are not representable in this case.

Q_n : Let $Q_n = DLD$, where L is the $n \times n$ Lehmer matrix [51, 52], with elements $L_{i,j} = \min(i, j) / \max(i, j)$, and D is the diagonal matrix with $D_{i,i} = i$. Thus Q is an

Table 4.1: Dixon is p-adic iteration, Wan is numeric-symbolic iteration using residual norm based continuation, Overlap is the confirmed continuation method we present here.. Times are in seconds.

Examples of numeric failure to converge			
matrix	Dixon	Wan	Overlap
J_{994}	2.27	1.77	0.0850
J_{995}	2.23	fail	0.0920
J_{1022}	2.40	fail	0.100
J_{1023}	2.38	fail	fail
J_{2000}	13.3	fail	fail
Q_{500}	2.07	fail	0.81
Q_{1000}	15.0	fail	7.29
Q_{2000}	121	fail	70.3
Q_{4000}	1460	fail	633

integral Brownian matrix [53] with $Q_{i,j} = \min(i, j)^2$ (“ Q ” is for quadratic). A closed form expression, $\det(Q_n) = 2^{-n}(2n)!/n!$ follows from [54].

Note that $Lx = b$ iff $x = Dy$ and $Qy = Db$ (also $De_1 = e_1$). Being an integer matrix, Q fits in our experimental framework while rational L does not.

Table 4.1 includes Q_n measurements concerning numeric difficulties. In his recent experiments, Steffy [42] used the Lehmer matrix as an example where Dixon’s method works but numeric-symbolic iteration does not. We include it here because it shows a striking difference between residual norm based continuation and overlap confirmed continuation in numeric-symbolic iteration. In fact, Wan’s code in LINBOX fails on Q_n for $n > 26$.

The examples of Q_n along with the remaining five classes of examples are used for our performance study shown in Table 4.2. These test cases are in many collections of matrices used for testing. A notable such collection was used by Steffy [42].

Three of our test matrices (Q_n , m_n , and M_n) are Brownian matrices [53] in that they have an “echelon” structure: that is, the elements obey $b_{i,j+1} = b_{i,j}$, $j > i$, and $b_{i+1,j} = b_{i,j}$, $i > j$, for all i, j . Many Brownian matrices have known closed form

results for inverses, determinants, factorization, etc. One source of special results is the following observation [53]. If the matrix P is taken to be a Jordan block corresponding to a repeated eigenvalue of -1 , then PBP^T is tridiagonal if and only if B is Brownian.

S_n : The $n \times n$ Hadamard matrix using Sylvester's definition. $S_1 = (1)$, $S_{2n} = \begin{pmatrix} S_n & S_n \\ S_n & -S_n \end{pmatrix}$. This definition results in n being a power of two. The determinant of S_n equals $n^{n/2}$, which is sharp for the Hadamard bound. Thus, for any integral right hand side, the solution is a dyadic rational vector. This provides a test of early termination due to a zero residual.

m_n : The $n \times n$ matrix with $m_{i,j} = \min(i, j)$. Because this a Brownian matrix[53], PBP^T is tridiagonal, and in this case, the tridiagonal matrix is the identity matrix. Thus, determinant of m_n is 1, so the solution is integral for any integral right hand side. This is another case where early termination due to zero residual is expected. But the entries in the inverse are larger than in the Hadamard matrix case, so more iterations may be needed for this example.

M_n : The $n \times n$ matrix with $M_{i,j} = \max(i, j)$. The determinant of this matrix is $(-1)^{n+1}n$, so the solution vector has denominator much smaller than the Hadamard bound predicts. The determinant of M_n is found by reversing its rows and columns, which does not change its determinant. The result is a Brownian matrix. Its tridiagonal form using the matrix P is the identity matrix — except for the value $(-1)^n n$ in the upper left corner.

The previous three test cases can benefit from early termination. Q_n and the following 2 are expected to benefit less from output sensitivity.

R_n : An $n \times n$ matrix with random entries in $(-100, 100)$.

Z_n : An $n \times n$ $\{0, 1\}$ -matrix with probability 1/2 of a 1 in a given position. This is meant to represent some commonly occurring applications. The LINBOX library is often used to compute Smith forms of incidence matrices, where invariant factor computation involves solving linear systems with random right hand sides.

Reported are run times on a 3.0 GHz Intel Pentium D processor in a Linux

2.6.32 environment. All codes used are in LINBOX as of svn revision 3639, and have since been included in the official LINBOX release. The experiments were run with right hand sides being e_1 , the first column of the identity matrix. This provides a direct comparison to Steffy’s examples [42] and in some cases allows checking a known solution formula. But for Q_n , M_n , and Z_n , the right hand sides used are random with entries in $(-100, 100)$. This is to create an interesting early termination situation in the case of Q_n and M_n (where the solution for rhs e_1 is obtained in the first iteration). For Z_n it is in view of the expected application.

S_{2^k} and m_n are examples where the determinant is a power of two and considerably less than the Hadamard bound. Thus an early termination due to a perfect dyadic expansion with residual zero can occur and no rational reconstruction is needed. Both forms of the Overlap algorithm verify this. The current implementation of Wan’s method does not check for an exactly zero residual, though there no reason it could not. The determinant (thus the denominator of solution vector) of S_n is $n = 2^k$ and the Hadamard bound is considerably larger, $n^{n/2}$. Output sensitive termination due to zero residual accounts for the factor of 10 or more speedups. The determinant of m_n is 1 and the Hadamard bound is larger than that of S_n . For right hand side e_1 the solution vector is $2e_2 - e_1$ so that essentially no iteration is required if early termination (Dixon) or zero residual detection (Overlap) is used. In these cases all the time is in matrix factorization which is about 4 times more costly modulo a prime (Dixon) than numerically using LAPACK (Overlap). Wan’s implementation lacks the early termination, thus performs a full iteration. That more than offsets the faster matrix factorization than in Dixon, making Wan’s implementation slowest for solving with the m_n family.

M_n and Q_n results show early termination saving a factor of about 2, the most available with sufficient dyadic approximation for a guaranteed rational reconstruction. Further speedup is possible from very early speculative reconstructions. We have not explored this.

In the data for the random entry matrix, R_n , and random $\{0, 1\}$ -matrix, Z_n , we

see variable speedups up to a factor of 1.8 over Dixon's p-adic lifting, sometimes slightly aided by early termination. Significant early termination is not generally expected for these matrix families.

The overlap method works well with sparse numeric solvers (both direct and iterative), those designed to solve systems where A is sparse. We have begun incorporating popular sparse numeric system solvers from packages such as SuperLU [55] and MATLAB. With these solvers, performance asymptotically better than Dixon's method can be expected. Figure 4.1 charts running time of an example computation comparing the competing dense and sparse exact solvers. The systems used in this example range from very sparse to barely sparse, increasing density along the x-axis of the chart. One may notice the crossover points between dotted and solid lines indicating the threshold for switching away from sparse specializations. The significant symbolic competition to sparse numeric-symbolic will be the method of Eberly, et al. [56].

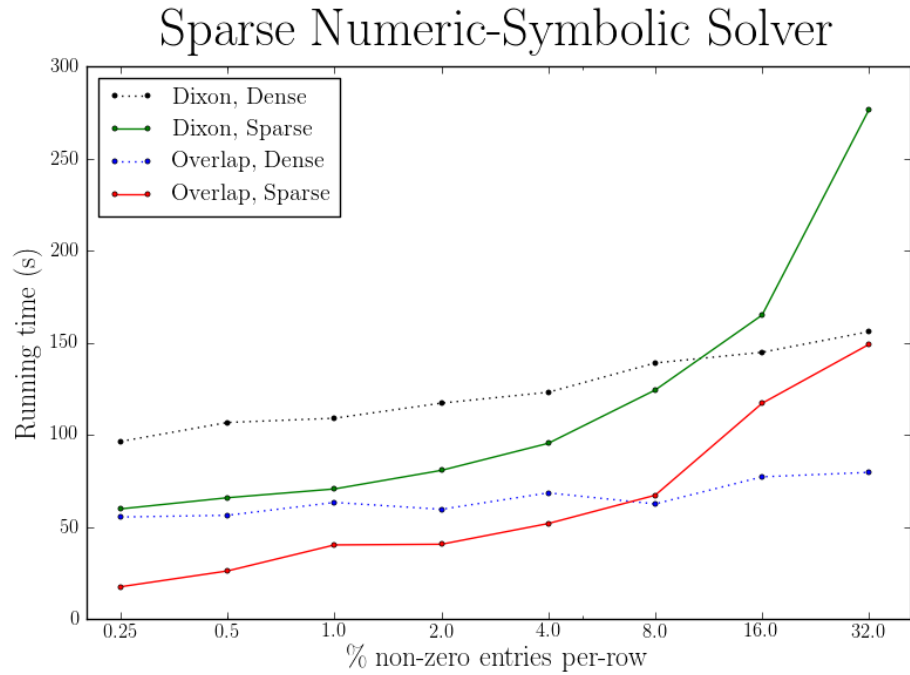


Figure 4.1: Dense and sparse system performance comparison between the Overlap method and Dixon’s method. The measurements are of time taken to solve systems order 2000, with randomly generated entries in $\{-100,100\}$ filling each row at the densities listed on the x-axis. There are two pairs of measurements, Dixon’s method (upper pair) and Overlap method (lower). The dotted lines in each case denote runtime of the standard dense approach, while the solid lines measure a specialization for sparse matrices. In the case of the numeric-symbolic solver, this specialization is specifically the use of SuperLU as the numeric solver.

Table 4.2: Dixon, Wan, and Overlap columns are as in Table 4.1. Ov-ET is Overlap with with early termination enabled. “mem” denotes out of memory. Times are in seconds.

Algorithm performance comparisons				
Matrix	Dixon	Wan	Overlap	Ov-ET
S_{512}	0.728	0.711	0.0723	0.0721
m_{500}	1.28	1.34	0.273	0.273
M_{500}	1.46	fail	1.06	0.562
Q_{500}	2.41	fail	2.98	1.39
R_{500}	1.09	1.04	1.05	0.931
Z_{500}	0.793	0.864	0.584	0.580
S_{1024}	4.58	4.75	0.380	0.371
m_{1000}	8.83	10.8	2.24	2.24
M_{1000}	10.2	fail	8.56	4.42
Q_{1000}	16.6	fail	24.5	17.4
R_{1000}	7.25	fail	6.87	6.48
Z_{1000}	6.04	6.38	4.41	4.46
S_{2048}	32.3	36.6	2.08	2.10
m_{2000}	72.0	89.6	17.1	17.0
M_{2000}	82.8	fail	75.0	37.8
Q_{2000}	137	fail	243	167
R_{2000}	54.6	fail	53.7	49.3
Z_{2000}	45.4	52.15	35.8	34.1
S_{4096}	255	297	11.7	11.7
m_{4000}	579	783	138	138
M_{4000}	628	fail	658	319
Q_{4000}	1519	fail	3274	2294
R_{4000}	380	fail	393	397
Z_{4000}	340	439	318	271
S_{8192}	2240	2517	77.6	82.6
m_{8000}	mem	6802	1133	1138
M_{8000}	mem	fail	6170.6	3049
Q_{8000}	mem	fail	33684	27367
R_{8000}	mem	fail	2625	2710
Z_{8000}	mem	5771	2584	2474

4.6 Summary

In this chapter we detailed a history of leading approaches to the problem of solving a rational linear system exactly. Specifically we compared and contrasted Dixon’s p-adic lifting algorithm with Wan’s numeric-symbolic iteration. The two schemes are asymptotically equivalent, with the numeric-symbolic approach likely to be faster on most problems due to the advantages of floating point arithmetic versus intermediate exact computations. However, the (only well-known) implementation of Wan’s idea in LINBOX was hardly reliable for a wide class of input problems. We addressed this shortcoming, simultaneously improving runtime performance, with our overlap method to provide *confirmed-continuation* of the algorithm. The key reason this improvement was successful is that it is adaptive to the level of accuracy provided by the numeric solver, and is much less pessimistic regarding intermediate results. Additionally, the improved rational reconstruction component allows for output-sensitive, speculative or guaranteed early termination, which has also been shown beneficial to certain examples. Having a robust rational system solver is not only an important routine to be used directly, but also an important kernel used by many solutions that LINBOX provides, for example computing null space basis, the last invariant factor, or the Smith normal form. Many applications stand to benefit from our improvement to the performance and stability of the numeric-symbolic solver.

Chapter 5

SUMMARY

In this thesis we have used LINBOX as a vehicle for developing solutions to select exact linear algebra problems. These solutions have in some cases improved on the performance of preexisting approaches, and in other cases enabled computation of previously unexplored problems. As computing hardware is advancing, so too must exact computational linear algebra's algorithms and computational methods.

In Chapter 2 we have markedly improved arithmetic over small prime finite fields in LINBOX. Performing faster arithmetic over these fields lends performance to the many algorithms in exact linear algebra of which field arithmetic is a building block.. These improvements have not only improved wall-clock performance on the bare hardware, but also lowered the memory requirements for storing the finite field data. Both benefits stand to help future LINBOX developers push the boundaries on the scope of computable problems. First, we outlined the more widely-known compression, bit-packing, which is quite flexible and even extendible. Our primary extension, that of *semi-normalization* has proven significantly more efficient for certain small-prime fields. Next, we detailed the lesser-known strategy of bit-slicing for \mathbb{F}_3 in LINBOX and demonstrated that it is without a doubt the state of the art in representing matrices consisting of this particular field's elements. We provide an implementation of these compression methods in LINBOX. We have demonstrated the efficacy of these compression schemes with repeatable experiments containing dependably regular performance improvements.

An immediate application of these advancements in finite field arithmetic appeared in Chapter 3. Here we calculated the 3-rank of a $3^{16} \times 3^{16}$ matrix, which involved computing with over 1.85 peta-entries. This project relied every bit on the efficient

compression schemes, but also required the development of a novel Monte Carlo algorithm when preexisting solutions proved to run too long or ballooned memory usage too large. Additionally, various flavors of parallelism were needed to solve this problem, especially considering the number of times the computation needed to be restarted due to bugs, oversights, heuristic adjustments, and the like. These failures that happened along the way taught valuable lessons about distributed computing algorithm design, especially when storing large amounts of data is an algorithmic requirement.

Specifically three types of parallelism were triumphantly melded together in order to solve this large problem. First, the word-level parallelism of bit-slicing ensured that each CPU cycle devoted to finite-field arithmetic was computing on sixty-four values at a time. Second, as the subject matrix of our rank calculation was not stored *a priori* but generated on-demand by a position-independent formula, shared-memory parallelism was employed. This was an ideal solution to quickly generating the needed matrix entries, especially considering our access to a super computer with highly efficient, 48-core nodes. Finally, speaking in terms of managing both long running time and large memory demands, a distributed decomposition or “chunking” of the problem into units of work manageable by these compute nodes was an absolute necessity. The goal was to spread computation, and by extension storage responsibility, to as many compute nodes as possible. To accomplish this delegation of tasks, an RPC-based, master-slave, work-queueing framework was developed and successfully employed.

In Chapter 4 I describe and evaluate the new, state of the art, numeric-symbolic rational linear system solver that we created. For many cases of wanting an exact solution to a linear system, our solver performs better than the previously leading exact algorithm, Dixon’s method. In all cases, the new solver outperforms and is less sensitive to troublesome input problems than its immediate predecessor, Wan’s numeric-symbolic method. The difference of the new method is what we call *confirmed-continuation*, which is a method of detecting optimistic overlap between iterations of the solver. In any case, the modularization of the highly-tuned numeric linear algebra kernel we choose to use ensures we can always integrate with the bleeding-edge of

scientific research in floating-point linear algebra. Many of these kernels have been specialized for specifically structured input, providing a great degree of flexibility in efficiently solving different systems exactly. Solving rational linear systems is a key solution offered by LINBOX to its users.

5.1 Future Work

With the foundations in place that have been vetted to solve known large problems, the final goal for bit-packing and bit-slicing implementations is to provide a clean, usable interface so that many LINBOX kernels and developers can take advantage of these new data representations. Hand-vectorizing the arithmetic loops employed by these compression schemes will certainly pay off, especially as chip manufacturers continue to push wider and wider registers and vectorization instruction sets. Regarding the large 3-rank problem, the new theoretical algorithm and implemented parallel framework are general enough to apply to graph families similar to Dickson, where the sequence of ranks is also sought. Each of these cases may require tweaking of the heuristic approach used to compress the rank of the large matrix into a manageable block size. Ever-larger computations will follow, in lock-step with the improvements to hardware and abundance of memory and disk storage space. Having arrived at the rank of $D(3, 8)$ in a few days, the asymptotic complexity suggests we can expect ongoing computations to take on the order of months to complete. It is truly exciting to push ever forward with this framework.

BIBLIOGRAPHY

- [1] J-G. Dumas, T. Gautier, M. Giesbrecht, P. Giorgi, B. Hovinen, E. Kaltofen, B. D. Saunders, W. Turner, and G. Villard. Linbox: A generic library for exact linear algebra. In *ICMS'02*, pages 40–50, 2002.
- [2] M. Flynn. Some computer organizations and their effectiveness. *Computers, IEEE Transactions on*, C-21(9):948–960, Sept 1972.
- [3] Brian W. Kernighan and Dennis M. Ritchie. *The C Programming Language*. Prentice Hall Professional Technical Reference, 2nd edition, 1988.
- [4] P.J. Plauger, Meng Lee, David Musser, and Alexander A. Stepanov. *C++ Standard Template Library*. Prentice Hall PTR, Upper Saddle River, NJ, USA, 1st edition, 2000.
- [5] T. J. Boothby and R. W. Bradshaw. Bitslicing and the Method of Four Russians Over Larger Finite Fields. *ArXiv e-prints*, January 2009.
- [6] Martin Albrecht, Gregory Bard, and William Hart. Efficient multiplication of dense matrices over $\text{gf}(2)$. *CoRR*, abs/0811.1714, 2008.
- [7] Martin Albrecht and Gregory Bard. *The M4RI Library – Version 20100817*. The M4RI Team, 2010.
- [8] Jeffrey Sheldon, Walter Lee, Ben Greenwald, and Saman Amarasinghe. Strength reduction of integer division and modulo operations. In HenryG. Dietz, editor, *Languages and Compilers for Parallel Computing*, volume 2624 of *Lecture Notes in Computer Science*, pages 254–273. Springer Berlin Heidelberg, 2003.
- [9] B. David Saunders and Bryan S. Youse. Large matrix, small rank. In *Proceedings of the 2009 international symposium on Symbolic and algebraic computation*, In Proc. of ISSAC 2009, pages 317–324, New York, NY, USA, 2009. ACM.
- [10] J G Dumas and G Villard. Computing the rank of large sparse matrices over finite fields. In *CASC'2002 Computer Algebra in Scientific Computing*, pages 22–27. Springer-Verlag, 2002.
- [11] B. A. LaMacchia and A.M. Odlyzko. Solving large sparse linear systems over finite fields. *Lecture Notes in Computer Science*, 537:109–133, 1991.

- [12] J-G. Dumas, B. D. Saunders, and G. Villard. Smith form via the valence: Experience with matrices from homology. In *Proc. of ISSAC'00*, pages 95–105. ACM Press, 2000.
- [13] J.-C. Faugère. Parallelization of Gröbner basis. In H. Hong, editor, *PASCO'94*, volume 5 of *Lecture notes series in computing*, pages 109–133, 1994.
- [14] Guobiao Weng, Weisheng Qiu, Zeying Wang, and Qing Xiang. Pseudo-paley graphs and skew hadamard difference sets from presemifields. *Designs, Codes and Cryptography*, 44(1-3):49–62, 2007.
- [15] J.P May, B.D. Saunders, and Z. Wan. Efficient matrix rank computation with application to the study of strongly regular graphs. In *In Proc. of ISSAC 2007*, pages 277–284. ACM Press, 2007.
- [16] Q. Xiang. Recent progress in algebraic design theory. *Finite Fields and Their Applications*, 11:622–653, 2005.
- [17] T. Cormen, C. Leiserson, R. Rivest, and C. Stein. *Introduction to Algorithms, Second edition*. MIT Press, 2001.
- [18] D. Wiedemann. Solving sparse linear equations over finite fields. *IEEE Trans. Inform. Theory*, 32:54–62, 1986.
- [19] E. Kaltofen and B. D. Saunders. On Wiedemann’s method of solving sparse linear systems. In *Applied Algebra, Algebraic Algorithms and Error-Correcting Codes*, volume 539 of *LNCS*, pages 29–38, 1991.
- [20] E. Kaltofen. On probabilistic analysis of randomization in hybrid symbolic-numeric algorithms, http://www4.ncsu.edu/~kaltofen/bibliography/07/K07_owr_abs.pdf. In *Oberwolfach Reports*, volume 4, 2007.
- [21] G. Cooperman and G. Havas. Elementary algebra revisited: Randomized algorithms. In P. Pardalos, S. Rajasekaran, and J. Rolim, editors, *Proc. of DIMACS Workshop on Randomization Methods in Algorithm Design*, number 43 in DIMACS Series in Discrete Mathematics and Theoretical Computer Science, pages 37–44. AMS, Providence, RI, 1998.
- [22] L. Chen, W. Eberly, E. Kaltofen, W. Turner, B. D. Saunders, and G. Villard. Efficient matrix preconditioners for black box linear algebra. *LAA 343-344, 2002*, pages 119–146, 2002.
- [23] W. Turner. Preconditioners for singular black box matrices. In *Proc. of ISSAC'05*, pages 332–339, New York, NY, USA, 2005. ACM Press.
- [24] E. Kaltofen and B. D. Saunders. On Wiedemann’s method of solving sparse linear systems. In *Proc. AAECC-9*, volume 539 of *Lect. Notes Comput. Sci.*, pages 29–38. Springer Verlag, 1991.

- [25] J.T. Schwartz. Fast probabilistic algorithms for verification of polynomial identities. *J. ACM*, pages 27:701–717, 1980.
- [26] R. Zippel. Interpolating polynomials from their values. *J. Symb. Comp.*, 9(3):375–403, 1990.
- [27] S. L. Ma. A survey of partial difference sets. *Designs, Codes and Cryptography*, 4:221–261, 1994.
- [28] Thierry Gautier, Jean-Louis Roch, and Gilles Villard. Givaro, a C++ for algebraic computations. <http://givaro.forge.imag.fr>.
- [29] Edsger W. Dijkstra. The origin of concurrent programming. chapter Cooperating sequential processes, pages 65–138. Springer-Verlag New York, Inc., New York, NY, USA, 2002.
- [30] William Gropp, Ewing Lusk, and Anthony Skjellum. *Using MPI (2Nd Ed.): Portable Parallel Programming with the Message-passing Interface*. MIT Press, Cambridge, MA, USA, 1999.
- [31] Bryan Youse. Finite field/rank code suite. <https://bitbucket.org/bryouse/finite-field-rank-suite>.
- [32] OpenMP Architecture Review Board. OpenMP application program interface version 3.0, May 2008.
- [33] Donald E. Knuth. *The Art of Computer Programming, Volume 2 (3rd Ed.): Seminumerical Algorithms*. Addison-Wesley Longman Publishing Co., Inc., Boston, MA, USA, 1997.
- [34] Zhengdong Wan. An algorithm to solve integer linear systems exactly using numerical methods. *Journal of Symbolic Computation*, 41:621–632, 2006.
- [35] Zhengdong Wan. *Computing the Smith Forms of Integer Matrices and Solving Related Problems*. PhD thesis, University of Delaware, Newark, DE, 2005.
- [36] Keith O. Geddes and Wei Wei Zheng. Exploiting fast hardware floating point in high precision computation. In J. Rafael Sendra, editor, *ISSAC*, pages 111–118. ACM, 2003.
- [37] Alicja Smoktunowicz and Jolanta Sokolnicka. Binary cascades iterative refinement in doubled-mantissa arithmetics. *BIT*, 24(1):123–127, 1984.
- [38] Andrzej Kielbasiński. Iterative refinement for linear systems in variable-precision arithmetic. *BIT*, 21(1):97–103, 1981.
- [39] J. D. Dixon. Exact solution of linear equations using p -adic expansion. *Numer. Math.*, pages 137–141, 1982.

- [40] Nicholas J. Higham. *Accuracy and Stability of Numerical Algorithms*. Society for Industrial and Applied Mathematics, Philadelphia, PA, USA, 2nd edition, 2002.
- [41] James H. Wilkinson. *Rounding Errors in Algebraic Processes*. Dover Publications, Incorporated, 1994.
- [42] Daniel Steffy. Exact solutions to linear systems of equations using output sensitive lifting. *ACM Communications in Computer Algebra*, 44(4):160–182, 2010.
- [43] The LinBox Team. LinBox, a C++ library for exact linear algebra. <http://www.linalg.org/>.
- [44] Z. Chen and A. Storjohann. A BLAS based C library for exact linear algebra on integer matrices. In *Proc. of ISSAC'05*, pages 92–99. ACM Press, 2005.
- [45] T. Mulders and A. Storjohann. Certified dense linear system solving. *Journal of symbolic computation*, 37(4), 2004.
- [46] Torbjörn Granlund and the GMP development team. *GNU MP: The GNU Multiple Precision Arithmetic Library*, 5.0.5 edition, 2012. <http://gmplib.org/>.
- [47] Mark van Hoeij and Michael B. Monagan. A modular gcd algorithm over number fields presented with multiple extensions. In Teo Mora, editor, *ISSAC*, pages 109–116. ACM, 2002.
- [48] Joachim Von Zur Gathen and Jurgen Gerhard. *Modern Computer Algebra*. Cambridge University Press, New York, NY, USA, 2 edition, 2003.
- [49] Stanley Cabay. Exact solution of linear equations. In *Proceedings of the second ACM symposium on Symbolic and algebraic manipulation*, SYMSAC '71, pages 392–398, New York, NY, USA, 1971. ACM.
- [50] Bernhard Beckermann. The condition number of real Vandermonde, Krylov and positive definite Hankel matrices. *Numerische Mathematik*, 85:553–577, 1997.
- [51] John Todd. *Basic Numerical Mathematics, Vol. 2: Numerical Algebra*. Birkhäuser, Basel, and Academic Press, New York, 1977.
- [52] D. H. Lehmer. Solutions to problem E710, proposed by D. H. Lehmer: The inverse of a matrix, November 1946.
- [53] M. J. C. Gover and S. Barnett. Brownian matrices: properties and extensions. *International Journal of Systems Science*, 17(2):381–386, 1986.
- [54] E. Kilic and P. Stanica. The Lehmer matrix and its recursive analogue. *Journal of Combinatorial Mathematics and Combinatorial Computing*, 74(2):195–205, 2010.
- [55] *SuperLU User's Guide*: <http://www.nersc.gov/~xiaoye/SuperLU/>, 2003.

- [56] W. Eberly, M. Giesbrecht, P. Giorgi, A. Storjohann, and G. Villard. Solving sparse rational linear systems. In *Proc. of ISSAC'06*, pages 63–70. ACM Press, 2006.

Appendix A

REMOTE OBJECTS WITH PYRO

Setting up objects for remote procedure calls is made easy by the PyRO (Python Remote Objects) package. The scenario is that the master Python script from Section 3.3.3.1 wants to share the **BlockManager** object across the network to machines that will serve as workers (be they producers or consumers). The code to set this up is a simple snippet:

```
import Pyro4

... define BlockManager ...

# make a Pyro daemon
daemon=Pyro4.Daemon(host="chimera.cis.udel.edu")
# find the name server
nameserver=Pyro4.locateNS("chimera.cis.udel.edu")

manager=BlockManager() # the central, shared manager

uri=daemon.register(manager) # register as a PyRO object
ns.register("manager", uri) # register in the name server

daemon.requestLoop() # event loop server; wait for remote calls
```

There are two components at play here. First, creating a daemon and registering the **BlockManager** object with this daemon. The daemon is then started; here PyRO loops indefinitely, waiting for remote hosts to connect. Second, registering the object with a PyRO *name server*. The name server is a separate process, started independently, that maps the long URI PyRO allocates for our object to an easy-to-remember name. This is the same concept behind the broadly used DNS system on the Internet, which relates numeric IP addresses into memorable hostnames. Thus, instead of a long

string of seemingly random characters, remote workers can simply ask the name server for **"manager"**. Here we show the name server is running on the same host as our daemon, but that need not be the case.

Now, all that is left is for clients to retrieve the object for remote procedure calls:

```
import Pyro4

# find the name server
nameserver=Pyro4.locateNS("chimera.cis.udel.edu")
uri=nameserver.lookup("manager")
manager=Pyro4.Proxy(uri)
```

Here, we query the nameserver for the common name we allocated to this object during the set-up above, **"manager"**. We receive the URI and then can obtain a proxy for this object. At the end of this snippet, **manager** is, for all intents and purposes, the single remote instance of **BlockManager** as created by the master script. Its methods (e.g. **get_work()**) can be called as though it were a local object. In this fashion, modifications of the object's queues will automatically propagate to all remote workers, enabling seamless work-sharing without the threat of work duplication.

Appendix B

\mathbb{F}_3 BIT-SLICING “STEPPER”

As explained in Section 2.3 and specifically demonstrated by Algorithm 5, bit-slicing data is an involved process containing pointer arithmetic, bit-shifting and masking operations. When initializing a bit-sliced matrix or vector, it would be no quick and simple task, computationally speaking, to perform calls to LINBOX’s `setEntry()` for each \mathbb{F}_3 element to be encoded. This is where the concept of a “Stepper” comes in. Rather than insert elements entry-by-entry, insertions can be pooled until there are enough of them to fill up the *sliced words*. Again, *sliced words* are the machine words comprising *sliced units*, which themselves are the building blocks of bit-slicing. A class which is intended to be subclassed is used for this purpose:

```
class Stepper {  
    public:  
        inline void step(uint8_t e) {  
            _store[_i--] = e;  
            if(_i > _width) flush();  
        }  
  
        virtual inline void flush() = 0;  
  
        inline void row(){  
            if(_i != _width-1) flush();  
        }  
  
    private:  
        uint8_t* _store;  
        size_t _i;  
        size_t _width;  
};
```

The **Stepper** interface contains three functions:

- **step**: Takes an \mathbb{F}_3 value (representable with a byte) as the sole argument. It stores this value in a local array called `_store` which is to store the exact same number of values as our bit-sliced machine word has bits (in general, 64). If this array fills up, it is flushed:
- **flush**: This does the heavy lifting of the **Stepper**, and is delegated to subclasses for customization. It performs a bulk operation using the pooled \mathbb{F}_3 data contained in `_store`.
- **row**: This forces a `flush()` call in the event we are stepping through a matrix data structure and have reached the end of a row.

With this simple interface in mind, let's examine how an actual bit-sliced matrix might be populated by examining a subclass of **Stepper**:

```

template<class Matrix>
class SlicedMatrixStepper : public Stepper {
    typedef typename Matrix::RawIterator RawIterator;
    typedef typename Matrix::SlicedUnit SlicedUnit;

public:
    SlicedMatrixStepper(Matrix &A) : _r(_A.rawBegin()) {
        _width = sizeof( typename Matrix::Domain::Word_T ) * 8;
        _i = _width - 1;
        _store = new uint8_t[_width];
    }

    inline void flush() {
        SlicedUnit &t = (*_r);
        t.zero();
        for(size_t i = _i + 1; i < _width; ++i) {
            t <<= 1;
            t.b1 |= ((_store[i] & 2) >> 1);
            t.b0 |= ((_store[i] & 1) | t.b1);
        }
        _i = _width-1;
        ++_r;
    }

private:
        RawIterator _r;
};

```

Here, we define a constructor that accepts a bit-sliced matrix as argument. These matrices have the concept of a **RawIterator**, which will cycle through each entry of the matrix, component-wise. In the case of bit-sliced matrices, each component is a *sliced unit*, thus generally encompasses 64 entries. The constructor sets up the private data members we saw introduced in the “interface” code listing.

Finally we see a definition of **flush()**. Here we take the data from our storage array **_store** and insert it into our matrix (by way of a temporary *sliced unit* that we accessed via our raw-iterator). Flushing our cache of data in this manner means we do not have to negative-mask and zero out data prior to the actual insertion step. We simply shift our *sliced unit* a single bit to the left and logical-OR in the new data. Upon finishing our flush, we increment our iterator and reset our counter, **_i**.

B.1 File-stepper

The second implementation of the “Stepper” interface has to do with writing data from a source directly to file. The format of this file is pure bit-sliced data. These files are encoded in a purely binary format, even without metadata, and only make sense to be interpreted as bit-sliced matrices when read back into memory later. This functionality was almost necessary, and highly desirable, when dealing with the just-in-time data generated in Section 3.3. Being able to write essentially stream data directly to file without first populating a matrix within main memory enabled many machines to pitch into the data generation efforts, which would otherwise be limited by their memory capacity. Here is a listing of the **FileStepper** class:

```

#include <fstream>
template<class Matrix>
class FileStepper : public Stepper {
    typedef typename Matrix::SlicedUnit SlicedUnit;

public:
    FileStepper(const char * filename="filestep.bin") {
        out.open(filename, ios::out | ios::binary);
        _width = sizeof( typename Matrix::Domain::Word_T ) * 8;
        _i = _width - 1;
        _store = new uint8_t[_width];
    }

    ~FileStepper() { out.close(); }

    virtual inline void flush(){
        SlicedUnit t;
        t.zero();
        for(size_t i = _i + 1; i < _width; ++i){
            t <<= 1;
            if(_store[i] > 1) t |= 1;
            else t.b0 |= _store[i];
        }
        out.write((char *)&t, sizeof(SlicedUnit));

        _i = _width-1;
    }

private:
    ofstream out;
};

```

Functionality is very similar to the `SlicedMatrixStepper`, but the constructor takes as argument a filename to write to rather than a bit-sliced matrix to populate. The call to `flush()` works mostly the same, but makes sure to append the temporary *sliced unit* created from the input to the file.